MODELLING THE OCEANOGRAPHIC TRANSPORT OF YOUNG CAPE ANCHOVY *ENGRAULIS CAPENSIS* BY ADVECTIVE PROCESSES OFF SOUTH AFRICA

submitted in partial fulfilment of the requirements for
the degree of MASTER OF SCIENCE in Marine Biology
(Zoology Department, University of Cape Town)

Candidate: Lynne Jane Shannon

Supervisors: Prof. J.G. Field

Mr G. Nelson

Dr R.J.M. Crawford

Even the birds and animals have much they could teach you;

ask the creatures of earth and sea for their wisdom.

All of them know that the Lord's hand made them.

Job 12 verses 7-9

DECLARATION

I hereby declare that the backbone of the work presented in this thesis is my own, that the detailed planning and fitting of data to this model, manipulation of results into the format I desired and the manipulation of the model required when applying it to the altered advection scenarios were done by myself. The model used in this thesis was developed under the guidance of and in collaboration with Dr G. Nelson. One approach addressing altered advection was undertaken by myself and Dr A.J. Boyd (Chapters Three and Five). Dr R. J. M. Crawford supervised another approach (Chapter Six). All the adaptations necessary to apply the model in these ways, the statistics and the collating of results were done by myself. Interpretation of results was done mainly by myself, but Dr Boyd and Dr Crawford aided me at times. Sensitivity testing (Chapter Two) and the work on the influence of spawner distributions on distributions of young-of-the-year anchovy were initiated and carried through by myself, although I consulted Dr Boyd on some aspects of Chapter Four. Technical and other assistance has been fully acknowledged in the acknowledgements. I have fully acknowledged the assistance and guidance I received. No part of the work towards this thesis has been submitted for any other degree at any other institution.

CONTENTS

CHAPTER THREE

MODIFYING THE FLOW FIELD ABOVE THE THERMOCLINE IN AN ATTEMPT TO IMPROVE SIMULATION OF ANCHOVY TRANSPORT

page

CHAPTER FOUR

IMPORTANCE OF SPAWNER DISTRIBUTION FOR ANCHOVY SURVIVAL

page

CHAPTER FIVE

POTENTIAL EFFECTS OF WEAKER AND STRONGER ADVECTION

CHAPTER SIX

A SECOND APPROACH TO INVESTIGATE THE POTENTIAL EFFECTS OF ALTERED WESTWARD ADVECTION

CHAPTER SEVEN

FUTURE OBJECTIVES AND CONCLUSIONS

APPENDIX A: MANUAL FOR USE OF THE MODEL

page

ACKNOWLEDGEMENTS

I am greatly indebted and immensely grateful to Mr G. Nelson and thank him for all the time and effort he devoted to construction of the model. Without his hard work, enthusiasm and the thought provoking discussions that arose, this model would not have been possible.

Dr R.J.M. Crawford is thanked for his much appreciated advice and constructive criticisms of this thesis, Prof. J.G. Field for his guidance through the project and helpful suggestions, and Dr A.J. Boyd for enthusiastically supervising the first section on altered advection. Special thanks are extended to Dr A.I.L. Payne for encouraging me and believing in me, and to Sea Fisheries Research Institute for granting me the opportunity to undertake this study.

Mr A. P. van Dalsen and staff of the Reprographic Section at Sea Fisheries Research Institute are thanked for fitting many of my figures into their tight schedule at short notice - their efforts are greatly appreciated. I also thank Messrs S. Bloomer for his constructive criticism of this thesis and all the time spent perfecting the graphics, G. Oberholster for his kind assistance in the extraction and manipulation of ADCP data, and his endless encouragement and support, and M. Prowse for his help with the extraction of acoustic data. Thank you Mom for always being there to offer a sympathetic ear and sound advice.

The Sea Fishery Fund is acknowledged for supporting the study. The Benguela Ecology Programme is thanked for funding participation at the "Climate and Survival" symposium held at Victoria falls, Zimbabwe, in February 1994, at which preliminary results were presented.

ABSTRACT

A Monte-Carlo type model has been developed to investigate the importance of passive transport by currents above the thermocline for anchovy recruitment off South Africa. Simulation studies indicate that mean year-class strength of Cape anchovy is relatively robust to altered advective processes off South Africa. This occurs despite the fact that changed flow alters the likelihood of offshore advection and hence losses of anchovy from the system. Two different approaches have been taken to address the effects of altered advection, and the applicability of each is discussed. One approach involves altering westward advection in proportion to the mean current field (derived from Acoustic Doppler Current Profiler measurements), and the other, altering westward and northward advection by the addition of fixed offshore current velocities. The proportional approach did not affect year-class strength significantly, whereas the other approach, which incorporated large changes in the flow field, yielded statistically significant differences in predicted year-class strengths between advection scenarios. Reduced flow in the latter approach led to a mean year-class strength 2.7 times stronger than a proposed base flow scenario (which incorporated westward and northward drift in addition to the ADCP currents), whereas enhanced flow resulted in a mean year-class strength of similar magnitude to that of the base flow scenario.

Changed flow may alter the geographic distribution of eggs and larvae, which might in turn influence recruitment of young-of-the-year anchovy to the South African purse-seine fishery. The north-flowing shelf-edge jet current plays an important role in transporting anchovy eggs and larvae from spawning grounds in the south to nursery areas further north along the west coast of South Africa. Enhanced model advection westward and northward from the spawning grounds in the south serves to transport anchovy into the region of the jet current. However,

advection into unproductive waters offshore is also enhanced and prevents good recruitment under these flow conditions. On the other hand, reduced westward and northward advection in the model, shown through wind records to characterise El-Niño years in coastal areas of South Africa, serves to retain anchovy reproductive products and often transports young anchovy into coastal areas, preventing offshore loss. Therefore the advection model suggests that good year-class strengths (in terms of numbers) are likely to be supported in years when westward and northward advection are reduced. A further reduction in westward advection may be less favourable by causing advective losses offshore along the south coast of South Africa. This may be viewed in terms of an "optimal environmental window" hypothesis, where reduced westward advection is favourable for anchovy survival off South Africa, but further reduction of westward advection as well as enhanced westward advection appear unfavourable. It is concluded that although passive transport of anchovy in South African waters is relatively robust, it may account for a substantial proportion of recruitment variability.

The model addresses changes in wind-induced advection. Oceanic advection has not been modelled and is likely to be the dominant influence on anchovy recruitment in some years. The distribution of spawning adults seems to be important for the ultimate destination of young of the year. In years when spawners are particularly concentrated in offshore areas, the likelihood of model advective losses is high. One example is provided by modelling spawning in 1988. During November of 1988, a high density of spawners was found on the outer edge of the Western Agulhas Bank. Model advective losses of eggs and larvae resulting from spawning in 1988 are at least double those in other years modelled. Model results suggest that anchovy benefit from spawning in the region of the Central Agulhas Bank. This region acts as a retention area to anchovy eggs and larvae, since mean currents measured here using an

Acoustic Doppler Current Profiler are weak. However, other factors such as those related to predators and prey in this region should be also be considered. It is likely that in addition to the passive transport of anchovy eggs and larvae, active swimming by older juveniles plays a role in distributing young-of-the-year anchovy.

CHAPTER ONE

SETTING THE SCENE

CHAPTER ONE

SETTING THE SCENE

1.1 BRIEF INTRODUCTION TO THE PHYSICAL OCEANOGRAPHY OF THE COAST OF SOUTH AFRICA

Before describing the life cycle of the Cape anchovy *Engraulis capensis*, it is necessary to set the scene by briefly outlining the main oceanographic features off South Africa. The ocean surrounding South Africa is dominated by two systems, namely the Agulhas Current system off the south coast and the southern Benguela system off the west coast (Figure 1.1). Shannon (1989) gave a comprehensive overview of the physical oceanography of the region.

The Agulhas Current region has recently been reviewed by Boyd and Shillington (1994). The Agulhas current characterises the area between 30°S and 36°S, flowing in a south-easterly direction along the coast and steered by the underlying bottom topography. It flows at an average speed of 1-2 $m.s^{-1}$ but can attain speeds of up to 2.6 $m.s^{-1}$. It is strongest at the surface but extends to depths of 2000 m or more. Between Port Shepstone and East London (Figure 1.1), the continental shelf is very narrow and the Agulhas Current flows strongly, slowing towards Port Elizabeth as the shelf begins to widen. Meanders in the current develop, particularly near Port Elizabeth (Figure 1.1), and have been described by Lutjeharms *et al.* (1989). Because of conservation of vorticity and other factors, the Agulhas Current is not maintained further than 36°S, and it retroflects anticlockwise as it approaches this limit (Shannon 1989). The positions of retroflection and the process whereby Agulhas rings break

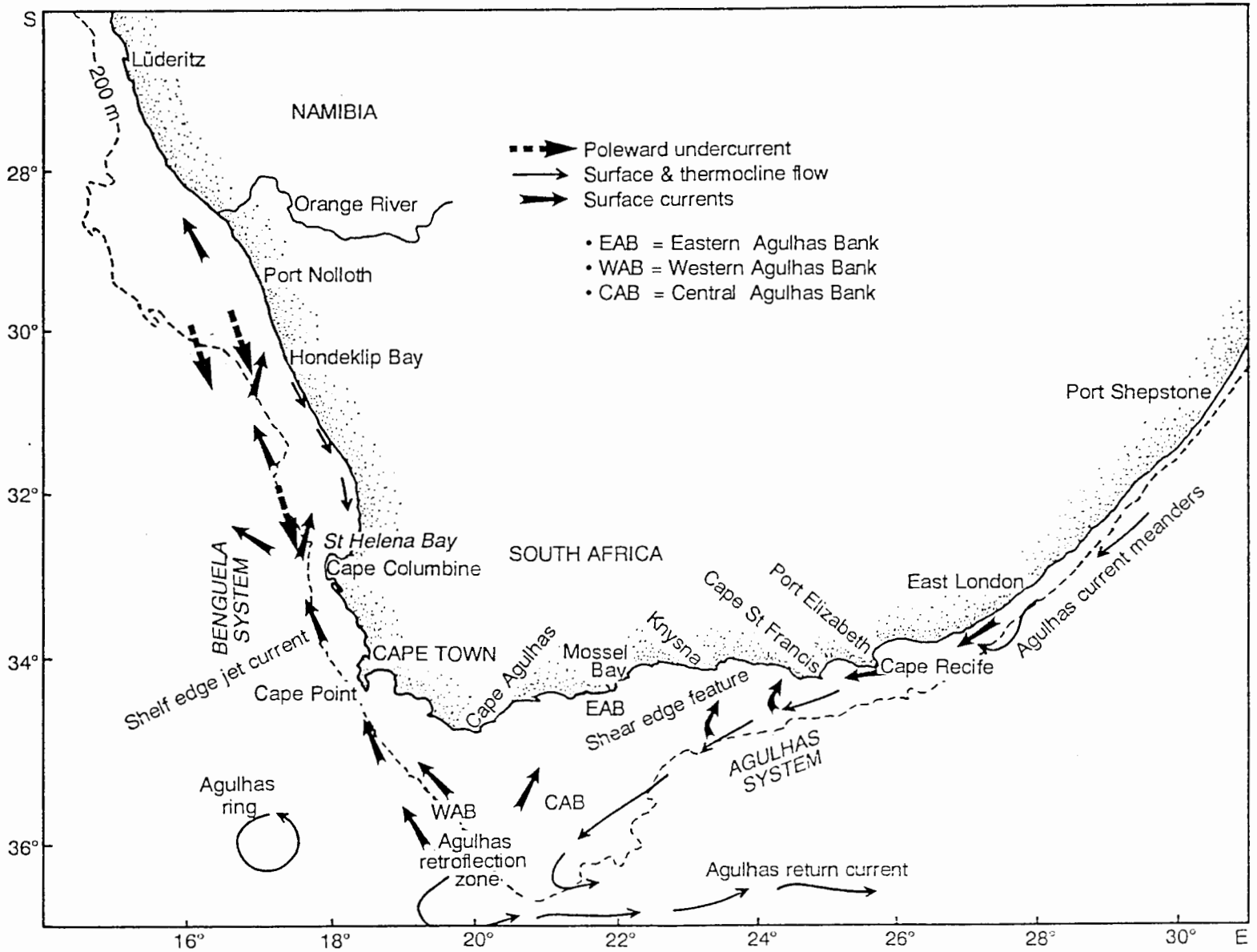

Figure 1.1 Shematic representation of the main oceanographic features off South Africa (adapted from Shannon 1989 and Shannon and Nelson in press)

off during retroflection and continue south and westward are described by Lutjeharms and van Ballegooyen (1988). Eastward-flowing countercurrents close inshore on the south-east Agulhas Bank have been measured using Acoustic Doppler Current Profilers (ADCPs), as have return currents along the outer parts of the Agulhas Bank (Boyd *et al.* 1992, Boyd and Oberholster 1994).

The Agulhas Bank is characterised by variable, weak currents (Boyd *et al.* 1992) and strong thermoclines develop here during the warm summer months (Shannon 1989). Westerly transport of biota from the eastern Agulhas Bank to the western Agulhas Bank has been proposed (Largier et al. 1992), based on observations of the physical oceanography of the region. Inshore, wind-induced upwelling occurs in summer, particularly in the regions of Capes such as Recife, St Francis and Agulhas (Shannon 1989).

Another prominent feature of the Agulhas region is the variable, semi-permanent, cool water ridge, extending from the eastern to the central Agulhas Bank. The cool ridge has been proposed to be of oceanographic origin (Swart and Largier 1987), although it has also been suggested to be strongly linked to coastal upwelling along the south coast (Swart and Largier 1987, Roberts 1993). Finally, it is possible that the widening of the shelf in the region between Port Elizabeth and Knysna (Figure 1.1) may result in divergent flow, likely to generate upwelling of the thermocline (Boyd and Shillington 1994).

The Benguela is one of the world's four eastern ocean boundary regions. Shannon and Nelson (in press) have recently reviewed the Benguela system in detail and include in their paper previously unpublished results, leading to the present understanding of the system. Wind-

induced upwelling is prevalent in many areas of the west coast, a major centre being off Lüderitz in Namibia (Figure 1.1). The semi-permanent plume of cool water acts as a biological barrier to species such as *E. capensis*, and serves to separate the Benguela region into two parts, namely the northern and the southern. It is the southern region which bounds the west coast of South Africa and which is described below.

The Benguela region is characterised by a permanent, baroclinic, equatorward-flowing shelf-edge jet current (Figure 1.1), first described by Bang and Andrews (1974). Reasons for the existence of shelf-edge jets are discussed at length by Shannon and Nelson (in press). The jet is located over the 300-400 m isobaths, between Cape Point and Childs Bank (in the region of 31°S and 16°E), and can attain speeds of up to 75 $cm.s^{-1}$, although this is far from the maximum speeds in the Agulhas current.

Equatorward flow within the boundaries of the 500 m isobath is slow in the region between Cape Town and Cape Columbine, and is due to widening of the shelf in this region as well as dynamic interaction of the jet with the poleward undercurrent (Nelson 1989). North of Cape columbine, current speeds return to approximately 35 $cm.s^{-1}$ (A. J. Boyd, Sea Fisheries Research Institute, pers. comm.). Near St Helena Bay, the jet current bifurcates into an offshore branch and a northward flow which partially enters St Helena Bay (Shannon 1985, Nelson 1991). North of St Helena Bay, flow curves onshore towards Hondeklip Bay and bounds a wide area to the east, where mean currents are weak (Boyd and Oberholster 1994). This feature is associated with upwelling tongues off Cape Columbine, which prevail during summer (Shannon and Nelson in press).

Beneath the north to north-westward flow of the Benguela current is a poleward undercurrent, extending below 120 m at the outer shelf and from as shallow as a few metres near the coast (Shannon and Nelson in press). Superimposed on the poleward flow are oscillatory components with periods of between 3 and 10 days, which can even reverse flow in both the upper and lower layers in some coastal regions (Shannon and Nelson in press).

Flow close inshore along the west coast is predominantly southward (Boyd *et al.* 1992). On the western Agulhas Bank, a convergent north-westerly current system has been located using an ADCP (Boyd *et al.* 1992). This feeds into the jet current on the west coast, off the Cape Peninsula.

In addition to the currents described above are the influences of filaments and eddies in the Benguela region. Some filaments are semi-permanent and cause instability in the shelf-edge jet and poleward undercurrent (Shannon and Nelson in press). Agenbag (1992) used satellite imagery to examine such a filament spreading out from near Dassen Island. Active transport away from the Benguela system by cold water filaments extending offshore, as well as the process by which they are formed, have been described by Shillington *et al.* (1992). Such filaments are frequently found in the north and south and near the Orange River mouth (Oranjemund). Additional forcing of these filaments by the interaction of warm-core Agulhas rings, shed in the Agulhas Current retroflection region, is recognised (Duncombe Rae *et al.* 1989, Lutjeharms *et al.* 1991 and Shillington *et al.* 1992).

Considering the often harsh and variable oceanographic conditions off South Africa, the Cape anchovy population must be sufficiently buffered to ensure survival.

1.2 LIFE HISTORY AND MIGRATION OF CAPE ANCHOVY

Spawning by the Cape anchovy *Engraulis capensis* takes place to the east of Cape Point (Crawford 1980), predominantly in the region of the Agulhas Bank (Figure 1.2). Since anchovy are pelagic spawners, their early reproductive products are transported by currents. Some eggs and larvae are transported northwards and westwards from spawning grounds in the south (Shelton and Hutchings 1982). Of particular importance in this process is the northward-flowing shelf-edge jet current (described in section 1.1) which attains speeds of between 25 and 75 $cm.s^{-1}$ (Boyd *et al.* 1992). Once north, young then migrate inshore to nursery areas along the coasts of the Western and Northern Cape Provinces, where they continue to grow before migrating southwards back to spawning areas (Figure 1.2) (Armstrong and Thomas 1989). It is during this southward migration, at the age of approximately six months, that young become susceptible to the purse-seine fishery (Armstrong and Thomas 1989). The Cape anchovy has been the major contributor to catches of South Africa's purse-seine fishery since the mid 1960s, when small-meshed (13mm stretched) nets were introduced. In 1993, anchovies contributed some R133 million to the South African economy in fish meal and oil.

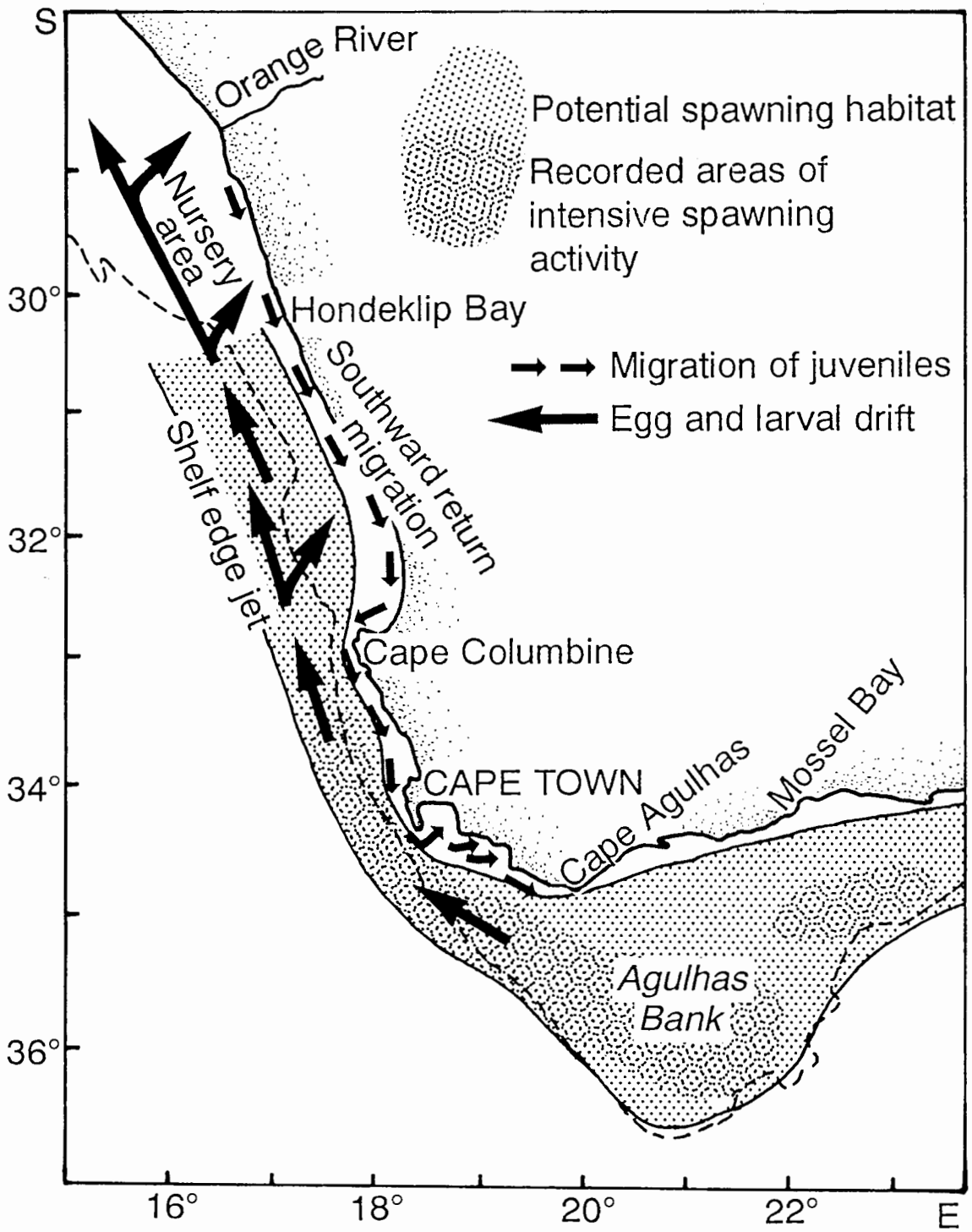

Figure 1.2 Map showing the migration of anchovy from spawning grounds to the nursery areas and back (adapted from Armstrong and Thomas 1989)

1.3 EFFECTS OF ENVIRONMENTAL FACTORS ON CLUPEOIDS

Populations of clupeoids are sensitive to environmental variability and are subject to large natural fluctuations in stock size (Shackleton 1987, Lluch-Belda *et al.* 1989, Lluch-Belda *et al.* 1992). Factors thought responsible for most of the natural variability in fish stocks include temperature, turbulence, transport, food, predation and population density (Parrish *et al.* 1983). The physical environment may impact fish populations in a number of ways - abundance and availability of food may be affected (e.g. Cushing and Dickson 1976, Lasker 1978); surface warming increases stratification, and may enhance food concentration in upper layers, possibly resulting in expansion of suitable habitats for some species (Bernal 1988); altered temperatures may influence growth and mortality of eggs and larvae (e.g. King *et al.* 1978, Brownell 1983, Lo 1985, Armstrong *et al.* 1988); advective processes important in the transport of fish may change, influencing mortalities, especially of young stages (e.g. Parrish *et al.* 1981).

Altered conditions arising from global environmental change may influence survival of the early life stages of anchovy, and hence the quantity of anchovy available to the fishery off South Africa (Shannon *et al.* 1988, Siegfried *et al.* 1990). The latter authors presented four scenarios which could possibly arise during global-warming induced change. One of these was altered wind stress, which itself could present a few possibilities for altered offshore advection. Bakun (1990) proposed a mechanism whereby global greenhouse warming could lead to increased longshore wind stress, resulting in enhanced coastal upwelling. He pointed out that as yet there is little documented evidence that increased primary production actually promotes population growth and reproductive success of commercially-exploited fish species.

On the other hand, should the thermal gradient between equatorial and polar zones be reduced, upwelling may be reduced through lowered intensity of trade winds (Siegfried *et al.* 1990). This is in agreement with Hsieh and Boer (1992), who suspect that the effects of global warming on ocean productivity may be less pronounced and more complicated than Bakun (1990) suggested. They in fact predict a general weakening of open ocean upwelling and are of the opinion that there will not be an increase in coastal upwelling as a result of global warming. Instead of enhanced productivity, these authors predict a decrease in biological productivity. However, should upwelling along the south coast of South Africa increase, conditions for spawning by anchovy would become more favourable, and the area in which spawning could occur would expand further eastwards (Siegfried *et al.* 1990). However, increased upwelling may be likely only as a transient, intermediate phase (Siegfried *et al.* 1990). Evidently there is much debate regarding the consequences of global climate change. However, one thing that has been predicted with confidence is that major and sudden changes in marine populations will result from global climate change (Bakun 1994).

Some modelling studies have suggested that global warming may result in El-Niño events having more severe effects, such as more extreme wet and dry periods (Zebiak and Cane 1991, Meehl *et al.* 1993 and G. A. Meehl, NCAR, pers. comm.). Between the summers of 1990/91 and 1992/93, South Africa experienced the effects of the most prolonged El-Niño event recorded. This period was characterised by reduced frequency of south-easterly winds (J. Taunton-Clark, Sea Fisheries Research Institute, pers. comm.). During the austral summer of 1993/94, south-easterly winds blew more strongly than during the previous two summers, but had returned to below normal levels by spring 1994 (J. Taunton-Clark, Sea Fisheries Research Institute, pers. comm.). It is possible that part of the reason for poor anchovy

recruitment in 1994 was wind-induced offshore transport of eggs and larvae in the surface waters during the summer of 1993/94, which led to greater losses of anchovy by advection. The impacts that altered intensity or frequency of El-Niño events will have on the South African anchovy stock are unknown. The suitable approach is to model the effects of a number of different advection scenarios which could result as the climate changes.

1.4 RATIONALE FOR MODELLING TRANSPORT PROCESSES

Due to the fact that most time series of fisheries are fairly short, statistical analysis is limited. Parrish *et al.* (1981) therefore suggested that a few dominant environmental variables be examined for effects on fisheries. The authors proposed that in coastal fisheries of California, surface drift of fish eggs and larvae is a significant factor.

A model was developed to simulate spawning of anchovy eggs and the subsequent transport of reproductive products six months after spawning. Young of the year retained in and near to coastal regions were assumed to contribute to year-class strength, whereas batches of eggs and larvae transported to areas far offshore and unfavourable for survival were considered to have been lost from the system.

Two different approaches looking at various scenarios of altered advection were investigated using the model, results of which are discussed in this thesis. Firstly, the Acoustic Doppler Current Profile (ADCP) flow field was modified in the model by altering current vectors in different areas by the addition or subtraction of components, in order to obtain realistic

distributions of young-of-the-year anchovy and advective losses. Reasons for doing this are discussed in section 3.2 of Chapter Three, and stem from the fact that ADCP measurements in the upper 25 m of the water column are considered unreliable and are therefore not used in the current averaging process (A. J. Boyd, Sea Fisheries Research Institute, pers. comm.). Once a flow field which yielded reasonable spatial distributions of young of the year and losses was established, each of the seven spawner distributions from 1986 to 1992 was modelled using the new field. Following this, scenarios of enhanced and reduced flow relative to the new flow field were considered. The second approach involved addition and subtraction of fixed proportions (viz. 25% and 50%) from unmodified easterly velocity components.

Transport of fish eggs and larvae has been the centre of much discussion, (for example the review paper by Norcross and Shaw, 1984), and has been shown to affect the recruitment success of many fish species. Berntsen *et al.* (1994) used a three-dimensional model of transport of particles to represent the transport of sandeel larvae (*Ammodytes sp.*) in the North Sea. They found that retention of larvae was extremely important for good year-class strengths to be attained. A numerical model of advection and diffusion of eggs and larvae of the Japanese sardine (*Sardinops melanostictus*) indicated that survival of sardine is significantly affected by the offshore drift current of the region, induced by the winter monsoon (Kasai *et al.* 1992). Norwegian capelin (*Mallotus villosus*) and herring (*Clupae herengus*) stocks are supplied by the transport of fish by currents from Iceland to the Norwegian coast (Bjørke and Sætre 1994). By means of a three dimensional advection model of North sea herring, Bartsch *et al.* (1989) showed that environmental modelling can improve the understanding of interannual variability in fish recruitment.

Many fish species rely on transport of eggs and larvae from spawning grounds to nursery areas by currents (Cushing 1986). As already mentioned, one such species is *Engraulis capensis* (Shelton and Hutchings 1982). The objectives of this thesis are to model the transport of anchovy by oceanographic processes influencing year-class strength of the Cape anchovy *Engraulis capensis* off South Africa, and to investigate implications of altered advective processes for abundance and the spatial distribution of young-of-the-year anchovy.

CHAPTER TWO

SIMULATION OF TRANSPORT OF EARLY LIFE STAGES

OF ANCHOVY *ENGRAULIS CAPENSIS* OFF SOUTH AFRICA

CHAPTER TWO

SIMULATION OF TRANSPORT OF EARLY LIFE STAGES OF ANCHOVY *ENGRAULIS CAPENSIS* OFF SOUTH AFRICA

2.1 INTRODUCTION TO THE MODEL

This chapter describes a model constructed to simulate transport of early life stages of Cape anchovy *Engraulis capensis* from the areas of spawning to nursery areas off South Africa. It computes year-class strength and distribution of young-of-the-year anchovy under chosen current fields. Sensitivity of the model to two physical parameters (namely turbulence and diffusion) is investigated.

Figure 2.1 aids in conceptualization of the model. The model uses empirical data on currents and spawner biomass at discrete grid points around the South African coast. It allows for a maximum grid array (memory space) of 100 by 100. The model uses a rectangular grid, a constant temperature field of water, historical distributions of spawner biomass and a constant velocity field to which random components may be added to simulate variability in the flow field (due to filaments and eddies). The dimensions of blocks in the grid are a matter of preference. The model space fills an irregular area of computer memory space (Figure 2.2). The grid can be rotated so as to obtain better alignment with the coast and better resolution where strong currents occur. For the purposes of this thesis, a horizontally-orientated, rectangular grid of 0.25 by 0.25 degree (latitude and longitude) blocks containing Acoustic Doppler Current Profile (ADCP) data was used (Figure 2.3). Grid dimensions of quarter

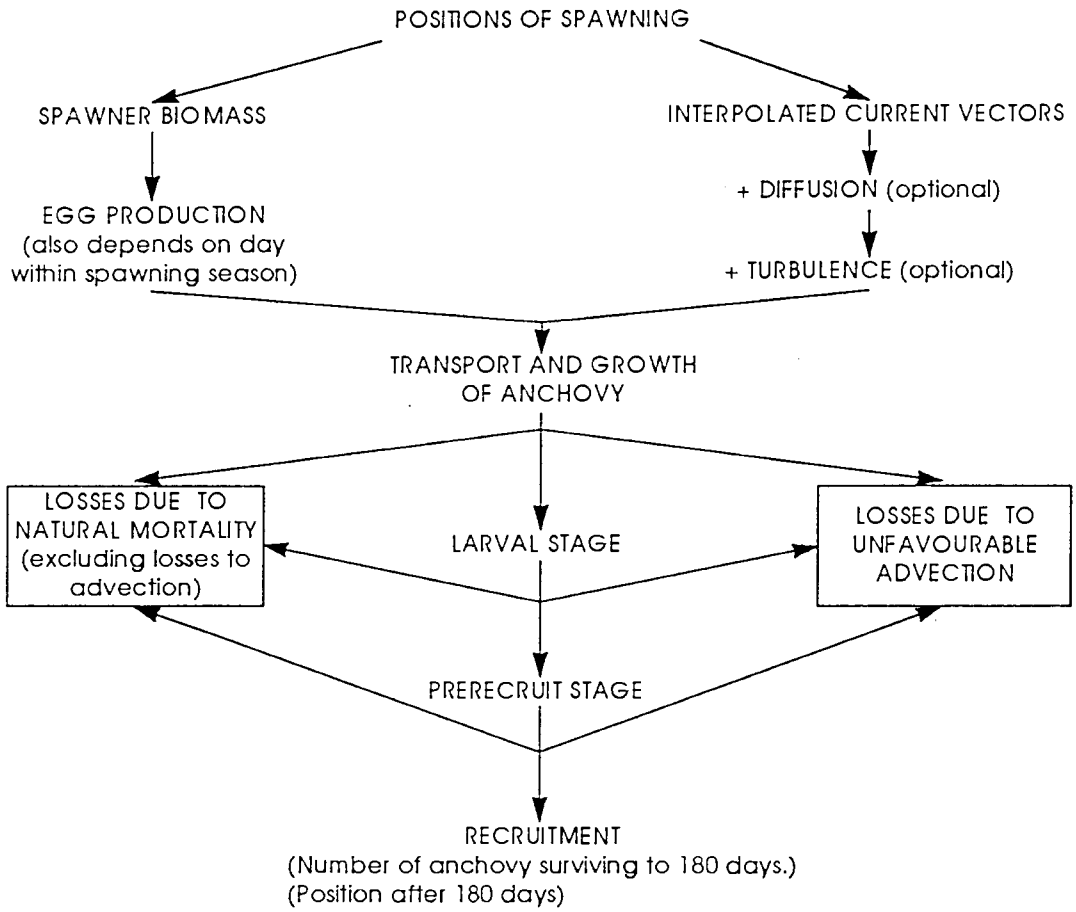

Figure 2.1 Conceptual diagram of model

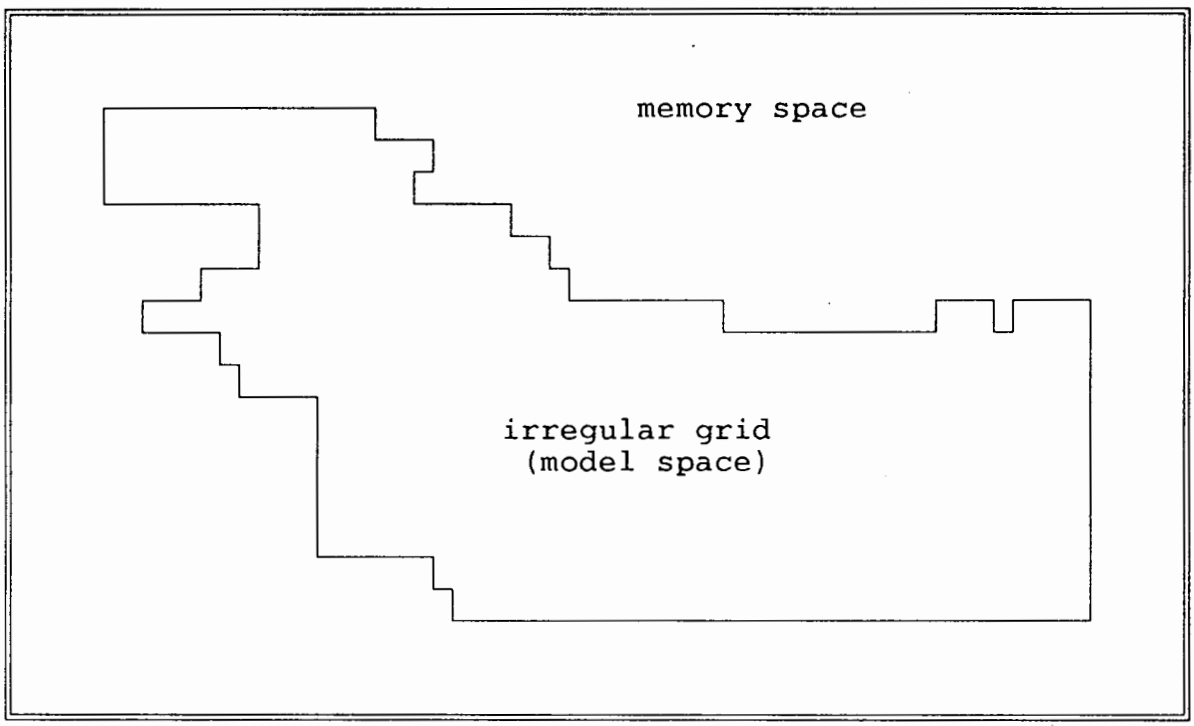

Figure 2.2 Conceptual representation of the terms computer (memory) space and model (grid) space.

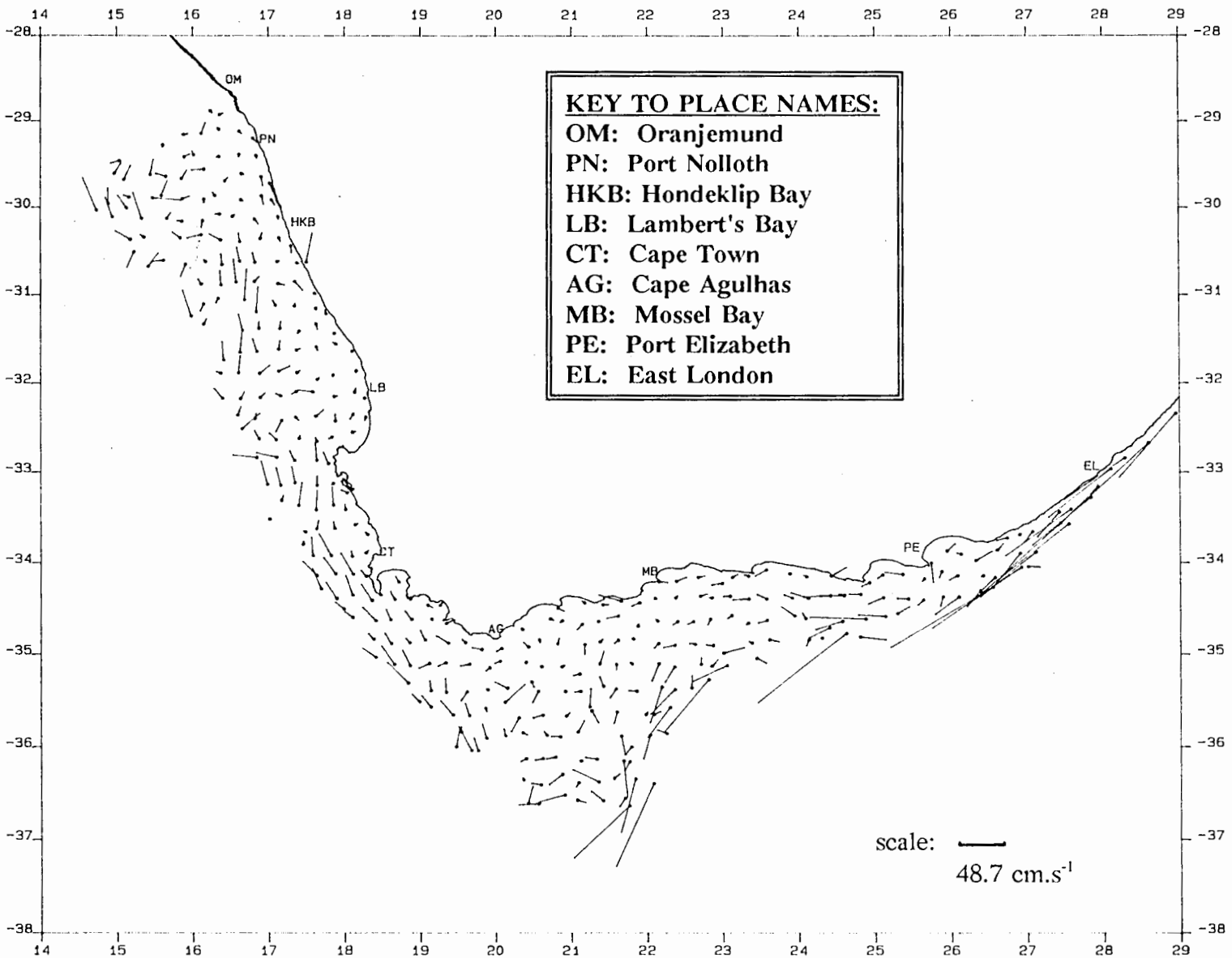

Figure 2.3 Means of 30 and 50 m ADCP current vectors, averaged into quarter degree blocks

degree blocks were converted to kilometres, calculated using the method of Raisz (1948) (Appendix A, page A.9). The grid covered the west coast, Agulhas Bank and east coast from 29°00'S to 36°45'S and 15°00'E to 28°00'E. Blocks outside the grid and offshore blocks within the grid but lacking ADCP data (i.e. not within the routine survey area and therefore presumed to be beyond the distribution of anchovy) are considered as sinks; any reproductive product entering these blocks was presumed lost from the system.

Mortalities of eggs, larvae and prerecruits resulting from processes other than transport were modelled independently as numbers lost per unit time. Duration of egg, larval and prerecruit stages were set to constant values and mortality rates of eggs, larvae and prerecruits remained constant throughout the spawning season and across the spatial distribution.

2.2 MODEL DESCRIPTION

2.2.1 SPAWNING AND EGG PRODUCTION

Cape anchovy off South Africa spawn mainly between October and January (e.g. Crawford 1980), although spawning may extend to the end of March (Y.C. Melo, Sea Fisheries Research Institute, pers. comm.). In the model, the spawning season of anchovy was assumed to commence on 1 October and continue to 31 March. Most spawning takes place to the south of Cape Columbine between 33 and 35°S and around Cape Point between 18 and 21°E (Crawford 1980, Shelton and Hutchings 1982). In the model, eggs were produced by a fixed initial abundance of spawners.

The number of eggs spawned per day was computed as:

$$E = \frac{B}{W} rSf$$

.....equation 2.1

where E is egg production per day,

B is spawner biomass (kilograms),

W is mean weight of a female anchovy (kilograms),

r is mean proportion of females (by mass),

S is mean proportion of females spawning on any one day (spawning fraction), and

f is mean batch fecundity (eggs produced in a day by a spawning female).

Values of parameters used in the model are tabulated in Table 2.1.

Table 2.1 **Parameters (from Sea Fisheries Research Institute records) and the years for which averages were used to calculate the overall means for input into the egg production algorithm.**

VARIABLE	YEARS	MEAN
Mean spawner biomass	1984-1992	$1172X10^6$ kg
Mean female proportion by mass (r)	1984-1992	0.53
Mean female mass (W)	1984-1992	0.01242 kg
Mean spawner fraction (S)	November 1985-1992	0.104/day
	February/ March 1987	0.069/day (Melo 1992)
Mean batch fecundity	1984-1992	6749 eggs/female/batch

The model is aimed at investigating recruitment resulting from a *fixed* spawner biomass, but also to examine the importance of the geographical distributions of spawners, for which information over a nine-year period was available from acoustic surveys. In order to fulfil both these prerequisites, average anchovy density weighted by length of acoustic intervals was calculated for each 0.25 by 0.25 degree block in each year. (Acoustic intervals are those distances across which acoustic signals were integrated). The average weighted density in each block was then converted to a fraction of the total sum of weighted densities for that year in all blocks and multiplied by the average spawner biomass for the nine-year period. Unfortunately, there were problems in the spawner biomass database for spawning in 1984 and 1985, and although the mean was taken for the nine-year period, detailed distributions of spawners were only reliable for the years from 1986 to 1992. A batch of eggs is defined as the total number of eggs produced per day by all females in a quarter degree block. The size of a batch depends on the day within the spawning season, owing to variation over the season of the spawning fraction of females (S) per day. This differs from the biological term batch fecundity (f), which is defined as the mean number of eggs produced per female per spawning session. In the model, it should be noted that because a single batch of eggs was released each day within the spawning season from each quarter degree block containing spawners, and due to the fact that spawner distributions varied between years, the sum of batches released during the spawning season depended on the spatial distribution of spawners and therefore differed between years. The size of batches released per day depended on the observed concentration of spawners in each quarter degree block each year. It should be stressed that because *total* spawner biomass was fixed, *total* egg productions were equivalent in all years.

The number of spawners was decreased to account for natural mortality of spawning anchovy during the spawning season. To account for arrival and growth of adults at the spawning ground from September to mid-November, the number of spawners was only reduced from the 15 November onwards, i.e. it was assumed that the increase in spawner biomass as a result of growth and new arrivals at the spawning grounds balanced spawner mortality during the early part of the spawning season. Mortality rate used here is "m" in the algorithm

$$A_{t_s} = A_{t_0} e^{-m(t_s - t_0)}$$

.....equation 2.2

where A_{ts} is the spawner biomass at time t_S and A_{t0} is the spawner biomass at time t_0, i.e. 15 November. An annual instantaneous mortality rate of 1.33 (corresponding to an hourly survival rate of 0.9998) is used in the management of *E. capensis* (Valdés-Szeinfeld and Cochrane 1992). Butler *et al.* (1993) documented a daily instantaneous mortality rate of 0.0021 (corresponding to an hourly survival rate of 0.9999) for the northern anchovy *Engraulis mordax*. Based on these two estimates, an average hourly survival rate of 0.9999 was used in the model. An hourly mortality rate was used in the model in order to accommodate the hourly time-step necessary to obtain adequate resolution in the Lagrangian simulation of eggs and larvae. Note that since mortality rates for *E. capensis* are poorly known, it is unreasonable to include more significant figures in survival rates.

It was assumed that the proportion of females (r) remained constant throughout the spawning season. Spawning by anchovy is not of uniform intensity throughout the spawning season. Periods of peak spawning intensity are followed by periods of spawning minima (Lasker and Smith 1977, Shelton 1979), reflecting the larger fraction of females spawning per day (*S*) at

the peak of the spawning season and the smaller fraction towards its end (Table 2.1 and Hunter and Goldberg 1980). For modelling purposes, a curve of *S* as a function of time was fitted for *E. capensis*. Curves derived from hyperbolic tangent functions were merged to give a suitable approximation to the trend expected from the available data. This function has a plateau representing the highest value of S and two tails (the early and late parts of the spawning season) which may be asymmetric, depending on the choice of characteristic rise and fall time scales. The model fitted was:

$$S = 1.0 - e^{-[10.6(1-2x)]+1}$$

.....equation 2.3

where

$$x = \frac{abs(d)}{K}$$

.....equation 2.4.

and abs(*d*) = absolute number of days from 1 November to the day of spawning,

K = the constant which determines the width of the "plateau" of largest S and was assigned the value of 376.

The egg production algorithm assumed that all females produce the same number of eggs per batch and that batch fecundity (f) remained constant throughout the duration of the spawning season. These are approximations that may not necessarily be true. Valdés-Szeinfeld and Melo (unpublished) found that larger anchovy, and therefore usually older, produce more eggs and that these eggs are bigger than eggs produced by smaller females. Larger eggs may have larger survival rates and hence contribute disproportionately to successful recruitment. Size-dependent batch fecundity has also been reported for northern anchovy, *E. mordax* (Hunter

et al. 1985). Similar batch fecundities have been found at the start and end of the spawning season of northern anchovy (Hunter and Leong 1981), although Parrish *et al.* (1986) suggest that batch fecundity may vary over the spawning season.

2.2.2 EGG SURVIVAL

An average instantaneous egg mortality of 0.01 per hour was measured for anchovy off South Africa over the period 1986-1988 (Valdés *et al.* 1987, Valdés-Szeinfeld 1991, unpublished records of Sea Fisheries Research Institute). This corresponds to a 79% daily survival rate, which is comparable to the 78% average daily survival rate reported for northern anchovy (Piquelle and Hewitt 1983).

King *et al.* (1978), related time (y hours) from blastodermal cap stage until hatching to temperature (T°C) for *E. capensis* as follows:

$$y = 43787.93T^{-2.41}$$

.....equation 2.5.

Using the relation

$$\ln(y) = 5.02 - 0.155T$$

.....equation 2.6

presented by Lo (1985) for the northern anchovy, an estimate of time from spawning until blastodermal cap stage (y hours) at a specified temperature (T°C) was calculated, since no similar relationship for *E. capensis* is available. An average temperature of 17°C was selected as a representative temperature for the upper mixed layer in the spawning region over the

Agulhas Bank (Anders 1965, Armstrong *et al.* 1988, Shelton 1979). From the two relations, time from spawning until hatching is described by the algorithm

$$Y = 43787e^{-2.41\ln(T)} + e^{5.02-0.155T}$$

.....equation 2.7

which gives Y = 58 hours at a water temperature of 17°C. This agrees closely with the 2.5-day (60-hour) estimate mentioned by Armstrong and Thomas (1989). Therefore for model purposes, larvae were assumed to appear 59 hours after spawning had taken place (refer to Appendix A, Figure A.3).

2.2.3 SURVIVAL OF LARVAE AND PRERECRUITS

Some larvae and prerecruits are transported from spawning grounds to nursery grounds. The main region of transport is between 35 and 33°S, 15 and 18°E and the main nursery area stretches from 30 to 33°S, 16°E to the coast, although the Orange River region may also be important (Boyd and Hewitson 1983, Hampton 1992).

Laboratory experiments carried out on *E. capensis* by Brownell (1983) at temperatures between 18.5 and 19.5°C suggested an average daily larval mortality rate of 6.1% over the period until 30 days post-hatch. This value corresponds to an instantaneous daily mortality rate of 6.3%, comparable to that of 5% assumed by Smith (1985) on the basis of other known data for the late larval stage of northern anchovy *E. mordax*. However, the instantaneous daily mortality rate of early larvae of northern anchovy was found to be 16% (Hewitt and

Methot 1982). The instantaneous daily mortality of late juveniles and prerecruits of the northern anchovy was estimated to be 1% by Smith (1985) and 0.31% by Butler *et al.* (1993), corresponding to average hourly survival rates of 0.9996 and 0.9999 respectively. Mortality rates of juvenile *E. capensis* at the stage when they enter the nursery grounds are as yet unknown (J.D. Hewitson, Sea Fisheries Research Institute, pers. comm.). For this reason, the mortality rate of prerecruits was adjusted until the mean year-class strength produced by the model under documented flow was comparable to the average of 135.598 $X10^9$ anchovy estimated from acoustic surveys undertaken by Sea Fisheries Research Institute in October, November and December from 1986 to 1993 (calculated from unpublished records of Sea Fisheries Research Institute). Prerecruit survival was eventually set at 0.9981 per hour, corresponding to approximately 4.5% mortality per day (equivalent to daily instantaneous mortality of 0.046, i.e. 4.6%).

Larvae were assumed to grow into prerecruits approximately 101 days after spawning had occurred, since anchovy are classified as pre-recruits at an age of 3-4 months (J.D. Hewitson, Sea Fisheries Research Institute, pers. comm.). The time taken for prerecruits to grow to the stage at which they enter the fishery is then another 79 days, if it is accepted that Cape anchovy become susceptible to fishing gear at an age of approximately 180 days. The recruit fishery generally operates off South Africa's west coast in the austral autumn or winter, approximately six months after spawning commences (Crawford 1980).

2.2.4 ADVECTIVE PROCESSES

Transport simulated by the model depends on the flow field chosen to be modelled. Therefore choice of the flow field to be used is important and results obtained using the model should always be considered in conjunction with the flow field chosen. In the applications of the model used in work towards this thesis, transport of eggs, larvae and prerecruits from one block to an adjacent block was computed from mean current vectors above the thermocline, obtained from Acoustic Doppler Current Profile (ADCP) data (Figure 2.2). Time steps of one hour were used in the model. ADCP data were collected during cruises undertaken between September and March from 1989 to 1993 (refer to Appendix A, Table A.1). The ADCP identifies semi-permanent "structures" such as the shelf-edge jet off the west coast of South Africa (Boyd *et al.* 1992) whenever they are measured. The variance in such cases is small. Where transient features such as eddies and filaments occur, many observations are necessary to identify mean ambient flow. With only fifteen cruises contributing to the ADCP data base used to generate flow in the model, the variance of northerly and easterly current components was sometimes greater than the mean measured in a quarter degree block, in some cases by an order of magnitude. Therefore, it was decided to incorporate variability without adding a component based on variance to the average values, as was initially intended, because it would then have been necessary to make arbitrary restrictions on variability. Instead, the model simulated transient features by adding random components to the ADCP averages over selected periods (**lapse periods**). For purposes of this thesis, random components are termed **turbulence** and **diffusion** and are based on a rectangular distribution. This means that there is equal probability that any value of a random component from a defined spectrum (between zero and a specified maximum amplitude) will be selected. Transient features simulated in

this way typically operate on time scales of 12 to 24 hours, representing spatial scales of 10 to 20km (G. Nelson, Sea Fisheries Research Institute, pers. comm.)

Random easterly and northerly velocity vector components representing **turbulence** are kept constant for the duration of each selected lapse period, after which a new set of random components is generated for the following lapse period. For further details of this process Appendix A (section 3 part d 13) should be consulted.

In addition, random components representing smaller scale **diffusion** of less than 1 $cm.s^{-1}$, applicable to objects as small as eggs and larvae, were added to the ADCP averages. The time scale was fixed at one hour and the spatial scale was the order of meters (Appendix A, section d 13).

Each batch of eggs to be "released" in the model was randomly allocated a **seed integer**, which was used to initiate a repeatable sequence of random numbers for the addition of these random components (refer to Appendix A, page A5). In this manner, the path travelled by a particular batch, and depending on the sequence of random components added along the way, could be repeated and re-examined should this be necessary.

The 2-dimensional approach taken in this modelling study was favoured over using a 3-dimensional model for two reasons. Firstly, the ocean around South Africa is characterised by both eastern and western boundary current systems (Chapter One, section 1.1) which interact with one another, thereby strongly influencing the distribution and survival strategies of marine biota. It is extremely difficult to model two current systems in a single 3-

dimensional model. Boundary conditions are almost impossible to determine, unless one focuses on a smaller part of the coastline. However, to model transport and survival of anchovy in South African waters, both the west and south coasts need to be modelled together. Secondly, means of current measurements above the thermocline represent what is happening far better than fewer measurements at discrete depths within the surface layer. For these reasons and because Cape anchovy eggs and larvae occur predominantly above the thermocline (Shelton and Hutchings 1982), and since prerecruits are also most abundant in this region (O'Toole and Hampton 1989, J.D. Hewitson, Sea Fisheries Research Institute, pers. comm.), the zone of water through which young anchovy are passively transported can be considered 2-dimensional. Therefore use of a fixed current field based on ADCP measurements to which random perturbations are added was viewed as the best approach to achieve the objectives (Chapter One, section 1.1) of this study. Furthermore, use of a 2-dimensional model facilitates a "Monte-Carlo" type approach (repeated simulations using random components to introduce perturbations into the flow field) not feasible using a 3-dimensional model in which vertical flux has to be considered.

2.2.5 YEAR-CLASS STRENGTH

Year-class strength was computed as the sum of all individuals not advected offshore to sink areas and which obtained an age of 180 days, usually equivalent to a length of 7.0 to 8 cm (Bloomer 1994).

2.2.6 DISTRIBUTION OF YOUNG OF THE YEAR

The distribution of young of the year, as modelled under particular flow conditions, was examined in four strata (Figure 2.4), namely within the boundaries of the grid between:

i) the northern boundary at 29°S and Cape Columbine at 33°S,

ii) Cape Columbine at 33°S and Cape Agulhas at 20°E,

iii) Cape Agulhas at 20°E and Mossel Bay at 22°E and

iv) Mossel Bay at 22°E and the eastern boundary at 28°E.

2.3 SENSITIVITY TO PHYSICAL PARAMETERS

Owing to the time-consuming process of modelling transport of all batches spawned in a season, a small test input file (termed a release file) was compiled. Mean spawner biomass (Table 2.1) was divided by the total number of 0.25 by 0.25 degree blocks in which spawning occurred during at least one of the seven years from 1986 to 1992 (viz. 226 blocks). Egg production based on this value of spawner biomass was calculated for 15 November only. Therefore unlike other applications of the model, batches of *equal* size were released at the mid-points of all spawner blocks and tracked for 180 days.

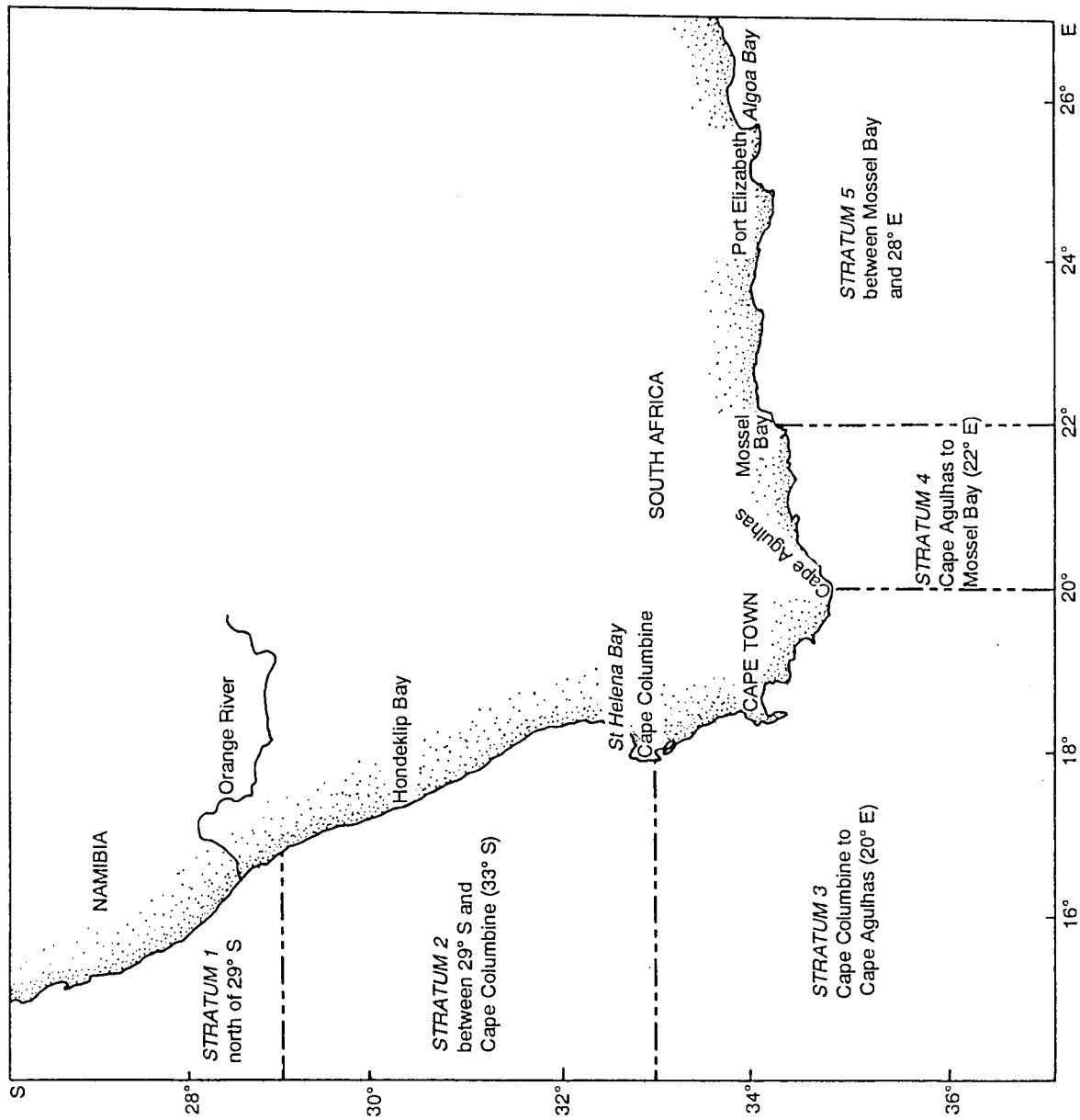

Figure 2.4 **Strata for which young of the year were summed (strata 2 to 5) and from which advective losses were summed (strata 1 to 5)**

2.3.1 TESTS CONDUCTED

The analysis tools of Microsoft Excel were used to perform statistical analyses. The test file was run using maximum turbulence amplitudes of 5, 10, 15, 20, 25 and 30 $cm.s^{-1}$, at lapse periods of 6, 12, 24, 36, 48, 60, 72, 84, 96, 120 and 144 hours. A two-factor ANOVA test (Model I) without replication was performed on both year-class strength and total advective losses in order to test for significant differences resulting from different turbulence options. Following this, five test files were compiled and each was randomly allocated a different set of seed integers (one integer for each of the 226 batches of eggs to be released). The files were run at maximum diffusion amplitudes at increments of 0.1 $cm.s^{-1}$, from 0.0 to 1.0 $cm.s^{-1}$. Similarly, the five files were run at the specified lapse rates between 6 and 144 hours, for a turbulence amplitude of 30 $cm.s^{-1}$. Two-factor ANOVA tests (Model I) without replication were performed to test whether seed integer allocation significantly affected year-class strength and advection. In the process, maximum diffusion amplitude was tested for significant effects on year-class strength and total number of anchovy lost to advection (referred to as total advective losses).

2.3.2 RESULTS OF SENSITIVITY TESTS

From here onward statistical terms are abbreviated as follows:

SS: Sum of squares

df: degrees of freedom

MS: Mean square

$F_{calculated}$: Calculated F-statistic

p-value: Probability value

$F_{critical}$: critical F-statistic for the 5% level of significance

TURBULENCE

Tabulated below are results of the two-factor ANOVA test without replication, performed on year-class strength and total advective losses at turbulence amplitudes and lapse periods specified in section 2.3.1. Both lapse period and maximum turbulence amplitude showed significant effects on year-class strength (Table 2.2) and total advective losses (Table 2.3). The effect of lapse period on year-class strength ($p=3.11x10^{-6}$) was more significant than on advective losses ($p=0.036$).

Table 2.2 **Summary of results of two-factor ANOVA without replication, performed on year-class strength (numbersX10^9) obtained under different maximum turbulence amplitudes (cm.s^{-1}) and lapse periods (h).**

SOURCE OF VARIATION	SS	df	MS	F calculated	p-VALUE	F critical
LAPSE PERIOD (h)	0.007874	10	0.000787	6.381641	$3.11x10^{-6}$	2.026141
MAXIMUM TURBULENCE AMPLITUDE (cm.s^{-1})	0.001936	5	0.000387	3.138241	0.015341	2.400412
ERROR	0.006169	50	0.000123			
TOTAL	0.015979	65				

Table 2.3 **Summary of results of two-factor ANOVA without replication, performed on total advective losses (numbersX10^{12}) obtained under different maximum turbulence amplitudes (cm.s^{-1}) and lapse periods (h).**

SOURCE OF VARIATION	SS	df	MS	F calculated	p-VALUE	F critical
LAPSE PERIOD (h)	0.015667	10	0.001567	2.166604	0.035809	2.026141
MAXIMUM TURBULENCE AMPLITUDE (cm.s^{-1})	0.012263	5	0.002453	3.39165	0.010257	2.400412
ERROR	0.036156	50	0.000723			
TOTAL	0.064086	65				

Tables 2.4 and 2.5 list means and coefficients of variation of year-class strength and advective losses, obtained using given turbulence amplitudes and lapse periods respectively. Variation is much greater between advective loss values than between year-class strength under the set of turbulence options investigated. As expected, advective losses and year-class strength showed greater variation between runs at shorter lapse periods and at higher levels of turbulence (also refer to Appendix C, Tables C.1 and C.2, in which percentage changes from baseline are tabulated).

Table 2.4 **Means and coefficients of variation (CVX100%) of year-class strength (numbersX10^9) and advective losses (numbersX10^{12}) of the 11 specified lapse rate runs when 6 turbulence amplitudes (cm.s^{-1}) were tested.**

	YEAR-CLASS STRENGTH (NUMBERSX10^9)		ADVECTIVE LOSSES (NUMBERSX10^{12})	
MAXIMUM TURBULENCE AMPLITUDE (cm.s^{-1})	MEAN	CV (%)	MEAN	CV (%)
5	3.180559	1.19X10^{-6}	1.159039	0.211205
10	3.183366	0.196188	1.156182	0.580192
15	3.180559	0.307015	1.158439	1.543898
20	3.179155	0.403676	1.161817	1.821321
25	3.172137	0.700741	1.182229	3.619023
30	3.167926	0.780352	1.191729	4.223292

Table 2.5 **Means and coefficients of variation (CVX100%) of year-class strength (numbersX10^9) and advective losses (numbersX10^{12}) of the 6 tested maximum turbulence amplitude runs when 11 specified lapse periods were tested.**

	YEAR-CLASS STRENGTH (NUMBERSX10^9)		ADVECTIVE LOSSES (NUMBERSX10^{12})	
LAPSE PERIOD (h)	MEAN	CV (%)	MEAN	CV (%)
6	3.154826	0.911214	1.194422	6.196708
12	3.167693	0.569806	1.184454	4.263134
24	3.170266	0.251499	1.187967	2.081741
36	3.180559	0	1.158144	0.148064
48	3.193425	0.197373	1.146768	0.448752
60	3.167692	0.479229	1.179006	2.432158
72	3.180559	0	1.164337	0.105376
84	3.180559	0	1.167828	0.83425
96	3.193425	0.197373	1.147577	0.464712
120	3.180559	0.307015	1.156999	0.70698
144	3.180559	0	1.163132	0.077839

IMPORTANCE OF SEED INTEGER ALLOCATION

A maximum turbulence amplitude of 30 cm.s^{-1} at the specified lapse periods was tested for significant effects on year-class strength and advective losses when the five files containing different starting seeds were run. As found in the section on turbulence above, Tables 2.6 and 2.7 again show that lapse periods significantly affect both year-class strength and advective loss totals. Seed integer files gave significantly different year-class strength and advective losses at specified lapse rates.

Table 2.6 **Summary of results of two-factor ANOVA without replication, performed on year-class strength (numbersX10^9) obtained under 30 cm.s^{-1} maximum turbulence amplitudes, specified lapse periods (h) and using five different seed files.**

SOURCE OF VARIATION	SS	df	MS	F calculated	p-VALUE	F critical
LAPSE PERIOD (h)	0.008894	10	0.000889	2.756271	0.011028	2.07725
SEED FILE	0.006259	4	0.001565	4.849006	0.002773	2.605972
ERROR	0.012907	40	0.000323			
TOTAL	0.02806	54				

Table 2.7 **Summary of results of two-factor ANOVA without replication, performed on total advective losses (numbersX10^{12}) obtained under 30 cm.s^{-1} maximum turbulence amplitudes, specified lapse periods (h) and using five different seed files.**

SOURCE OF VARIATION	SS	df	MS	F calculated	p-VALUE	F critical
LAPSE PERIOD (h)	0.046497	10	0.00465	2.953305	0.007145	2.07725
SEED FILE	0.03364	4	0.00841	5.341814	0.001526	2.605972
ERROR	0.062976	40	0.001574			
TOTAL	0.143113	54				

Unlike the turbulence case, year-class strength was exactly the same for all tested values of smaller scale diffusion used to run the five seed files. Diffusion was tested for significant effects on advective losses when the five seed files were run. Two-factor ANOVA without replication also showed that different levels of maximum diffusion amplitude of random components did not alter total advective loss values significantly ($p=0.997$) (Table 2.8). However, large diffusion amplitudes resulted in greater deviations of advective losses from those when no diffusion was modelled (Appendix C.3). Significant differences in advective losses occurred between the five files containing different random sequences of seed integers (Table 2.8).

Table 2.8 **Summary of results of two-factor ANOVA without replication, performed on total advective losses (numbersX10^{12}) obtained under different maximum diffusion amplitudes (cm.s^{-1}) using five different seed files.**

SOURCE OF VARIATION	SS	df	MS	F calculated	p-VALUE	F critical
DIFFUSION AMPLITUDE (cm.s^{-1})	5.03X10^{-6}	10	5.03X10^{-7}	0.176546	0.997078	2.07725
SEED FILE	0.000355	4	8.88X10^{-5}	31.16497	8.27X10^{-12}	2.605972
ERROR	0.000114	40	2.85X10^{-6}			
TOTAL	0.000474	54				

2.3.3 CONCLUSIONS DRAWN FROM SENSITIVITY TESTS

The model described in this chapter was tested for sensitivity to two physical components, namely turbulence and diffusion, about which the operator is required to make decisions prior to running the model. It was found that the model is sensitive to the choice of large scale turbulence amplitudes and lapse periods, as two-factor ANOVA without replication yielded significant results (Tables 2.2, 2.3, 2.6 and 2.7).

In contrast to turbulence, the smaller scale diffusion component, altering velocity vector components by between 0.0 and 1.0 cm.s^{-1}, was found not to affect year-class strength and total advective losses significantly (Table 2.8). It is viewed as functioning merely to add more realism in terms of dispersion of anchovy batches in space, and may become important in regions where current shear is high, for example near Cape Columbine (G. Nelson, Sea Fisheries Research Institute, pers. comm.).

Allocation of seed integers to records in the release file seems to be important. Seed integers are used to initiate the generation of repeatable sequences of random numbers for the addition of turbulence and diffusion components to the path traversed by each batch of anchovy.

Tables 2.6, 2.7 and 2.8 show that year-class strength and overall advective losses are sensitive to the sequence of chosen seed integers. This implies that survival of anchovy is sensitive to the path traversed through a turbulent flow field. The greatest variation in survival and advective losses occurred at smaller lapse periods and higher turbulence amplitudes (Tables 2.4 and 2.5). Reasons for this are as follows: firstly, new random components are generated more frequently at shorter lapse periods, resulting in a greater probability that both high and low amplitude random components will be added during the transport period, and secondly, since the distribution from which random selection of additional components takes place is rectangular, components are chosen from a wider spectrum when larger maximum turbulence amplitudes are specified.

Therefore when attempting to identify effects of different spawner distributions on anchovy transport, and if the turbulence and diffusion options in the model are selected, repeated simulation would be recommended. Release files having different sequences of seed integers allocated to otherwise identical records should then be used to obtain mean estimates of year-class strength and advective losses.

CHAPTER THREE

MODIFYING THE FLOW FIELD ABOVE THE THERMOCLINE

IN AN ATTEMPT TO IMPROVE SIMULATION

OF ANCHOVY TRANSPORT

CHAPTER THREE

MODELLING THE FLOW FIELD ABOVE THE THERMOCLINE IN AN ATTEMPT TO IMPROVE SIMULATION OF ANCHOVY TRANSPORT

3.1 THE MODEL APPLIED TO ALTERED ADVECTION

The model described in Chapter Two (sections 2.1 and 2.2) was used to investigate implications of altered advection for anchovy year-class strength, advective losses and the spatial distributions of the two. Various advection scenarios were modelled, each scenario being applied to the seven spawner distributions of anchovy recorded from 1986 to 1992 on acoustic surveys conducted between October and December (Hampton 1992). Daily egg production was calculated for each block for each day of the spawning season (i.e. 1 October to 31 March) using equation 2.1 (Chapter Two, section 2.2.1). Numbers of eggs and larvae were reduced by published mortality rates (Valdés-Szeinfeld *et al.* 1987, Brownell 1983, Table 3.1). Numbers of prerecruits were reduced by a daily mortality rate of 3.1% in the first approach to altered advection, and 4.5% in the second approach. The first rate resulted from crude tuning of the model to mean year-class strength calculated from May recruitment surveys (records of Sea Fisheries Research Institute). The second rate resulted from more precise tuning of the model, and was chosen to improve the match of mean strength of year classes produced by the model to the average year-class strength calculated from November spawner biomass surveys (Hampton 1992). This involved back-calculation of anchovy numbers by accounting for mortality which occurred in the period between recruitment and

subsequent spawning. The second rate of 4.5% was preferred since both egg production in the model and year-class strength to which the model was tuned were then based on November surveys only. This served to reduce additional uncertainty of a second set of surveys, which would have been introduced had year-class strength been tuned to the mean measured during May recruitment surveys.

Table 3.1 **Mortality rates used to investigate the effects of altered advection on survival and distribution of young-of-the-year anchovy**

STAGE OF DEVELOP-MENT	MORTALITY RATE	AVERAGE HOURLY SURVIVAL RATE (USED IN MODEL)	SOURCE OF MORTALITY RATE
egg	average instantaneous mortality rate of 0.01/hour	0.9900	Valdés *et al.* (1987)
larva	average mortality rate of 0.061/day	0.9974	Brownell (1983)
pre-recruit	average mortality rate of 1) 0.031/day and 2) 0.045/day	 1) 0.9987 (FIRST APPROACH) 2) 0.9981 (SECOND APPROACH: re-adjusted to give better estimates of year-class strength)	
post-recruit and adult	instantaneous mortality rate of 1.33/year instantaneous mortality rate of 0.0021/day (*E. mordax*)	 0.9999	Valdés-Szeinfeld and Cochrane (1992) Butler *et al.* 1993

Year-class strength was computed as the sum of all anchovy surviving to the age of 180 days and remaining within the flow field boundaries or collecting in coastal areas. Anchovy crossing the southern (36°45'S), northern (29°00'S), western (15°00'E) or eastern (28°E)

boundaries or entering blocks within these boundaries that lacked current data were summed as advective losses. Blocks lacking current data are those in offshore areas where survey cruises have not measured currents. Such blocks are presumed to be areas of loss since survey lines are extended offshore until no anchovy or anchovy eggs are found. Advective losses were apportioned to the five strata depicted in Figure 2.4 (Chapter Two).

3.2 RATIONALE

A preliminary study, in which altered advection was initially considered by adding proportional components to all east velocity components, and which is expanded upon in Chapter Six, showed little variation in year-class strength under different advection scenarios. This was contrary to what was expected, based on the importance previously attached to transport processes in the Benguela system (Crawford 1980, Shelton and Hutchings 1982, Boyd et al. 1992 and Hutchings and Boyd 1992). Therefore, before attempting to simulate the effects of altered advection by the simple addition of equal components to all northerly velocity components across the grid, and by adding larger components to all easterly velocity components, it was necessary to modify the basic averaged ADCP flow field at 30 m and 50 m, in order to obtain more realism in terms of distribution of young of the year and sites of advective losses. Since the model was based on ADCP data from depths above the thermocline but below 25 m (Chapter One, section 1.4), the influence of winds on surface currents was not incorporated. Bearing in mind that these data were collected mainly during El-Niño years, and that spawner data used extended prior to and after this period, when more intense south easterly winds were experienced, the flow field was modified by enhancing

westward and northward advection by different amounts over a) the entire area, b) only west of 20°E and c) just between Cape Columbine (33°S) and Cape Agulhas (20°E). Modifications and selection of an improved flow field were purely experimental and subjective, but based on knowledge acquired from surveys at sea and the research cited in this thesis.

The anchovy spawning distribution of November 1991 extended from Cape Town to Cape St Francis (Chapter One, Figure 1.1), fish being encountered between the coast and the shelf edge. For this reason, and because recruitment in 1992 was above expected (i.e. abnormally heavy advective losses were unlikely to have occurred), the 1991 spatial distribution of spawners was used to "tune" the advection flow field. This was done in order to achieve realistic spatial distributions of young of the year and advective losses. At the stage when this work was completed, prerecruit mortality rate had only been roughly "tuned" and was set to a 3.1% daily mortality rate (corresponding to an hourly survival rate of 0.9987 - Table 3.1), which yielded year-class strengths similar to the mean measured during May recruitment surveys (records of Sea Fisheries Research Institute).

Initially diffusion and turbulence were not incorporated i.e. the flow field was based on ADCP averages alone and all batches released in a particular block followed the same track each day of the spawning season. Then random components of i) diffusion, with maximum amplitudes of 0.9 $cm.s^{-1}$ and ii) turbulence, with maximum amplitudes of 10 $cm.s^{-1}$ were added.

Various advection options were tested before selection of a "new" baseline flow field. Some of these in turn became scenarios relative to that new field (investigated in Chapter Five). For example the original flow field became a case of reduced westward flow.

Once what was thought to be a reasonable attempt at a baseline flow field was found, the seven spawner distributions were run using this particular version of the model, in order to compare year-class strength and advective losses resulting from different distributions of spawning anchovy. To allow for comparison of year-class strengths occurring from different spawner distributions (i.e. in different years), random turbulence and diffusion components were excluded from these runs.

3.3 IN SEARCH OF A MORE REALISTIC BASELINE FLOW FIELD

The number of anchovy surviving to 180 days (recruits) and the number of anchovy crossing one of the offshore "loss" boundaries at some stage during the six month period are tabulated in Table 3.2 (1991 spawning distribution was used). Below is a key to the sixteen different advection scenarios tested during the quest for a more realistic baseline flow field.

Key to advection scenarios:

0 unaltered flow field

1 all westerly components enhanced by 5 $cm.s^{-1}$

2 only westerly components west of 20°E (Cape Agulhas) enhanced by 5 $cm.s^{-1}$

3 westerly components west of 20°E (Cape Agulhas) enhanced by 5 $cm.s^{-1}$ and northerly components west of 20°E (Cape Agulhas) enhanced by 2 $cm.s^{-1}$

4 westerly components west of 20°E (Cape Agulhas) enhanced by 10 $cm.s^{-1}$ and northerly components west of 20°E (Cape Agulhas) enhanced by 4 $cm.s^{-1}$

5 westerly components between Cape Columbine (33°S) and Cape Agulhas (20°E) enhanced by 5 $cm.s^{-1}$, northerly components between Cape Columbine (33°S) and Cape Agulhas (20°E) enhanced by 2 $cm.s^{-1}$, and elsewhere westerly components enhanced by 2 $cm.s^{-1}$ and northerly components unaltered

6 westerly components between Cape Columbine (33°S) and Cape Agulhas (20°E) enhanced by 10 $cm.s^{-1}$, northerly components between Cape Columbine (33°S) and Cape Agulhas (20°E) enhanced by 4 $cm.s^{-1}$, and elsewhere westerly components enhanced by 4 $cm.s^{-1}$ and northerly components unaltered

7 westerly components between Cape Columbine (33°S) and Cape Agulhas (20°E) enhanced by 10 $cm.s^{-1}$, elsewhere westerly components enhanced by 4 $cm.s^{-1}$, northerly components unaltered everywhere

Table 3.2 **Numbers of young of the year and advective losses obtained by simulation when altered advection scenarios were modelled (see key on previous page).**

A "t" following a scenario number indicates that the scenario was modelled with a maximum turbulence amplitude of 10 $cm.s^{-1}$, a lapse time of 72 hours and a maximum diffusion amplitude of 0.9 $cm.s^{-1}$. A "T" indicates that the scenario was modelled with a maximum turbulence amplitude of 30 $cm.s^{-1}$, a lapse time of 72 hours and a maximum diffusion amplitude of 0.9 $cm.s^{-1}$.

ADVECTION SCENARIO	NUMBER OF ANCHOVY SURVIVING TO 180 DAYS (NOS. X 10^9); % SURVIVING IN PARENTHESES	% OF YOUNG OF THE YEAR ACCUMULATING OFFSHORE BUT WITHIN GRID BOUNDARIES (AS APPOSED TO COASTAL ZONES)	NUMBER OF ANCHOVY LOST THROUGH ADVECTION ACROSS A BOUNDARY (NOS. X 10^{12})	NUMBER OF BATCHES LOST BY ADVECTION AVERAGE TIME OF LOSS IN PARENTHESES (HOURS AFTER SPAWNING)	% BATCHES LOST
0	440.63 (0.0090)	71.0	179.53	549 (405)	3.1
0t	439.80 (0.0090)	66.1	180.86	517 (350)	2.9
0T	438.32 (0.0090)	62.4	183.75	578 (351)	3.2
1	132.04 (0.0027)	74.5	134.56	12078 (2020)	67.3
1t	122.69 (0.0025)	70.5	116.91	12013 (2049)	67.0
2	175.85 (0.0036)	79.0	267.95	7686 (1570)	42.9
2t	176.67 (0.0036)	73.0	269.59	7498 (1550)	41.8
3	190.51 (0.0039)	73.2	242.98	6954 (1589)	38.6
3t	189.68 (0.0039)	67.4	246.36	6922 (1586)	38.6
4	190.16 (0.0039)	73.1	506.49	7137 (680)	39.8
4t	189.42 (0.0039)	67.2	508.50	7055 (671)	39.3
5	199.84 (0.0041)	71.0	228.80	6222 (1535)	34.7
5t	199.82 (0.0041)	70.7	230.57	6223 (1529)	34.7
6	241.33 (0.0050)	78.0	322.73	6039 (680)	33.7
6t	236.06 (0.0048)	69.6	323.41	6204 (787)	34.6
7	227.02 (0.0047)	82.9	624.57	6588 (409)	36.7
7t	221.66 (0.0045)	80.6	626.00	6803 (519)	37.9

Figure 3.1 (and Appendix B, Table B.1) shows the number of young of the year accumulating in each of the four strata (strata 2 to 5 in Chapter Two, Figure 2.4) under each of the seventeen scenarios. Numbers of anchovy lost by unfavourable advective processes from each of the five strata (strata 1 to 5 in Chapter Two, Figure 2.4) are presented in Figure 3.2 and Appendix B, Table B.2. Note that stratum 5 is omitted from Figure 3.2 since no advective losses occurred here when any of the seventeen advection scenarios were modelled.

For purposes of the remaining discussion in this thesis, the area between Cape Agulhas and Mossel Bay (stratum 4) is defined as the Central Agulhas Bank (CAB), and the stretch to the east of Mossel Bay (stratum 5) is referred to as the Eastern Agulhas Bank (EAB). Stratum 3 is subdivided into the west coast, between Cape Columbine and Cape Point (Chapter One, Figure 1.1), and the Western Agulhas Bank (WAB), extending from Cape Point to Cape Agulhas.

The spawning distribution of November 1991 (records of Sea Fisheries Research Institute) covered a broad area (Figure 3.3) and led to fairly good recruitment in 1992. For these reasons, it was used as a "typical" distribution on which to explore modified flow fields, in order to obtain a realistic baseline flow field. Results under the original flow field based on ADCP averages between September and March were found to be reasonable with respect to distribution of young-of-the-year anchovy (after 180 days), in that abundance increased westwards. The large proportion of young-of-the-year anchovy accumulating inshore between Cape Columbine and Cape Agulhas (30.5% of the year-class when turbulence was included, scenario 0t, Appendix B, Table B.1), possibly mainly in False Bay, was viewed as unrealistic. It is likely that fish found in False Bay in 1991 remained in the bay when modelled and

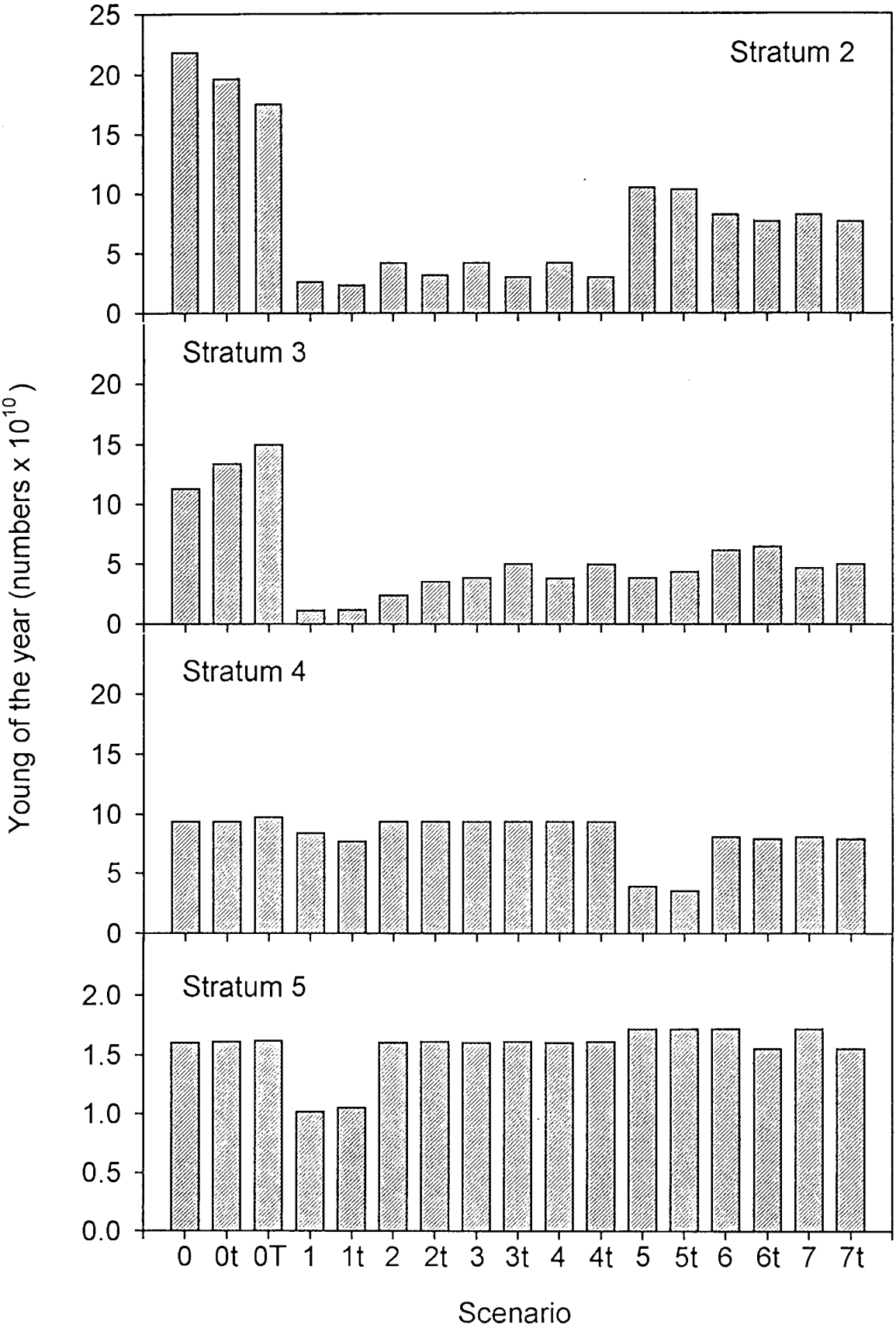

Figure 3.1 Numbers of young of the year accumulating in strata 2 to 5 respectively for each of the advection scenarios modelled (the y-axis scale in stratum 2 differs from the rest)

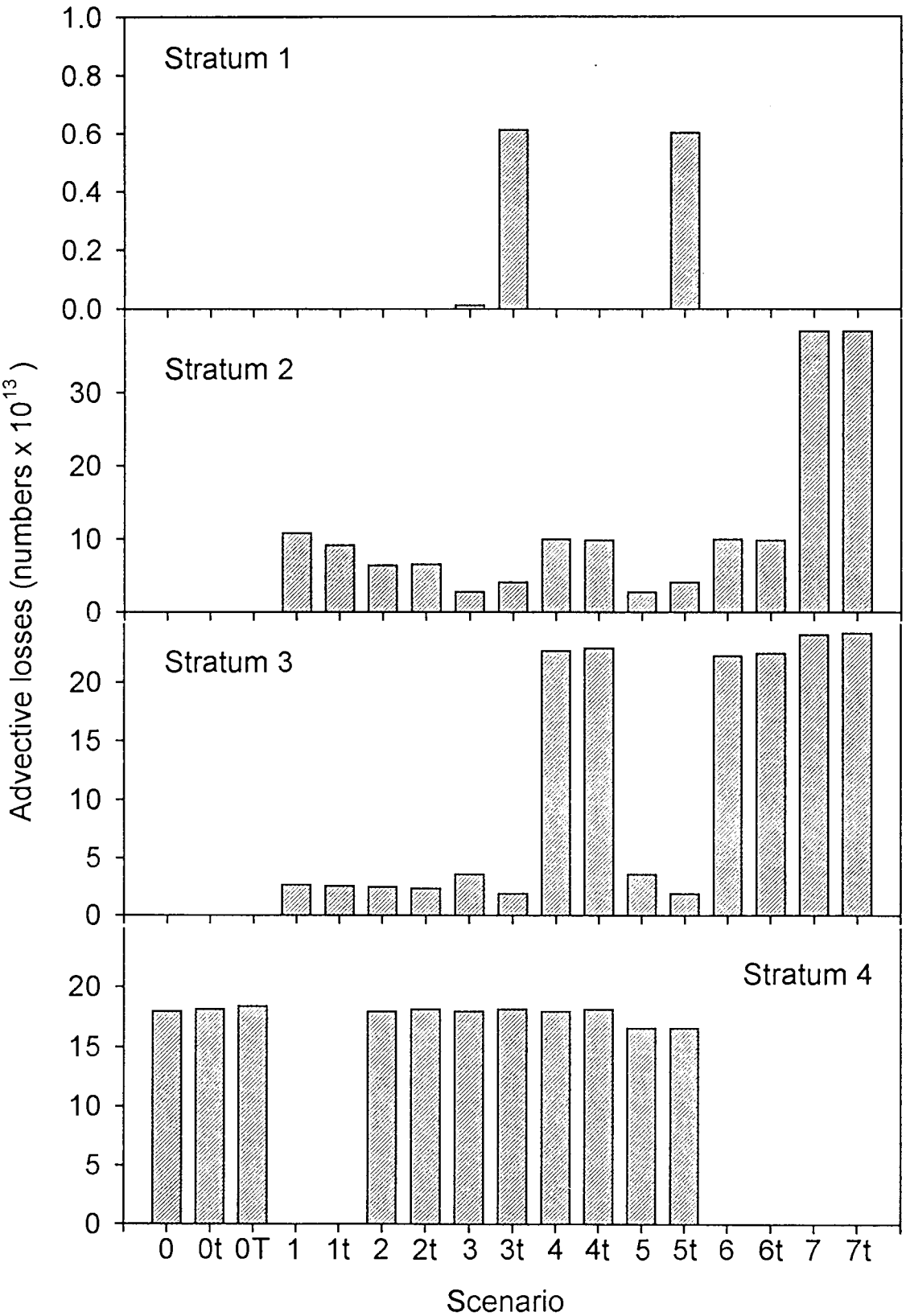

Figure 3.2 Numbers of anchovy lost by advection from strata 1 to 4 respectively for each of the advection scenarios modelled (no advective losses occurred from strata 5 when any of the advection scenarios were modelled) (y-axis scales differ between strata)

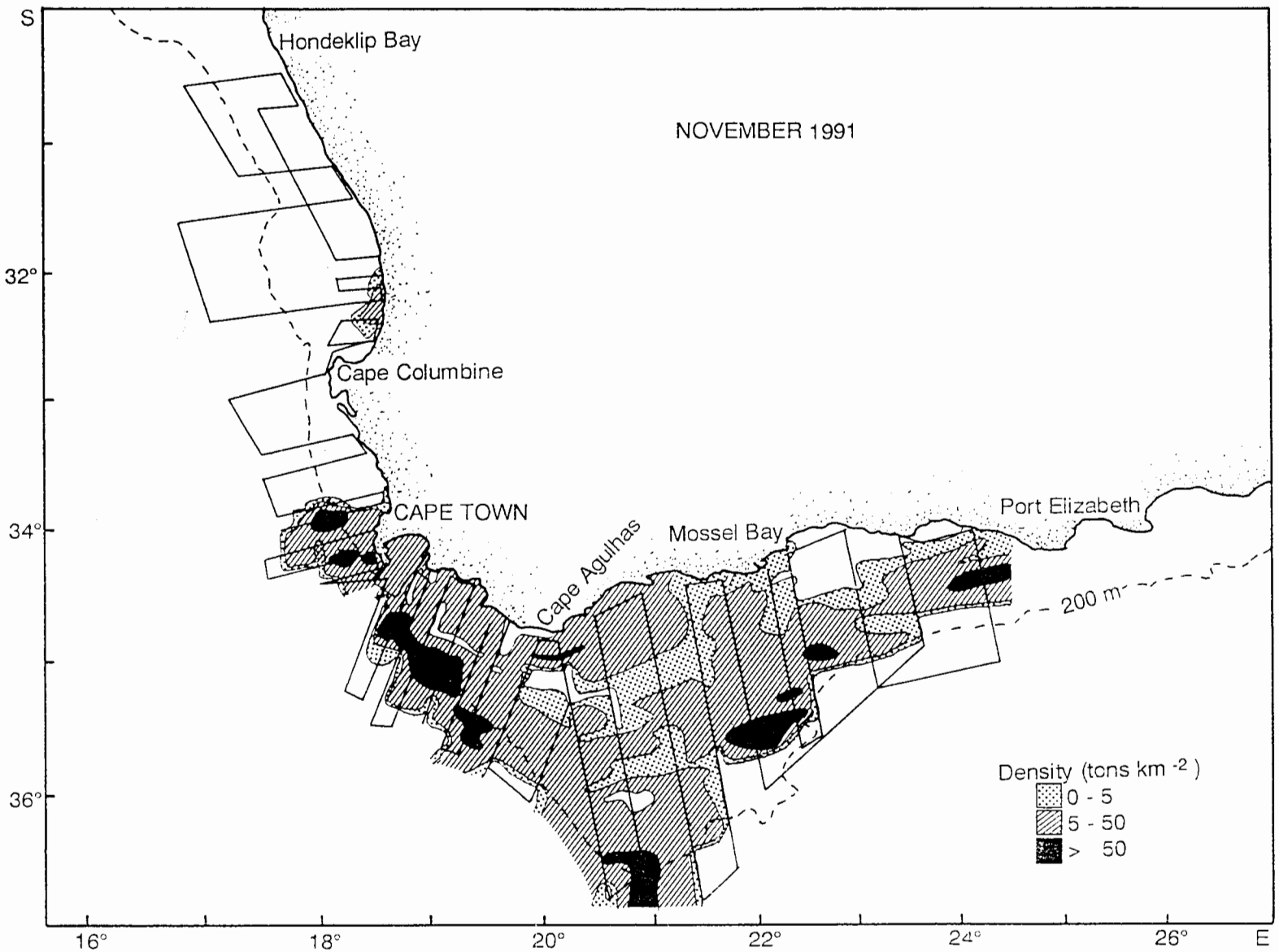

Figure 3.3 **Distribution of spawners in November 1991 (this was the distribution used for testing the different advection scenarios)**

comprised a maximum of 10%. The flow field was also viewed as unreasonable in that all advective losses occurring were restricted to the area between Cape Agulhas and Mossel Bay (stratum 4, Figure 3.2 and Appendix B, Table B.2), i.e. none occurred west of Cape Agulhas. Even though the Western Agulhas Bank region may well retain many of the batches, satellite imagery (e.g. Shannon *et al.* 1985) and egg distribution maps (Boyd *et al.* 1992) suggest advective losses offshore, often into food-poor areas beyond the shelf-edge jet current.

A first attempt at modification of the flow field was the simple addition of 5 $cm.s^{-1}$ westward advection over the entire grid (scenario 1), which gave rise to advective losses from strata 2 and 3 (Figure 3.2) but completely eliminated those east of Cape Agulhas (from strata 4), with the result that 64% of the model recruitment occurred on the Central Agulhas Bank (scenario 1, Figure 3.1 and Appendix B, Table B.1). Recruitment on the CAB remained mainly offshore whereas all recruitment to the east (in stratum 4) was close inshore. Some experimentation in terms of "more complex" modifications to the flow field was necessary. It was decided that only the spatial criteria (percentages rather than numbers) would be considered initially.

The next scenario added 5 $cm.s^{-1}$ to westward advection in the area west of Cape Agulhas only (scenario 2). Losses occurred in strata from 29°S to Mossel Bay, but the main effect of this run was substantially enhanced recruitment compared to the previous run (Table 3.2). Neither of these first two scenarios saw any anchovy transported from the WAB (part of stratum 3) to the CAB (stratum 4). However, the total number of young of the year accumulating east of Cape Agulhas appeared very stable in cases of enhanced westward advection, suggesting that westward transport is not dominant. The main problem with the scenario 2 was that recruitment between 29°S and Cape Columbine (stratum 2) remained too

low, at 17.9% of the year-class when turbulence was incorporated (scenario 2t in Figure 3.1 and Appendix B, Table B.1).

After further exploratory modelling was done, it was decided that in terms of distribution of both young of the year and advective losses, the most realistic modification of the seventeen resulted when westerly components between Cape Columbine (33°S) and Cape Agulhas (20°E) were enhanced by 5 cm.s^{-1}, northerly components between Cape Columbine (33°S) and Cape Agulhas (20°E) were enhanced by 2 cm.s^{-1}, and elsewhere westerly components were enhanced by 2 cm.s^{-1} and northerly components remained unaltered (scenario 5). The distinction between stratum 3 and the other strata was made initially because south easterly winds could be expected to intensify most between Cape Columbine and Cape Agulhas. This flow field gave satisfactory results. The majority of young of the year then accumulated north of Cape Columbine (52.5% in stratum 2), and year-class strength decreased to 19.2% in stratum 3, 19.7% in stratum 4 and 8.6% in stratum 5 in the east (scenario 5, Figure 3.1 and Appendix B, Table B.1). Most recruitment occurred offshore (i.e. away from the land-ocean boundary) apart from a fair number inshore in stratum 3, where accumulation of young-of-the-year anchovy in bays still prevailed, partly due to fish already present in False Bay in 1991 (Figure 3.3), and recruitment off the eastern Cape, where most young of the year either entered bays or had already moved westward before recruitment.

The spatial distribution of advective losses was also generally acceptable, with losses decreasing markedly from the CAB westwards. Some batches even crossed the northern boundary into stratum 1 when turbulence was incorporated (scenario 5t, Figure 3.2). Most losses on the CAB occurred relatively soon after spawning when compared with those

occurring in the west. Therefore losses in the west were of fish already about half way through their transport time and thus with reduced anticipated mortality ahead of them due to factors other than advection.

Other scenarios were also investigated (Figures 3.1 and 3.2) but were believed to detract from the scenario described above. Such runs could be viewed as potential scenarios of altered advection relative to this new "tuned" flow field, which was the one used to compare recruitment distributions resulting from the seven different spawner distributions. It is important to note the "tuning" process was based primarily on proportions not numbers. In so doing, the fit of model recruit numbers to numbers estimated from acoustic surveys was unintentionally improved through choice of the new baseline scenario, without adjusting the value of prerecruit mortality rate itself.

Relative to scenario 5, altered advection scenarios resulted in a decrease in year-class strength by a factor of as much as 1.6 (scenario 1t) and a maximum increase by a factor of 2.2 (scenario 0, Table 3.2). Advective losses decreased and increased by factors of as much as 2.0 (scenario 1t) and 2.7 (scenario 7t) respectively (Table 3.2). It is interesting that when scenario 1 was modelled, despite a substantial reduction in year-class strength compared to the unchanged flow field (scenario 0), losses due to advection were in fact less. Although in scenario 1 the number of batches that were lost due to advection was high, generally losses occurred late in the season (on average 84 days after spawning) and therefore anchovy were subject to mortality by causes other than advection for longer periods of time. Conversely, the large number of batches lost early in the season under scenarios 4 and 7, for example, contributed to heavy advective losses.

A two-tailed paired t-test was done to test for significant differences between year-class strength with and without the turbulence-diffusion option of 10 $cm.s^{-1}$ maximum turbulence amplitude at a lapse period of 72 hours and with a maximum diffusion amplitude of 0.9 $cm.s^{-1}$. Similarly, a paired t-test on total advective losses was performed (Table 3.3).

Table 3.3 **Summary of results of two paired t-tests, performed on a) year-class strength and b) total advective losses.**

	a) YEAR-CLASS STRENGTH	b) TOTAL ADVECTIVE LOSSES
CALCULATED t-TEST STATISTIC	2.148066	0.277141
CRITICAL t-TEST STATISTIC	2.364623	2.364623
P VALUE	0.06881	0.789678
CONCLUSION	no significant difference at 5% level	no significant difference at 5% level

The findings presented in Chapter 2 (section 2.3) showed that year-class strength and advective losses were sensitive to turbulence when a wide range of turbulence amplitudes (between 0 and 30 $cm.s^{-1}$) were compared. However, incorporation of diffusion and fairly conservative turbulence components (maximum amplitude of 10 $cm.s^{-1}$ at a lapse rate of 72 hours) was shown not to significantly affect year-class strength and total advective losses obtained under the seventeen scenarios modelled here (Table 3.3). Despite this, slight differences were visible in some cases, for example between scenario 1 and scenario 1t (Table 3.2). Even when turbulence did not have much effect (see scenario 0, 0t and 0T), it still played a role in the final positions of young of the year. For example, the same flow field without turbulence or diffusion (scenario 0) and again with diffusion and a large turbulence amplitude (scenario 0T) resulted in nearly a 9% difference in inshore versus offshore

accumulation of young of the year (Appendix B, Table B.1). In this particular case the shift occurred through more recruitment inshore in stratum 3 and less offshore recruitment in stratum 2 when turbulence was high (scenarios 0 versus 0t, Table B.1). However, in most scenarios turbulence did not make a difference to total numbers of young of the year or losses (Figures 3.1 and 3.2, Table 3.3). One of the objectives of the first approach in this chapter was to examine the effects of distribution of spawning anchovy on recruitment. For this reason, and to facilitate comparison with reduced and enhanced altered advection scenarios, all model runs in Chapters Four and Five were undertaken without the addition of diffusion and turbulence. In this way variation due to causes other than spawner distribution was minimised. However, it is noted that for other purposes addition of these components imparts more realism to results and can have significant effects on totals (year-class strength and total advective losses- Chapter Two, section 2.3.2). Hence modelling in Chapter Six includes random components.

CHAPTER FOUR

IMPORTANCE OF SPAWNER DISTRIBUTION

FOR ANCHOVY SURVIVAL

CHAPTER FOUR

IMPORTANCE OF SPAWNER DISTRIBUTION FOR ANCHOVY SURVIVAL

4.1 HOW THE SPATIAL DISTRIBUTION OF SPAWNERS INFLUENCES RECRUITMENT

This chapter explores recruitment patterns and numbers resulting from a *fixed* spawner biomass (mean of the seven years spawner biomass) while still accounting for interannual variations due to different spatial distributions of spawners. The new baseline flow field (scenario 5) was modelled using seven different spawner distributions (1986-1992).

Model numbers of young-of-the-year anchovy accumulating in the four regions (as named in Chapter Two, Figure 2.4) varied from year to year and were dependent on spawner distribution (Figure 4.1 and Appendix B, Table B.3). Young of the year accumulating west of Cape Agulhas (strata 2 and 3) comprised between 56% (from 1992 spawners) and 90 % (from 1988 spawners) of overall model young of the year surviving to 180 days (Figure 4.2 and Appendix B, Table B.4). This agrees with what would be expected based on distribution of spawners (Figures 4.3 c and g). In November 1992, spawners were spread across the entire Agulhas Bank (Figure 4.3 g) and hence accumulation of model young occurred in all regions. Spawners in 1988 were confined to the WAB and west coast (Figure 4.3 c), and since currents are generally westward and northward in this region, there was little chance of model recruitment east of Cape Agulhas.

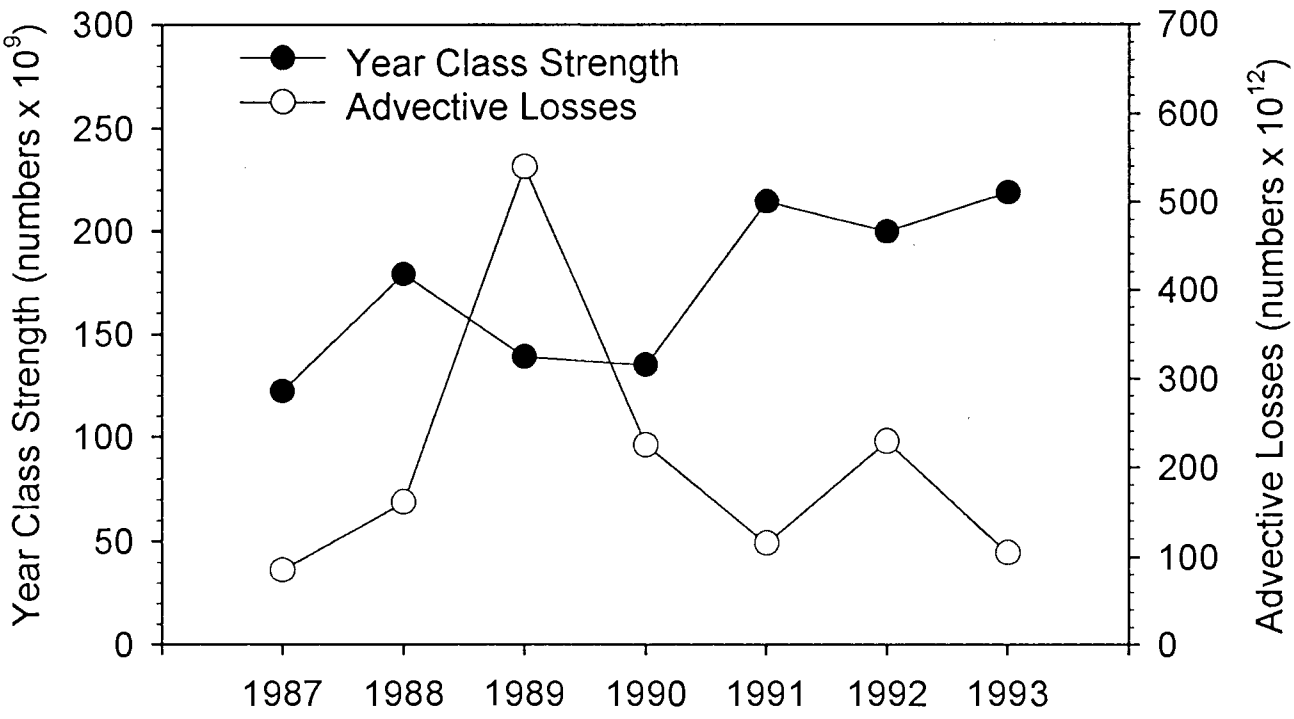

Figure 4.1 Year class strength and advective losses six months after spawning the previous summer (October to March) when scenario 5 (the improved baseline flowfield) was modelled

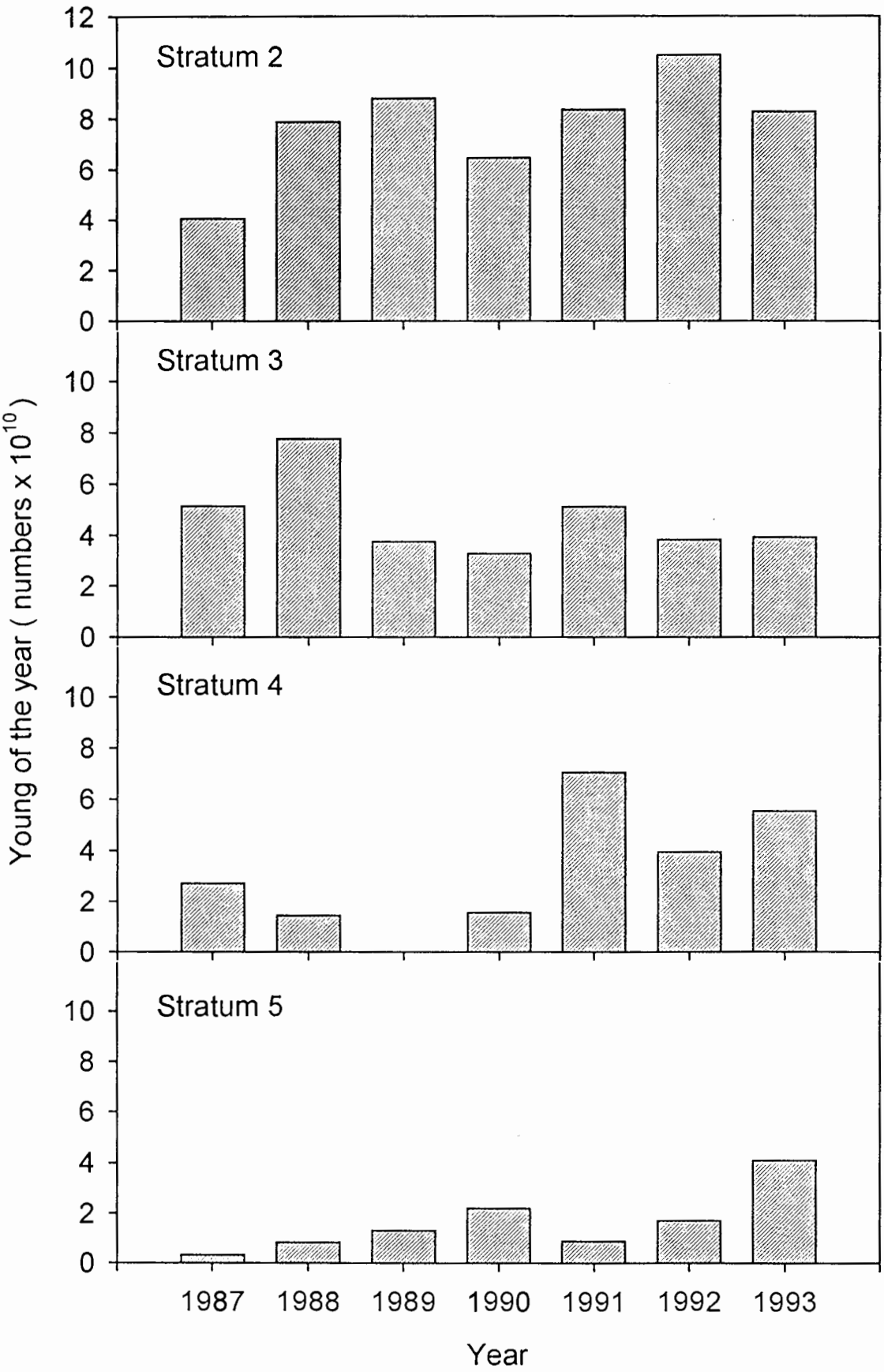

Figure 4.2 Numbers of young of the year accumulating each year in strata 2 to 5 respectively when scenario 5 (the improved baseline flowfield) was modelled (note that young of the year were spawned six months earlier, based on the spawner distribution of the previous year)
(the y-axis scale in stratum 2 differs from the rest)

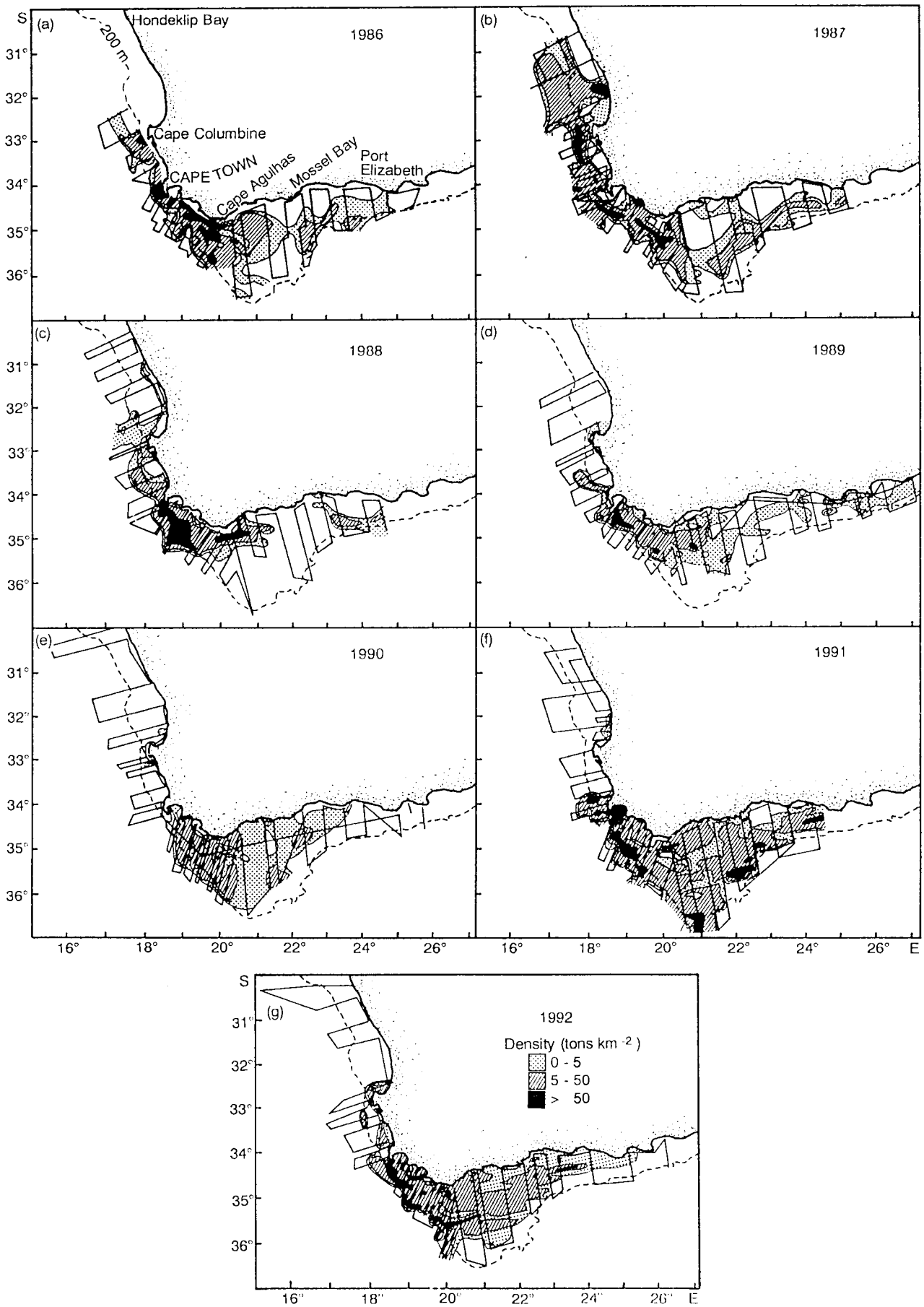

Figure 4.3 Distributions of anchovy in November of 1986 to 1993, from acoustic surveys (Hampton 1992 extended)

Model results showed that between 29°S and Cape Columbine, and on the CAB, young of the year were retained mostly offshore rather than very close inshore (strata 2 and 4 in Appendix B, Table B.4), whereas accumulation of young anchovy occurred predominantly inshore on the WAB and west coast as far north as 33°S (stratum 3). The latter agrees with acoustic observations; recruits are found in a narrow strip along the coast between Cape Columbine and Cape Town (Hampton 1992).

Relative proportions accumulating inshore versus offshore on the EAB showed interannual variation in the model (Appendix B, Table B.4). Total numbers of model young-of-the-year anchovy accumulating in different strata from year to year varied most on the CAB (stratum 4), where fewest young occurred in 1989 and most in 1991, corresponding to spawner distributions of 1988 and 1990 respectively (Figure 4.2). This is interesting as the 1991 winter survey on the west coast showed "normal" recruitment (from a low spawner biomass), yet subsequently 1991 recruitment was estimated as good, leading to the suggestion that many of these recruits may have come from the Agulhas Bank. It is important to note that the region east of Cape Agulhas is poorly covered during most recruitment surveys. In addition, the extent to which spawners on the CAB and EAB contribute to recruitment east of Cape Agulhas remains uncertain (Hampton 1992, Hutchings and Boyd 1992).

Model advective losses to the north (beyond 29°S, out of stratum 1) only occurred in 1988 and 1989, resulting from 1987 and 1988 spawners (Figure 4.4), as was expected for the two years in which spawners extended farthest up the west coast (Hampton 1992). Model losses between 29°S and Cape Columbine (stratum 2) were greatest in 1988 (Figure 4.4), since spawners were present in high densities in this region in November 1987 (Figure 4.3 b) and

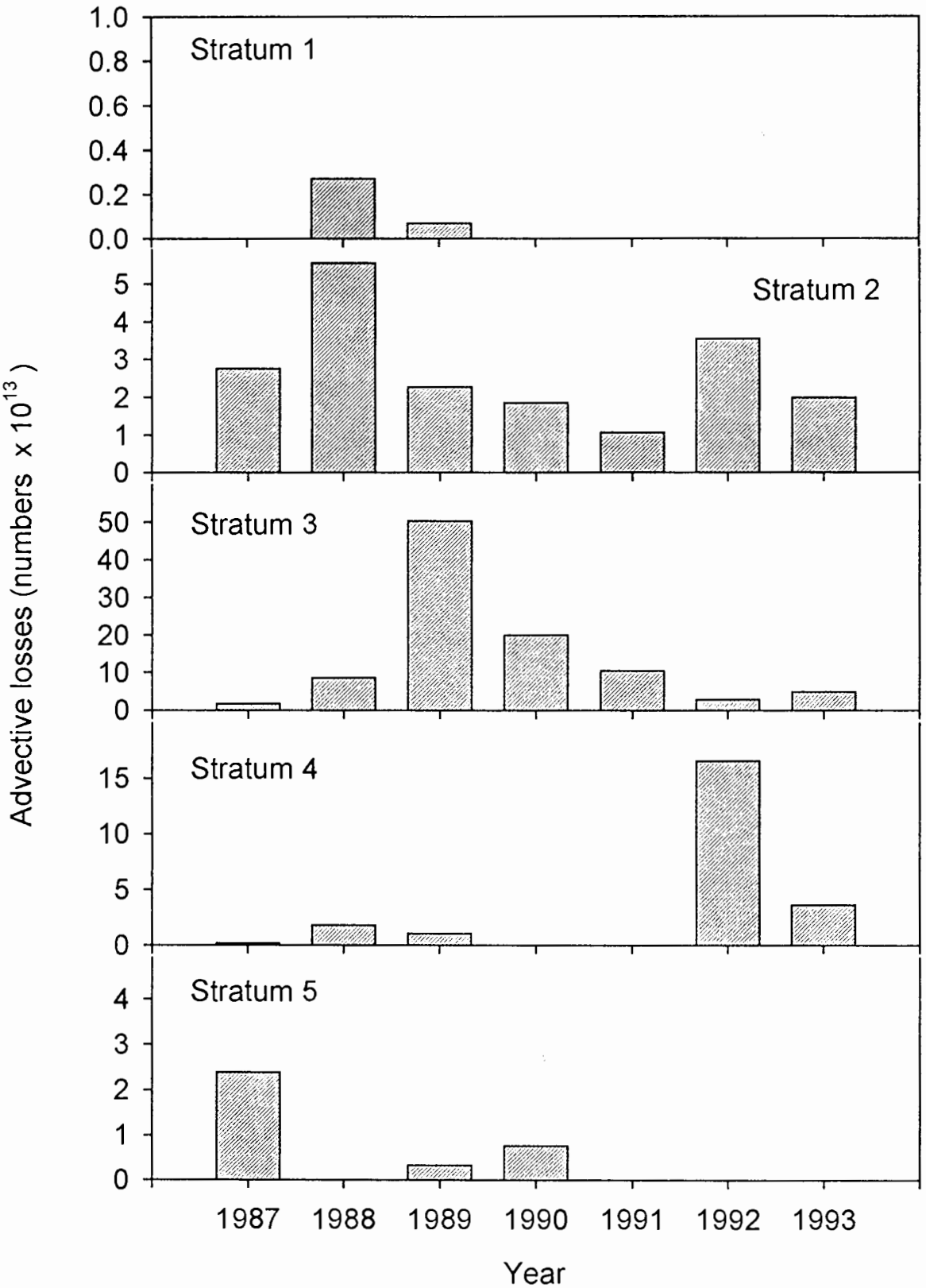

Figure 4.4 Numbers of anchovy lost by advection each year from strata 1 to 5 respectively when scenario 5 (the improved baseline flowfield) was modelled (note that young of the year were spawned six months earlier, based on the spawner distribution of the previous year)
(y-axis scales differ between strata)

were lowest in 1991, since few spawners were found here in November 1990 (Figure 4.3 e).

Model results showed that spawning in 1988 resulted in total advective losses that were at least double those experienced in other years (Figure 4.1 and Appendix B, Table B.3). Extra losses occurred between Cape Columbine and Cape Agulhas (ie. from stratum 3, Figure 4.4 and Appendix B, Table B.5), and resulted from the very high concentration of spawning anchovy on the outer edge of the WAB in 1988 (Figure 4.3 c). A possible reason for the abundance of spawners in this region was the occurrence of warm water closer inshore in 1988 than is usually observed. The resulting 1989 recruitment was low, although this was attributed to factors other than advection at that stage.

Anchovy spawning and transport modelled using spawning distributions of 1989 and 1990 resulted in no losses from the CAB (i.e. from stratum 4, Figure 4.4 and Appendix B, Table B.5), seemingly because spawning there during these years was confined inshore (Figure 4.3 d and e). The high density of spawners far offshore south of Mossel Bay in 1991 (Figure 4.3 g) explains the heavy model losses here by winter 1992 (stratum 4, Figure 4.4).

Strong offshore currents at the edge of the 200m isobath east of Mossel Bay (Boyd *et al.* 1992) were responsible for the model losses occurring when spawning was concentrated offshore in this region, such as in 1986, 1988 and 1989 (Figure 4.3 a, c and d). A quasi-permanent, cool subsurface ridge on the EAB, which has appeared frequently in results of November surveys and in satellite imagery (Swart and Largier 1987), was prominent in 1987, 1988 and 1989 and again in 1991, although only weakly (Boyd and Shillington 1994). The cool ridge served to restrict anchovy spawning to the outer edge of the EAB in these years.

How the ridge affects the life cycle of anchovy remains to be formally described. In other years spawning took place slightly farther inshore on the EAB, and model reproductive products seem to have been efficiently transported westward.

The greatly reduced model advective losses (by an order of magnitude) of eggs and larvae spawned in 1986, and the relatively light losses resulting from spawning in 1990 and 1992 (Figure 4.1 and Appendix B, Table B.3) may be explained by the abundance of spawners on the CAB and the absence of dense concentrations far offshore along the WAB and EAB, where losses are probable (Figure 4.3 a, e and g). It seems that the weak circulation on the CAB between September and March reduces offshore losses of reproductive products from this region and serves to enhance survival of anchovy to 180 days. Spawners were not present in vast numbers particularly far offshore in 1987 (Figure 4.3 b) and therefore model eggs and larvae were not subjected to unusually heavy offshore losses. However, model young of 1987 did not benefit to the same extent from the CAB "retention mechanism" as young of 1986, 1990 and 1992 (Figure 4.2 and Appendix B, Table B.3), since there was a noticeable absence of spawners from a large part of the CAB (Figure 4.3 b).

4.2 POSSIBLE ADDITIONAL FACTORS INFLUENCING RECRUITMENT

It can be concluded that in the model, distribution of spawning anchovy is very important in the ultimate distribution of young of the year surviving to six months. With regard to the number of surviving young-of-the-year anchovy, the model leads to at most a twofold difference due to advection alone in the different years (Figure 4.5). In contrast, acoustically-

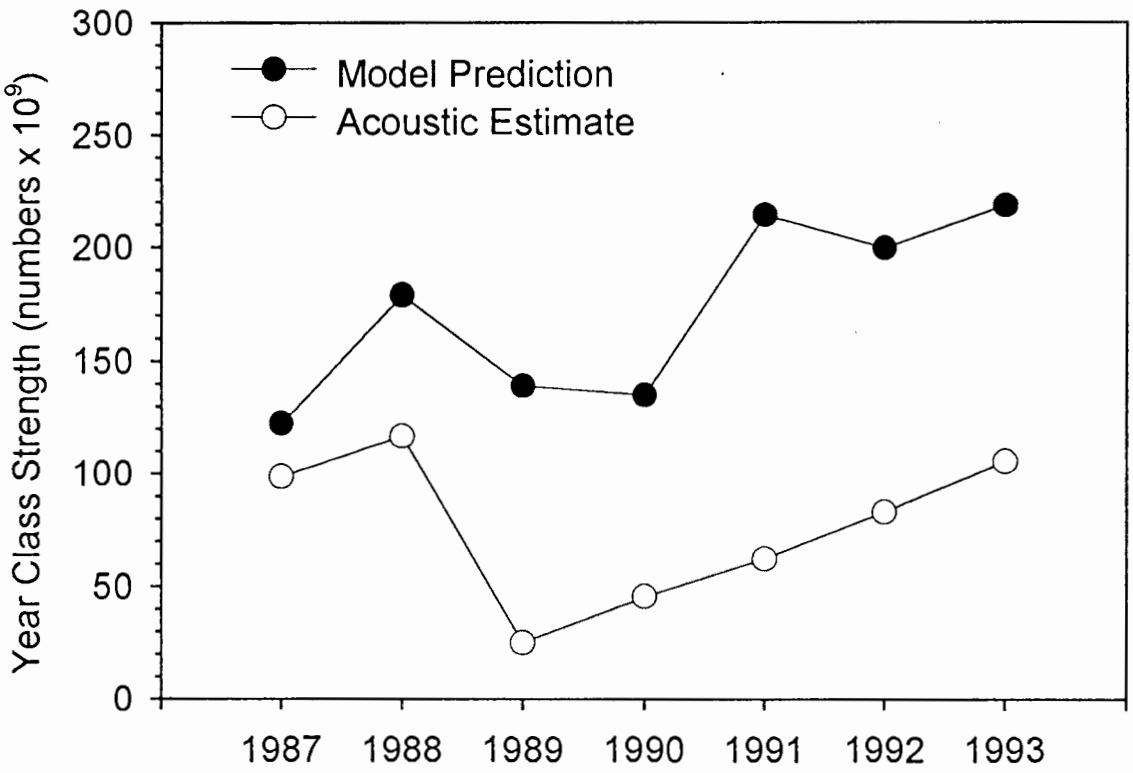

Figure 4.5 Comparison of acoustic estimate of year class strength in winter (May-June) with that when scenario 5 (the improved baseline flowfield) was modelled

derived estimates of year-class strengths vary almost five-fold, as shown in Figure 4.5 (Hampton 1992 and unpublished records of Sea Fisheries Research Institute). This order of interannual variability in numbers surviving suggests that in most years factors other than advective processes must also influence recruitment. However, the suppressed variation in model numbers would be explained in part by the fact that although relative spawner distributions were used, numbers of eggs spawned were always based on the mean spawner biomass of the seven years (refer to Chapter Two, section 2.2.1).

Anchovy are believed to take advantage of the north-flowing jet current and the coastal southward current between St Helena Bay and Cape Point (Nelson and Hutchings 1987). However, it is likely that passive transport is supplemented by active swimming. Active swimming by prerecruits eastwards out of the northward-flowing jet current into nursery areas is vital to the survival and success of anchovy off South Africa (Nelson and Hutchings 1987). Since large numbers of anchovy have been detected between Lambert's Bay and St Helena Bay during acoustic surveys (Hampton 1987), it is likely that active swimming by older juvenile anchovy plays an important role in concentrating recruits in this region.

In addition, although the model finds spawning on the CAB to be favoured by retention, this area may not necessarily be favourable for survival of anchovy in terms of other factors. The abundance and distribution of predators and prey of anchovy need to be considered relative to spawning position. In particular, the implications of cannibalism of eggs by spawning adults (Valdés *et al.* 1987, Valdés-Szeinfeld and Cochrane 1992) will vary with spawning distribution and abundance on the WAB, CAB and EAB.

CHAPTER FIVE

POTENTIAL EFFECTS OF

WEAKER AND STRONGER ADVECTION

CHAPTER FIVE

POTENTIAL EFFECTS OF WEAKER AND STRONGER ADVECTION

5.1 A FIRST APPROACH TO MODELLING THE EFFECTS OF ALTERED ADVECTION

Enhanced and reduced versions of the new baseline flow field were modelled without turbulence or diffusion, and results were compared to the unaltered (new baseline) flow field. Statistical testing was done using the analysis tools of Microsoft EXCEL. Two factor analysis of variance (Model I ANOVA) tests without replication were used to test the null hypothesis that year-class strengths in the seven years under the three advection scenarios were not significantly different from one another. Two factor ANOVA tests (Model I) with replication were run to test the null hypothesis that the three advection scenarios showed no significant difference in number of young of the year accumulating in the four geographic strata (strata 2 to 5, as named in Chapter Two, Figure 2.4). In a similar fashion, reduced, normal and enhanced flow scenarios were tested for significant differences between total advective losses from all strata and between advective losses occurring from the five strata (strata 1 to 5, as named in Figure 2.4).

Scenario 0 (the original unaltered flow field) was used as the reduced flow scenario relative to the new baseline flow field (scenario 5), in which the westerly components between Cape Columbine (33°S) and Cape Agulhas (20°E) were enhanced by 5 $cm.s^{-1}$, northerly components between Cape Columbine (33°S) and Cape Agulhas (20°E) were enhanced by 2 $cm.s^{-1}$, and

elsewhere westerly components were enhanced by 2 cm.s^{-1} and northerly components were unaltered. Scenario 6, in which the westerly components between Cape Columbine (33°S) and Cape Agulhas (20°E) were enhanced by 10 cm.s^{-1}, northerly components between Cape Columbine (33°S) and Cape Agulhas (20°E) were enhanced by 4 cm.s^{-1}, and elsewhere westerly components were enhanced by 4 cm.s^{-1} and northerly components were unaltered, served as the enhanced flow scenario.

5.2 MEAN YEAR-CLASS STRENGTH AND DISTRIBUTION OF YOUNG-OF-THE -YEAR ANCHOVY

When flow was reduced, model year-class strength was 2.7 times stronger than the new baseline flow case, but enhanced flow resulted in a mean year-class strength similar in magnitude to that of the unaltered case (Figure 5.1). The fact that the coefficient of variation of year-class strength for reduced flow was less than one quarter that of unaltered flow (Appendix B, Table B.6) means that reduced flow dramatically reduced interannual variability in year-class strength. The modelled percentage of young of the year accumulating away from the coast increased only slightly from reduced to enhanced flow, although interannual variability of this percentage under enhanced flow was almost double those under reduced and unaltered flow (Appendix B, Table B.6). The model showed that as advection increased from reduced to unaltered to enhanced flow, the percentages of young of the year accumulating north of Cape Columbine (i.e. in stratum 2) decreased (Figure 5.2). In all three advection scenarios, most model recruits were found offshore in this area, i.e. recruits were not restricted to bays (Appendix B, Table B.7).

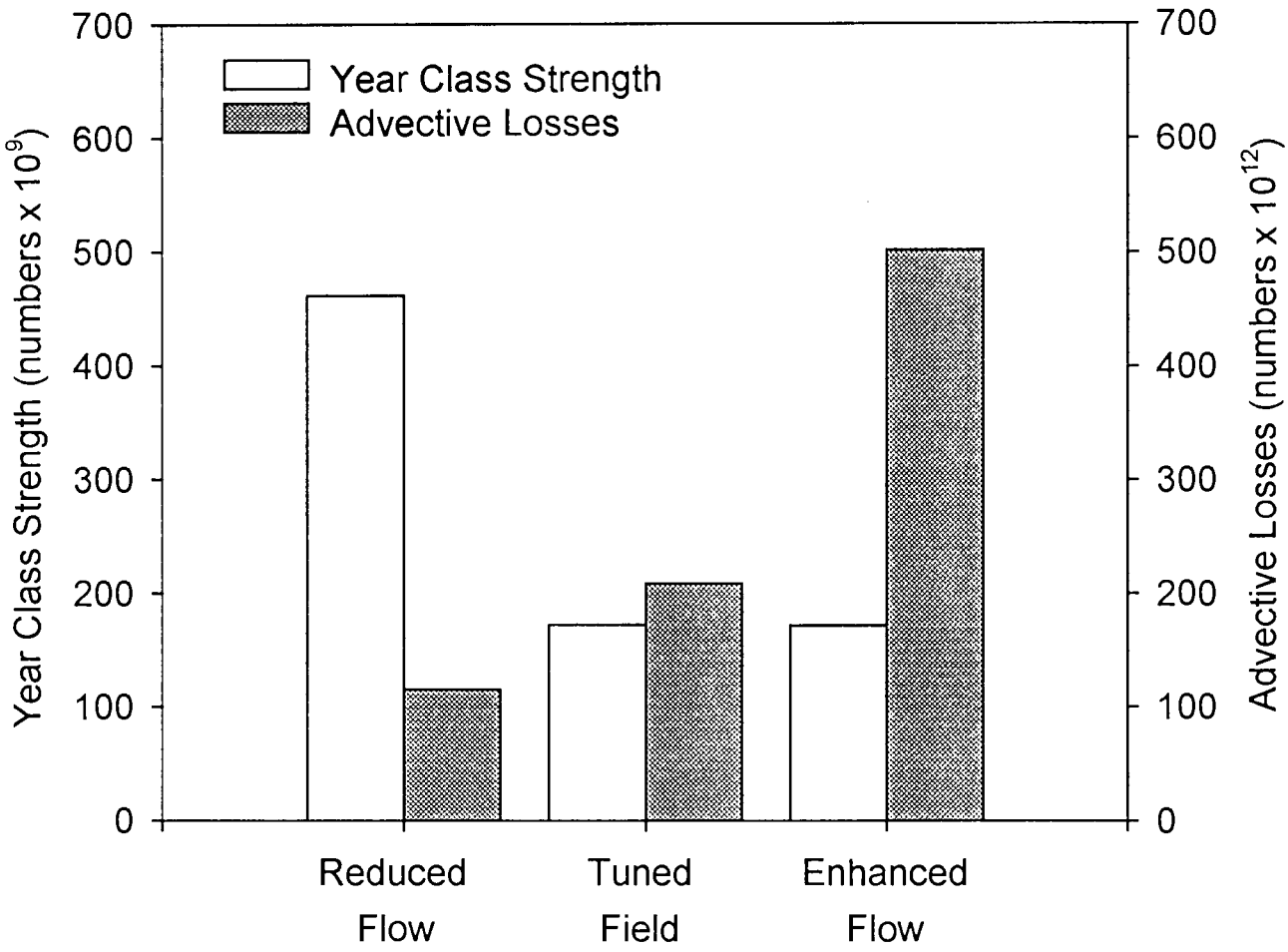

Figure 5.1 Comparison of model year class strength and advective losses (means of seven years) between the three advection scenarios

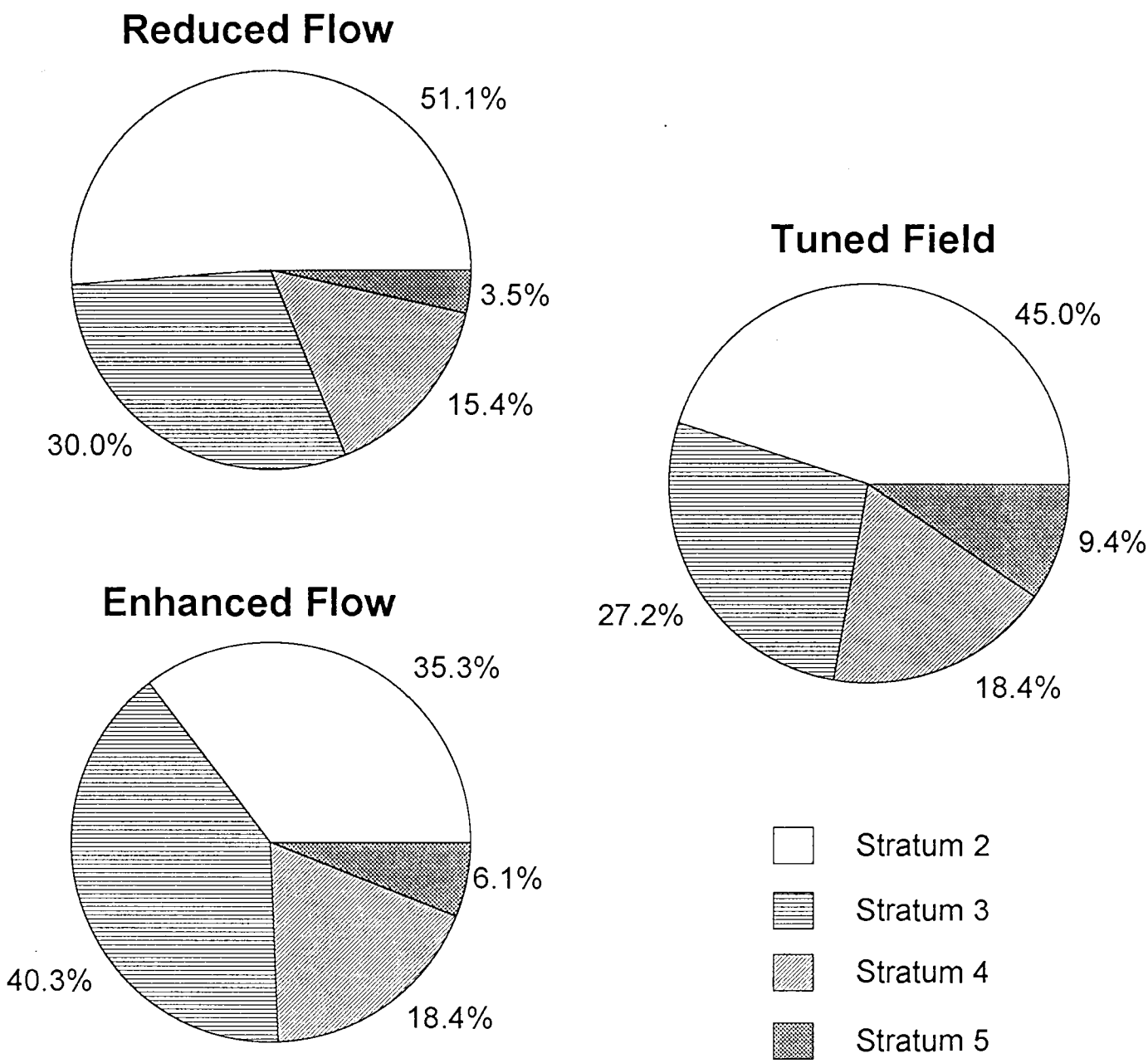

Figure 5.2 Pie charts comparing percentages of young of the year accumulating in strata 2 to 5 when each of the three advection scenarios were modelled

Under both reduced and unaltered (tuned) flow, the numbers and percentages of model young of the year decreased from stratum 2 to stratum 5, ie. eastwards around the coast (Figure 5.2 and Appendix B, Table B.7). However, modelling enhanced flow resulted in slightly more young accumulating between Cape Columbine and Cape Agulhas (stratum 3) than north of Cape Columbine (stratum 2).

It is interesting to note that reduced and unaltered flow scenarios resulted in almost identical numbers of model young of the year accumulating east of Mossel Bay (stratum 5), with fewer accumulating here when north west advection was enhanced (scenario 6, Appendix B, Table B.7). Numbers between Cape Agulhas and Mossel Bay (stratum 4) were similar under baseline and enhanced flow scenarios, and greater when flow was reduced (Appendix B, Table B.7).

5.3 LOSSES DUE TO ADVECTION

Model advective losses for the reduced flow field were 0.55 times those of the unaltered flow field, whereas model advective losses when flow was enhanced were 2.4 times greater than those of the unaltered flow scenario (Figure 5.1). The mean percentage of batches lost by advection followed a trend similar to year-class strength, i.e. it was similar under unaltered and enhanced flow scenarios but much lower when flow was reduced (only 0.11 times those of the other two scenarios, Appendix B, Table B.6). When flow was reduced, the mean average hour (after spawning) at which advective losses occurred was 16% of that obtained from the baseline flow scenario (Appendix B, Table B.6). Mean average hour of advective

loss was 46% of that of the baseline case when flow was enhanced (Appendix B, Table B.6).

Modelling reduced flow resulted in interannual variability in time of advective loss almost six times greater than was the case for unaltered flow (Appendix B, Table B.6). Reduced flow showed the largest interannual variations in advective losses of the three advection scenarios, but the smallest in year-class strengths (Section 5.2 and Appendix B, Table B.6). This is presumably because batches spawned far offshore were lost early, whereas offshore advection of batches spawned near (but not quite at) the offshore boundaries was delayed by enhanced onshore advection (reduced westward and northward flow), although losses still occurred eventually. However, during this time, other mortality factors reduced numbers, so little difference between numbers surviving per year (year-class strengths) resulted.

Modelling normal flow (tuned baseline) resulted in losses from all regions, with the highest numbers and percentages of advective losses occurring between Cape Columbine and Cape Agulhas (68.2% in stratum 3, Figure 5.3). The very small losses which occurred when batches were transported beyond 29°S under the other two scenarios, were absent when advection was enhanced (Figure 5.3, Appendix B, Table B.8). Enhanced advection led to reduced losses east of Cape Agulhas (i.e. from strata 4 and 5), where 1.1% of overall advective losses occurred, compared to 37.9% and 18.4% when flow was reduced and unaltered respectively (Figure 5.3). The heavier advective losses which occurred when flow was enhanced in the model (Figure 5.1) were the result of a considerable increase in losses from stratum 2 (numbers of advective losses increased by an order of magnitude from the baseline scenario, and from nothing under reduced flow, Figure 5.3 and Appendix B, Table B.8). Reduced flow virtually restricted model advective losses to the area east of Cape Agulhas (strata 3, 4 and 5).

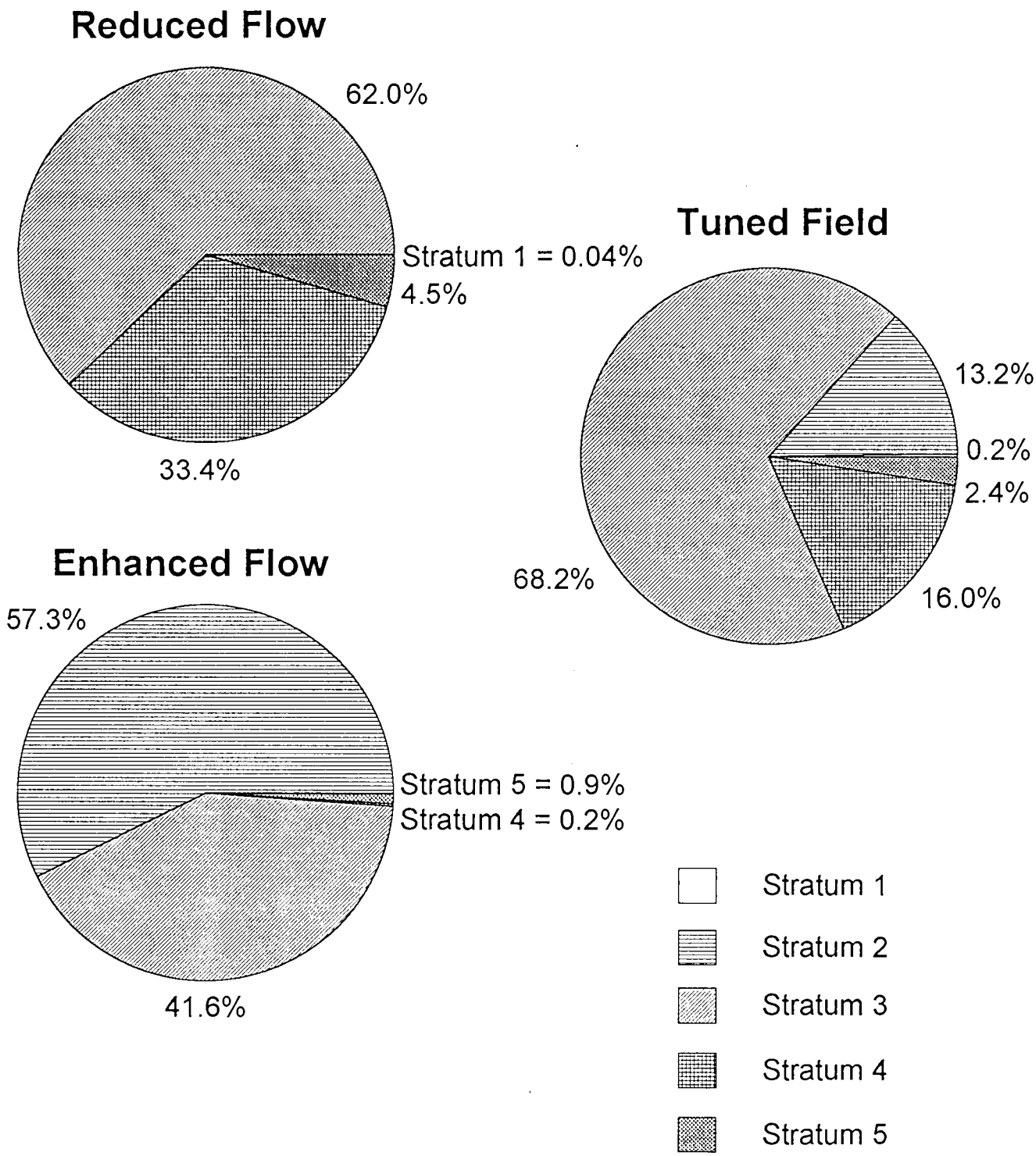

Figure 5.3 Pie charts comparing percentages of young of the year lost by advection from strata 1 to 5 when each of the three advection scenarios were modelled

5.4 SIGNIFICANT DIFFERENCES BETWEEN ALTERED ADVECTION SCENARIOS

Statistical analyses showed that the three advection scenarios differed significantly in their effects on both year-class strength and advective losses (Tables 5.1 and 5.2). Tables 5.3 and 5.4 show that both number of young of the year and number of advective losses per strata differed significantly between reduced, normal and enhanced advection scenarios. In addition, grouping results of the three advection scenarios showed that there were significant differences between number of young of the year accumulating in each of the four strata, as well as significant differences between number of advective losses occurring from the five loss strata. Since there was also evidence of an advection scenario by strata interaction in tests on both year-class strength and advective losses, it was concluded that there were significant differences in the way that the three advection scenarios affected recruitment in the four strata, and in the effect of advection scenarios on advective losses in the five strata from which losses occurred.

Both mean year-class strength and mean advective losses obtained under the three different advection scenarios (reduced, normal and enhanced) differed significantly from year to year (Tables 5.1 and 5.2). Since random components representing diffusion and turbulence were excluded from model runs in this investigation, interannual variation in overall advective losses and year-class strength was due to interannual variation in the distribution of spawners. Interannual differences in model year-class strength were less significant ($p=0.026$) than were interannual differences in model advective losses ($p<0.001$) (Tables 5.1 and 5.2). Interannual variation in model advective losses in each of the five loss strata (coefficients of variation,

Appendix B, Table B.8) as well as interannual variation in total model advective losses (Appendix B, Table B.6) were much larger than interannual variations in model recruitment in the four strata (coefficients of variation, Appendix B, Table B.7) and model year-class strengths (Appendix B, Table B.6). The reason for this is that advective losses are higher when losses occur soon after spawning (when there has been little opportunity for other mortality factors to act), and lower when losses only occur later. On the other hand, model recruitment is of a lower order and does not depend on timing - all 180-day old survivors are summed to give model year-class strength.

Table 5.1 **Summary of results of two factor ANOVA without replication, performed on year-class strength (numbersX10^{9}) obtained under reduced, normal and enhanced flow scenarios.**

SOURCE OF VARIATION	SS	df	MS	F calculated	P-VALUE	F critical (5%)
YEARS	18717.68	6	3119.613	3.669068	0.026375	2.996117
ADVECTION SCENARIOS	390800.3	2	195400.2	229.8159	$2.71\text{x}10^{-10}$	3.88529
ERROR	10202.96	12	850.2466			
TOTAL	419721	20				

Table 5.2 **Summary of results of two factor ANOVA without replication, performed on total advective losses (numbersX10^{12}) obtained under reduced, normal and enhanced flow scenarios.**

SOURCE OF VARIATION	SS	df	MS	F calculated	P-VALUE	F critical (5%)
YEARS	624338.5	7	89191.21	9.715143	0.000191	2.764196
ADVECTION SCENARIOS	496689.4	2	248344.7	27.05092	$1.55\text{X}10^{-5}$	3.73889
ERROR	128528.9	14	9180.638			
TOTAL	1249557	23				

Table 5.3 **Summary of results of two factor ANOVA with replication, performed on numbers of young of the year ($X10^{10}$) in four strata, obtained under reduced, normal and enhanced flow scenarios.**

SOURCE OF VARIATION	SS	df	MS	F calculated	P-VALUE	F critical (5%)
STRATA	1456.351	3	485.4504	81.84012	$3.81x10^{-23}$	2.731809
ADVECTION SCENARIOS	979.7817	2	489.8909	82.58871	$2.3x10^{-19}$	3.123901
INTERACTION	724.2377	6	120.7063	20.34938	$8.98x10^{-14}$	2.227402
WITHIN SUBGROUPS (ERROR)	427.0819	72	5.931693			
TOTAL	3587.453	83				

Table 5.4 **Summary of results of two factor ANOVA with replication, performed on advective losses (numbers$X10^{13}$) in five strata, obtained under reduced, normal and enhanced flow scenarios.**

SOURCE OF VARIATION	SS	df	MS	F calculated	P-VALUE	F critical (5%)
STRATA	3408.772	4	852.193	13.055	$2.0x10^{-8}$	2.47293
ADVECTION SCENARIOS	1139.332	2	569.666	8.726883	0.000344	3.097696
INTERACTION	3100.535	8	387.5669	5.937252	$4.22x10^{-6}$	2.042988
WITHIN SUBGROUPS (ERROR)	5874.943	90	65.27714			
TOTAL	13523.58	104				

5.5 EFFECTS OF ALTERED ADVECTION ON TRANSPORT AND RECRUITMENT OF ANCHOVY

Modelling reduced flow yielded the strongest year-class and lowest advective losses (Figure 5.1). Given the unexpectedly low mean hour (after spawning) at which advective losses occurred when flow was reduced (scenario 0, Appendix B, Table B.6), it may have been expected that greater advective losses would have occurred owing to the reduced opportunity for other causes of natural mortality to have taken their toll. However, this was not the case since only a very small percentage of total batches released were lost to advection (11% that of the baseline case). Although mean percentages of batches lost to advection were similar for unaltered and enhanced flow scenarios, enhanced flow resulted in advective losses that were more than double those under the new baseline flow field. This was the result of advective losses occurring within the first month after spawning when flow was enhanced (Appendix B, Table B.6). Coefficients of variation suggest that interannual variations in advective losses (numbers), percentage of batches lost to advection and average hour at which advective losses occurred were greatest under the reduced flow scenario (Appendix B, Table B.6). However, reduced flow dampened interannual variability in year-class strength (Appendix B, Table B.6). The reasons for the variations in interannual variability are discussed in sections 5.3 and 5.4.

Enhanced advection seemed to move model anchovy westwards out of stratum 5, through stratum 4 and into stratum 3 (Figure 5.4, which is based on *numbers* presented in Appendix B, Tables B.7 and B.8). Although transport into the more productive waters of the west coast was enhanced, the likelihood of advection into unproductive offshore waters was also greater

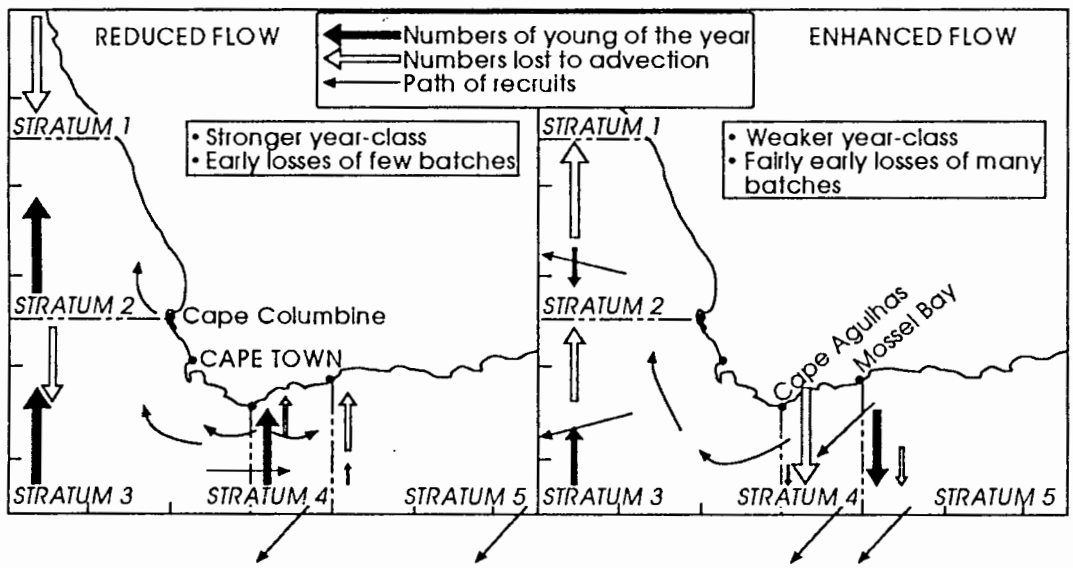

Figure 5.4 **Diagramatic representation of the effects of reducing and enhancing advection (relative to scenario 5, the improved baseline flowfield)**

(arrows representing numbers of young of the year and advective losses:
upward pointing arrows indicate an increase in numbers
downward pointing arrows indicate a decrease in numbers
size of arrows represents the magnitude of change)

in this region, thereby preventing good recruitment under this scenario. Since advection is generally northwards and westwards and because it was further enhanced, batches in offshore regions were lost to advection before reaching stratum 1 (no advective losses here). On the other hand, reduced advection facilitated accumulation of young of the year in all strata in the model (Figure 5.4). Advective losses were restricted to strata south and east of Cape Columbine (i.e. strata 3, 4 and 5), although some batches were lost from stratum 1 when spawning in 1988 was modelled.

CHAPTER SIX

A SECOND APPROACH TO INVESTIGATE THE

POTENTIAL EFFECTS OF ALTERED WESTWARD ADVECTION

CHAPTER SIX

A SECOND APPROACH TO INVESTIGATE THE POTENTIAL EFFECTS OF ALTERED WESTWARD ADVECTION

6.1 PROPORTIONAL ENHANCEMENT AND REDUCTION OF WESTWARD ADVECTION

A second approach to altered advection was taken in order to further explore the suggestion by a similar, smaller preliminary study that altering advection by a proportion of the measured currents yielded insignificant differences in year-class strength. This was in contrast to the significant differences in effects exerted on anchovy recruitment by the different advection scenarios investigated in Chapter Five.

Five versions of the model were run to investigate the effects of altering westward advection over the entire area under observation. An unchanged flow field based on sampled ADCP data was used, as well as versions that increased and decreased westward advection by both 25% and 50%. This approach differed from the first in that the altered amount was a fixed proportion of each measured velocity component, as opposed to a fixed amount added to or subtracted from each component irrespective of its original value. Additionally, the second version of the model simulated transient features such as eddies and filaments by adding random components (turbulence) with maximum amplitudes of 10 $cm.s^{-1}$ to the ADCP vectors over 72 hours, representing events on a maximum scale of ca. 26 km. Smaller scale diffusion (with a maximum amplitude of 0.9 $cm.s^{-1}$), having a fixed time scale of one hour and a spatial

scale the order of metres, was also added to current vectors (Chapter Two). Note that, unlike in chapters Four and Five, the original flow field was used and not an improved baseline field. It should also be noted that the second approach was undertaken after prerecruit mortality rate had been "tuned", and hence absolute numbers are not comparable between the two different approaches to altered advection. Therefore it is the trends that are important here.

6.2 MEAN YEAR-CLASS STRENGTH AND ADVECTIVE LOSSES

Mean number of anchovy surviving to recruitment (year-class strength) and mean number of anchovy lost due to unfavourable advection offshore for the cases when the flow field was unaltered and when westward advection was increased or decreased by 25% and 50% are shown in Figure 6.1 (standard deviations are tabulated in Appendix B, Table B.9). Westerly advection enhanced or reduced by 25% and 50% did not significantly impact on mean year-class strength ($p=0.298$, Table 6.1). When westerly advection was both increased to 150% and decreased to 50% of that when flow was unaltered, mean numbers of young-of-the-year anchovy dropped slightly to 96% of that under unaltered flow conditions. When westerly advection was decreased to 75%, year-class strength increased very slightly, but decreased slightly under the 125% westward advection scenario. Despite the non-significant difference between year-class strength in the seven years ($p=0.157$, Table 6.1), interannual variation was slightly greater when westward advection was reduced and enhanced to 50% and 150% respectively (coefficients of variation were 7%, compared to between 4% and 5% under the three other scenarios, Appendix B, Table B.9).

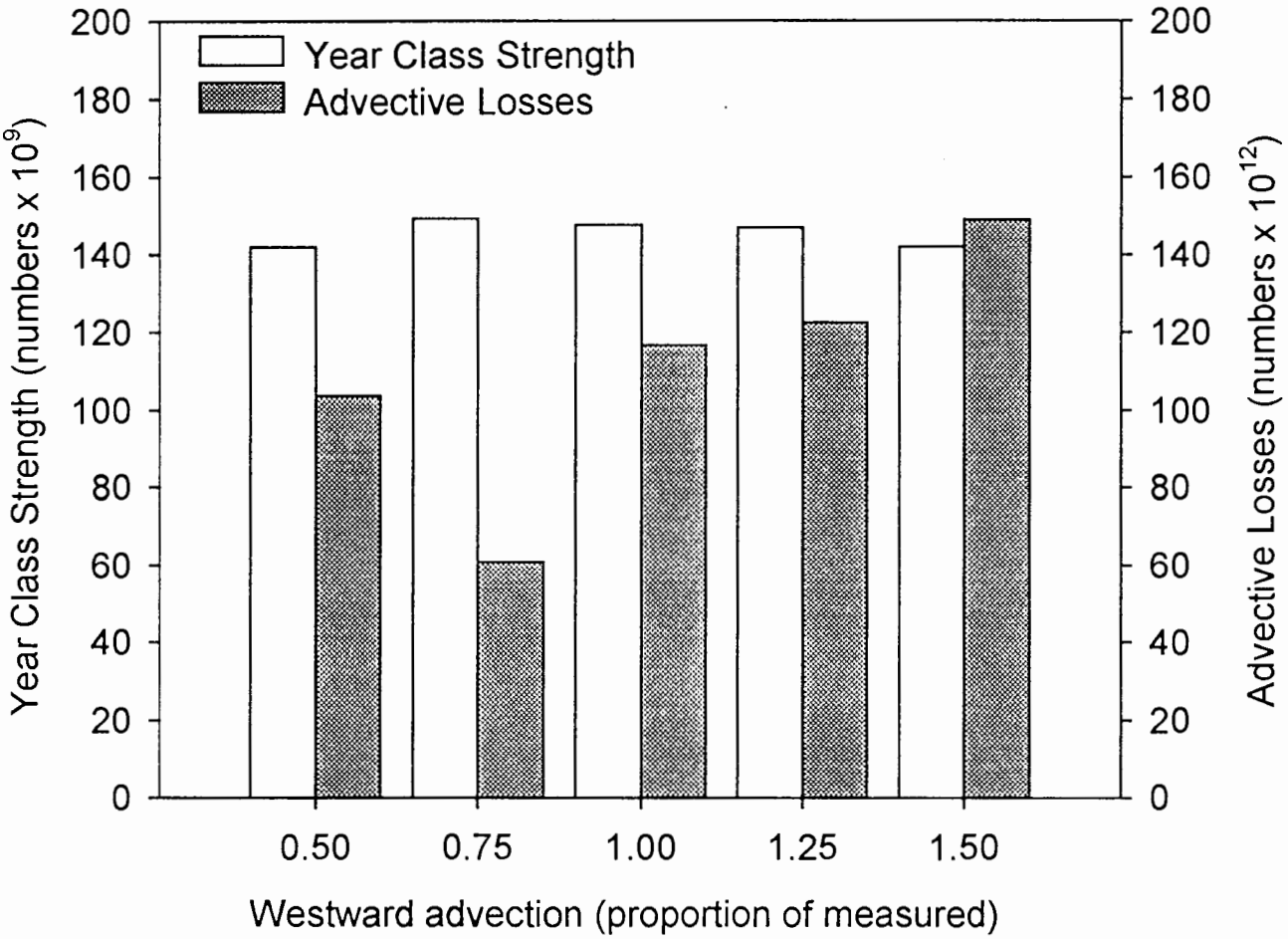

Figure 6.1 Comparison of model year class strengths and advective losses (means of seven years) when westward advection was altered by the indicated proportion

Advective losses of anchovy increased with increased westward advection, to as much as 128% of that under the unaltered flow scenario, when westward flow was 50% stronger (150% of the unaltered flow scenario). Advective losses decreased when westward flow slackened, to as little as 52% of that under unaltered flow conditions for a 25% decrease in flow (to 75% of the unaltered case, Figure 6.1 and Appendix B, Table B.9). Coefficients of variation of mean advective losses occurring under each of the five advection scenarios were very large (between 90% and 124%, Appendix B, Table B.9), and interannual variation was shown to be significant (p=0.018, Table 6.2). As was the case for year-class strength, advection scenarios did not impact significantly on total advective losses (p=0.613, Table 6.2).

Table 6.1 **Summary of results of the two-factor ANOVA without replication, performed on year-class strengths (numbersX10^9)**

SOURCE OF VARIATION	SS	df	MS	$F_{calculated}$	p-VALUE	$F_{critical}$ (5%)
YEARS	619.7568	6	103.2928	1.730758	0.156961	2.508187
ADVECTION SCENARIOS	310.3428	4	77.58569	1.300014	0.298158	2.776289
ERROR	1432.336	24	59.68067			
TOTAL	2362.436	34				

Table 6.2 **Summary of results of the two-factor ANOVA without replication, performed on total advective losses (numbersX10^{12})**

SOURCE OF VARIATION	SS	df	MS	$F_{calculated}$	p-VALUE	$F_{critical}$ (5%)
YEARS	209448	6	34908	3.234781	0.017915	2.508187
ADVECTION SCENARIOS	29313.39	4	7328.348	0.679088	0.613167	2.776289
ERROR	258995	24	10791.46			
TOTAL	497756.5	34				

6.3 RECRUITMENT IN DIFFERENT REGIONS

Advection scenarios were shown to have insignificant effects on year-class strength ($p=0.298$, Table 6.1) and on mean recruitment per strata ($p=0.963$, Table 6.3). However, some trends are noted.

Enhanced westward advection resulted in a northward shift in recruitment, so that more model young of the year accumulated in stratum 2, between 29°S and Cape Columbine, than was the case under unaltered or reduced flow scenarios (Figure 6.2 and Appendix B, Table B.10). Reduced westward advection caused fewer young of the year to accumulate in stratum 2, whereas more were found in stratum 3, between Cape Columbine and Cape Agulhas. There were not large differences between advection scenarios in numbers of young of the year occurring in strata 4 and 5 east of Cape Agulhas (Figure 6.2).

The percentage of anchovy surviving to 180 days that accumulated offshore, as opposed to coastal regions, increased and decreased substantially when westward advection was increased and decreased respectively (Appendix B.11).

Grouping of results obtained under all five scenarios showed significant differences between the number of six-month-old anchovy (termed recruits) accumulating in the various strata ($p=1.18X10^{-47}$, Table 6.3). Highest numbers of recruits accumulated west of Cape Agulhas (in strata 2 and 3) and fewest recruits were found east of Mossel Bay (stratum 5, Figure 6.2).

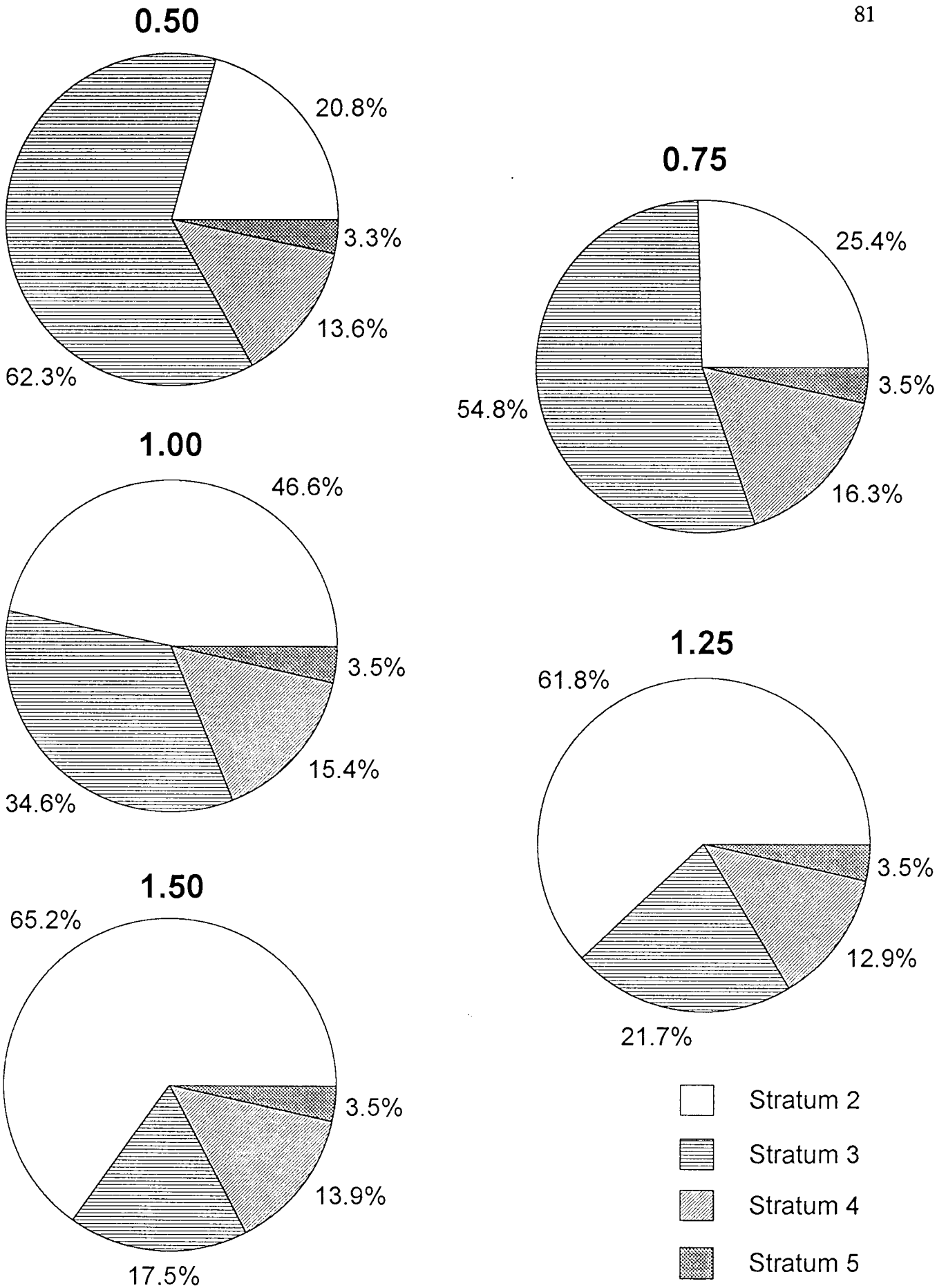

Figure 6.2 Pie charts comparing percentages of young of the year accumulating in strata 2 to 5 when each of the five westward advection scenarios were modelled (westward advection altered by the indicated proportion)

Table 6.3 **Summary of results obtained when a two-factor ANOVA with replication was performed on numbers of young of the year ($X10^{10}$) per strata, for westward advection altered proportionally.**

SOURCE OF VARIATION	SS	df	MS	F calculated	P-VALUE	F critical (5%)
STRATA	820.7396	3	273.5799	210.7878	$1.18X10^{-47}$	2.680167
ADVECTION SCENARIOS	0.775761	4	0.19394	0.149427	0.962934	2.447237
INTERACTION	471.7694	12	39.31412	30.29073	$9.93X10^{-31}$	1.833694
WITHIN SUBGROUPS (ERROR)	155.7471	120	1.297892			
TOTAL	1449.032	139				

6.4 ADVECTION ACROSS OFFSHORE BOUNDARIES

Altered advection scenarios did not affect total advective losses and advective losses per strata significantly (p=0.613, Table 6.2 and p=0.799, Table 6.4, respectively). However, the means of advective losses under the five advection scenarios differed significantly between strata ($p=4.57X10^{-5}$, Table 6.4). Losses across the northern boundary (29°S) were small (0.4% or less of total advective losses, under other flow scenarios, Figure 6.3).

Losses offshore (i.e. to the west) in stratum 2, to the north of Cape Columbine (33°S), only occurred when westward advection was enhanced, and then only comprised up to 2.1% of total advective losses when westward advection was increased to 150% (Figure 6.3 and Appendix B, Table B.12).

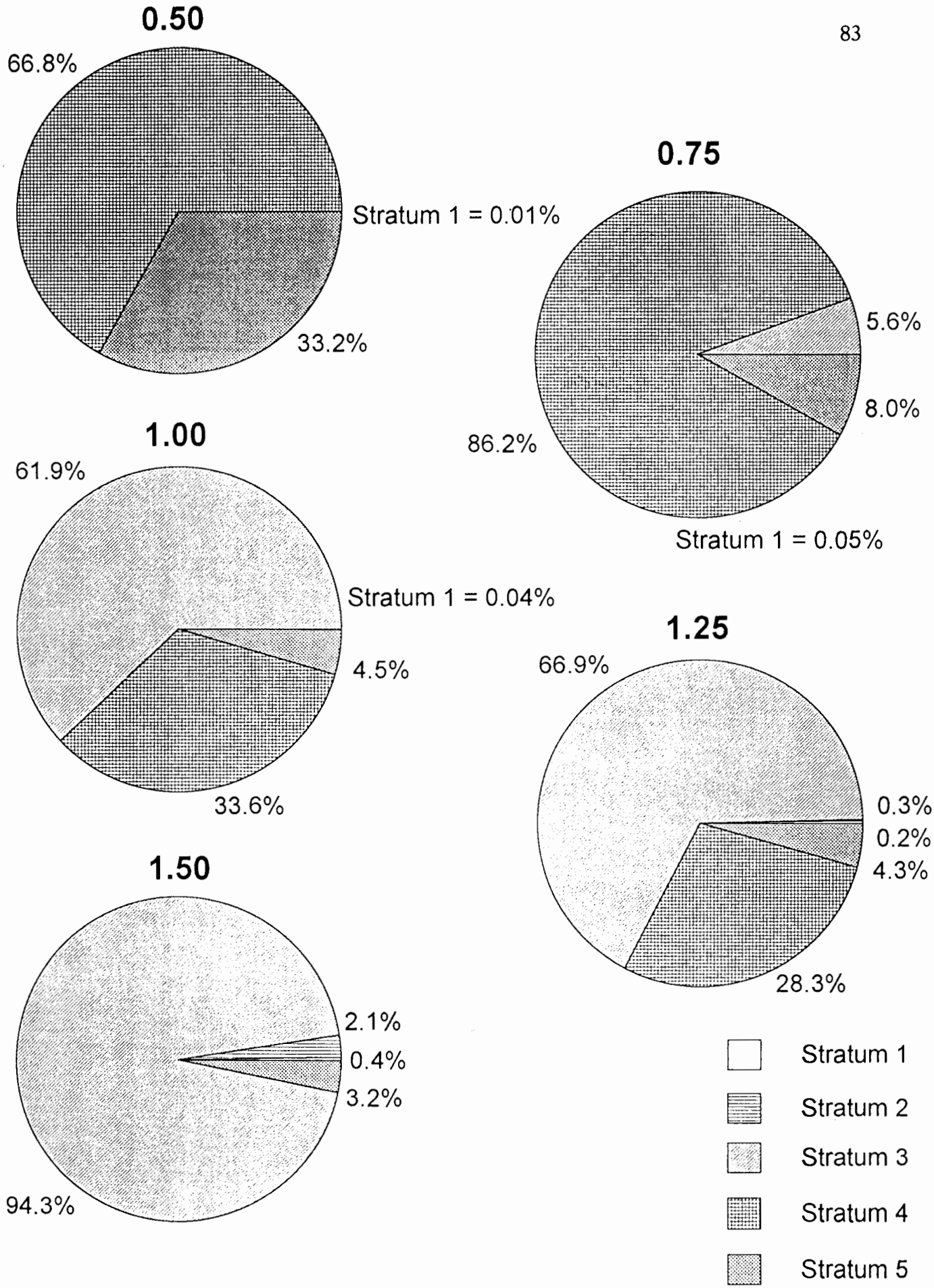

Figure 6.3 Pie charts comparing percentages of young of the year lost by advection from strata 1 to 5 when each of the five westward advection scenarios were modelled (westward advection altered by the indicated proportion)

The majority of advective losses occurred in strata 3 and 4, i.e. between Cape Columbine and Cape Agulhas (20°E) and between Cape Agulhas and Mossel Bay (22°E) respectively (Figure 6.3). Losses in stratum 3 increased as westward advection was increased and decreased with reduced westward advection. Conversely, the proportions of advective losses that occurred offshore in stratum 4 and in stratum 5 east of Mossel Bay were greater when westward advection was reduced, and visa versa.

Table 6.4 **Summary of results obtained when a two-factor ANOVA with replication was performed on advective losses (numbersX10^{13}) per strata, for westward advection altered proportionally.**

SOURCE OF VARIATION	SS	df	MS	F calculated	P-VALUE	F critical (5%)
STRATA	966.1662	4	241.5415	6.813988	4.57X10^{-5}	2.431968
ADVECTION SCENARIOS	58.62012	4	14.65503	0.413424	0.798772	2.431968
INTERACTION	1149.177	16	71.82359	2.026173	0.014759	1.711346
WITHIN SUBGROUPS (ERROR)	5317.185	150	35.4479			
TOTAL	7491.149	174				

6.5 IMPLICATIONS OF ALTERED WESTWARD ADVECTION FOR THE SOUTH AFRICAN ANCHOVY FISHERY

Despite the ANOVA tests not showing significant differences between scenarios in year-class strength and advective losses (Tables 6.1 and 6.2), interesting trends were observed and are discussed below.

As discussed in section 6.2, model year-class strength decreased as westward advection was increased, increased when westward advection was reduced to 75%, but decreased once more when westward advection was reduced to 50% (Figure 6.1). This may be viewed in terms of the "optimal environmental window" hypothesis (Cury and Roy 1989), where an intermediate level of enhanced eastward advection is favourable for anchovy survival off South Africa, but further enhancement of eastward advection and both levels of enhanced westward advection are unfavourable. Boyd *et al.* (submitted) found that there is a negative correlation between acoustically-derived recruitment (numbers of young-of-the-year anchovy) and south-easterly winds. Therefore by restricting offshore losses, the less intense south-easterly winds which occurred during the El-Niño period between 1990 and 1993 (J. Taunton-Clark. Sea Fisheries Research Institute, pers. comm.) may have been at least partly responsible for the increasing trend in anchovy numbers measured during these years. Conversely, as discussed in Chapter One (section 1.3), the return to strong south-easterlies during the summer of 1993/1994 (J. Taunton-Clark, Sea Fisheries Research Institute, pers. comm.) seems to have served to advect anchovy offshore, leading to the poor recruitment observed in 1994.

Enhanced westward advection moved anchovy into the region of the north-flowing jet current, so that a greater number accumulated between 29°S and Cape Columbine (stratum 2) than did under reduced flow and unaltered flow scenarios (Figure 6.2 and section 6.3). This supports Shelton's (1979) proposal that west coast recruitment could be reduced by eastward advection of anchovy reproductive products during sustained periods of westerly winds.

Losses across the northern boundary (29°S), (stratum 1), were small (Figure 6.3 and section 6.4) and occurred in the early part of the 180 day period (from scanning output data files). It is not certain whether batches of anchovy reaching this boundary continue northwards and recruit to the Namibian stock, or whether they return southwards to recruit to the South African stock (Badenhorst and Boyd 1980). Both scenarios are feasible, depending on prevailing environmental factors. It would be interesting to compare these two options. It therefore remains for simulation of the transport of batches to be repeated, with batches crossing the northern boundary to be reduced by natural mortality until 180 days and then those surviving to be added to year-class strength. On the other hand, neither scenario may hold. Relatively high densities of anchovy have been found in the region of the Orange River mouth in recent years (Hampton 1992), and are thought to be part of a resident population in this region.

Advective losses offshore (i.e. westwards) in stratum 2 north of Cape Columbine only occurred when westward advection was increased (Figure 6.3 and Appendix B, Table B.12). The fact that losses in this region were otherwise zero is related to the predominantly north-easterly flow in this region.

Under normal flow conditions, 62% of advective losses occurred in stratum 3, between Cape Columbine and Cape Agulhas, and a third occurred in stratum 4, between Cape Agulhas and Mossel Bay (Figure 6.3 and section 6.4). As westward advection was increased, losses offshore (i.e. to the west) in stratum 3 were enhanced, whereas losses offshore (i.e. to the south) in stratum 4 were substantially reduced. No losses occurred in the latter region when westward advection was increased to 150% and no batches were lost in stratum 3 under the 50% (i.e. reduced) westward advection scenario (Figure 6.3). Southward advection was greatly enhanced when westward advection was reduced, 86% of advective losses occurring to the south from stratum 4 when westward advection was reduced to 75%.

A further reduction in westward advection (to 50% of unaltered flow) served to transport anchovy eastward into stratum 5, east of Mossel Bay, counteracting the predominantly westward flow off the south coast of South Africa (Shelton and Hutchings 1982). Losses offshore in this region (i.e. to the south) then comprised 33% of total advective losses.

It was concluded that the geographic extent and magnitude of changes in current strength above the thermocline can influence the distribution of recruits and the extent of advective losses, although long-term changes in advective processes may not significantly alter mean year-class strength. This results from most of the mortality of early stages in the model arising from causes other than unfavourable advection. If this is correct, it means that the anchovy population off South Africa may be relatively robust to long-term changes in advective processes. However, it should be borne in mind that the full spectrum of advective processes in the ocean of South Africa was not modelled. For example, the influences of Agulhas rings (Duncombe Rae *et al.* 1992) and variability in the frontal jet stream off western

South Africa on year-class strength and the distribution of recruits were not considered. It should also be noted that interannual variation in year-class strength and especially advective losses in each stratum were large. Therefore distribution of the spawning stock is important in determining the likelihood of survival and ultimate destination of new recruits.

Increased westward advection results in fewer recruits being retained in coastal areas (numbers inshore, Appendix B, Table B.11), which may impact on the anchovy fishing industry in terms of fish availability.

CHAPTER SEVEN

FUTURE DEVELOPMENTS AND CONCLUSIONS

CHAPTER SEVEN

FUTURE DEVELOPMENTS AND CONCLUSIONS

7.1 LIMITATIONS OF THE MODEL

The accuracy of results produced by the model is limited by the precision of the current data and by the poorly known effects of environmental change on the ocean surrounding South Africa. Changes imposed on flow fields may result in divergence of flow and should be checked for this and adjusted if necessary. The model is itself limited by its assumptions and simplifications. However, this work has served to underline the importance of further research into possible mechanisms of environmental change in the ocean, in order to improve predictions of potential impacts on South Africa's living marine resources and thereby better equip managers to optimally manage and utilize such resources.

7.2 POSSIBILITIES FOR USE OF THE MODEL IN THE FUTURE

7.2.1. PROPOSED EXTENSION OF THE MODEL

At a modelling workshop held from 25 to 27 July 1994 under the auspices of the Benguela Ecology Programme (BEP) and the Joint Global Ocean Flux Study (JGOFS), the model was assessed in terms of potential for the development of additional versions. It was felt that the model would benefit from the addition of more biological constraints. These possibilities,

together with others arising during the analysis of results (particularly the proposed improvements of the quantification of advective losses), are discussed in the sections below.

Modelling swimming by juveniles and prerecruits

It is likely that juveniles are capable of swimming against currents, particularly those of the strength measured off western South Africa in autumn, when prerecruits begin migrating inshore (J.D. Hewitson, Sea Fisheries Research Institute, pers. comm.). Although in this thesis prerecruits are moved between areas in the same way as eggs and larvae, the option is available in the model to superimpose deterministic movement, equivalent to the swimming capability of prerecruits, towards inshore regions in the nursery area. Nelson and Hutchings (1987) presented a cruising speed of 3 $cm.s^{-1}$ for juvenile (10 week-old) Cape anchovy, as quoted to them by A.G. James and C.L. Brownell who undertook tank studies at Sea Fisheries Research Institute. It was suggested at the above-mentioned workshop that swimming speeds in the model be between one and two body lengths per second, and that swimming eastwards and onshore only be permitted along the west coast and during daylight hours (L. Hutchings, Sea Fisheries Research Institute, pers. comm.).

Modelling mortality rates

In further developments of the model, durations of egg, larval and prerecruit stages should be allowed to vary with temperature, and mortality should be permitted to vary across the distribution of anchovy, depending on local food availability, predation and physical conditions.

Changes in temperature affect the rate of anchovy egg and larval development (King *et al.* 1978, Brownell 1983, Lo 1985 and Armstrong *et al.* 1988). King *et al.* (1978) reported that the lowest lethal temperature at which eggs of *E. capensis* develop was 14°C. Using the time-temperature relations of King *et al.* (1978) and Lo (1985) already mentioned in Chapter Two, time from spawning to hatching will therefore assume a maximum of 93 hours, corresponding to the development period at 14°C. However, it should be noted that the work of King *et al.* (1978) was carried out on anchovy taken from water warmer than 14°C, and that this does not necessarily imply that anchovy eggs spawned in cooler areas do not develop at lower temperatures.

Higher temperatures may be advantageous since development is faster and duration of egg and larval stages having highest mortality rates is therefore shortened. In addition, altered temperature variability may influence anchovy year-class strength. Boyd (1980) found anchovy year-class strength off Namibia to be negatively correlated with variability of sea surface temperature.

Mortality of larvae resulting from starvation is an important consideration on the west coast (L. Hutchings, Sea Fisheries Research Institute, pers. comm.). Optimal feeding occurs in the region of the front, between 16 and 19°C. Advection into food-poor regions beyond the front will result in higher mortality of anchovy. In addition, the spatial distribution of predators and prey should be taken into account if mortality is to be fully modelled.

Hence it would be useful to incorporate an average or typical temperature field in the model, in order to allow differential mortality rates to be included. Furthermore, possible impacts of

global warming on water temperature could then be addressed, in a similar fashion to effects of altered advection scenarios as covered in Chapters Five and Six.

Modelling gonad atresia

Gonad atresia refers to the reabsorption of yolk from oocytes in the ovaries of fish. It depends on the level of energy reserves of fish, food availability, timing of the reproductive cycle and environmental conditions such as temperature (Hunter and Macewicz 1985). The percentages of atretic oocytes in ovaries of *E. capensis* in November-December from 1985 to 1993 generally ranged between 0.5 and 13.1 % (Melo in press, Y.C. Melo, Sea Fisheries Research Institute, pers. comm.). However, November 1988 saw the unusual situation where 16.9% of oocytes were atretic (Melo 1992). Such high levels of atresia are presumed to indicate low probability of spawning and likely curtailment of the spawning season (Y.C. Melo, Sea Fisheries Research Institute, pers. comm.). The possibility that atresia occurs in any one season was not incorporated into the model, so as to minimise variability in year-class strength *not* due to advective processes. Its effect on year-class strength may now be included as an additional cause of mortality.

Modelling advective processes

It is planned that a future version of the model will incorporate more detailed information on well-known "structures" such as the shelf-edge jet, an important mechanism in the transportation of anchovy larvae to nursery grounds (Shelton and Hutchings 1982), the inshore southward current between St Helena Bay and Cape Point (Nelson 1983, Lamberth and

Nelson 1987, Nelson and Polito 1987, Boyd *et al.* 1992), which aids return migration of new recruits to spawning grounds, surface drift, upwelling tongues, fronts and continental shelf waves (Nelson 1992). The "structures" will also be permitted to vary in time, incorporating "events" such as rings which have known effects on the physical conditions and advection in certain regions. For example, Duncombe Rae *et al.* (1992) proposed that part of the reason for the very poor 1989 anchovy year-class off South Africa was due to offshore entrainment of late stage larvae and prerecruits by an Agulhas ring.

Improved quantification of advective losses

Closer examination of results discussed in Chapter Four revealed some seemingly odd situations, which upon further analysis led to the conclusion that advective losses require improved quantification in the model. Timing of advective losses, as well as number and size of batches lost should be viewed together as they interact, often obscuring actual trends. An example of such a contradiction is discussed below.

When the seven years of spawning distributions were run under the "new" baseline flow (scenario 5, Chapter Four), fewer anchovy survived to 180 days when spawning occurred in 1989 than in 1991, corresponding to year-class strength of the winters of 1990 and 1992 (Appendix B, Table B.3 and Chapter Four, Figure 4.1). Contrary to the hypothesis that lower recruitment should result from greater advective losses, advective losses occurring by winter of 1992 were similar but slightly heavier than those of the winter of 1990. Additionally, one would then expect that greater advective losses from spawning in 1991 resulted from early advection across boundaries (with less time during which natural mortality could reduce

numbers) and that a larger percentage of batches released were lost to unfavourable advection. However, this was not the case (Appendix B, Table B.3). The complicating factor here is that batches are of unequal size, depending on spawning intensity in each block. Although a smaller percentage of batches was lost from 1991 spawning, and despite the later occurrence of losses, the unexpectedly heavy advective losses were a result of the loss of batches which must on average have been comprised of more individuals than those spawned in 1989.

It was concluded that the output of the model which best represented the overall effect of a particular scenario was total number of anchovy surviving to 180 days (i.e. year-class strength), rather than advective losses, number of batches lost and timing of losses alone. In an attempt to better quantify the impact of timing and batch size on advective losses, and therefore ultimately on recruitment, a new index should be introduced and tested, viz. average weighted hour of loss (H), calculated as

$$H = \frac{\sum (hr.Lva)}{(\sum Lva)}$$

equation 7.1

where hr= hour (after spawning) at which a batch was lost and

Lva= number of anchovy surviving in a batch at the time a loss boundary was crossed. This index requires the modification of both the main and processing programs and it is intended to be undertaken in the future.

A further improvement planned is to express advective losses as number of "would-be-recruits". That is, the absolute number of anchovy crossing a "loss" boundary at a particular time will be reduced by natural mortality until 180 days has passed. In this way, the number

of potential recruits (the sum of those surviving to 180 days and those that would have survived to 180 days if they had not crossed a "loss" boundary) could be compared to the number of recruits when advective losses are permitted, in order to better quantify the importance of advective losses in the recruitment process.

7.2.2 FUTURE OBJECTIVES

Probabilistic distribution of recruitment

Fisheries management procedures worldwide rely heavily on stochastic models, and since recruitment of clupeoid stocks fluctuate, it is important that such models be extended to incorporate variability in recruitment (Bergh and Butterworth 1987). A reasonable assumption, which is widely in use in these management procedures, is that recruitment has a log-normal probabilistic distribution, that is, most recruitment values lie close to the spawner stock-recruit relation, with the exception of a few high outliers (Walters 1984). This assumption is made in the assessment and management of the Cape anchovy stock. Repeated simulations of the model will be used to test the assumption's validity with respect to the influences of advection and egg and larval development.

A more accurate representation of the real statistical distributions of year-class strength might be obtained if random selection of a whole set of matching parameters (spawning distribution, batch fecundity etc.) obtained during one of the seven years between 1986 and 1992 is allowed.

To investigate the possible optimization of timing and position of spawning by anchovy off South Africa

Provided the natural oceanographic transport systems operate "normally", the coupling of these systems to spawning is advantageous to eggs and larvae in terms of transport to and from nursery grounds and areas conducive to survival (Norcross and Shaw 1984). Parrish *et al.* (1981) found that fish reproduction corresponds to surface transport mechanisms in the California Current region, indicating that the development of spatial and seasonal spawning characteristics of fish have been moulded by the minimization of advective loss of reproductive products. This led to a proposal by the authors that a possible cause of the large variability in recruitment in the major fisheries along the Californian coast has been the deviation from "normal" transport conditions, to which the reproductive strategies of fish are coupled.

Results of Power's (1986) model support the hypothesis formulated by Parrish *et al.* (1981) that northern anchovy, *E. mordax*, spawn in the California Bight at a time when least offshore transport of eggs and larvae occurs. Along similar lines, it is proposed that the model used in this thesis be applied to answer the following question: does *E. capensis* spawn at a time when losses of potential recruits resulting from advection are minimized?

In place of using ADCP data averaged over all months, ADCP data will be grouped into 3-month periods and four averages will be used. This will facilitate an investigation into recruitment success of spawning in different seasons. Some of the advection scenarios considered in Chapters Three, Five and Six could be re-modelled for spawning in different

seasons and different regions. In this way, the optimization of spawning and transport of *E. capensis* in the southern Benguela system will be addressed, and the possible impact of global environmental change on anchovy recruitment will be approached from a different perspective.

Finally, in addition to the potential optimization of timing of spawning, it is proposed that spawning distributions of *E. capensis* be studied in more detail in terms of optimization of spawning position. It has been found that fish such as Atlantic herring (Sinclair and Tremblay 1984) and cod (Hutchings *et al.* 1993) spawn in areas where retention of eggs and larvae is likely. Walters *et al.* (1992) modelled the transport of English sole in the Hecate Strait, British Columbia, and hypothesized that sole spawn in areas in which food supply is optimised and advective transport to unfavourable habitats is minimised. Therefore the authors proposed that observed spawning locations result from a trade-off between these two factors.

Cape anchovy avoid spawning in areas where offshore advection is likely (Shelton *et al.* 1985). The latter could be further examined using the model to simulate the release of batches of anchovy eggs in areas in which spawners are *not* usually found. Model tracking of such batches to determine positions after six months as well as advective losses during transport should prove useful. This work would build on that covered in Chapter Four, in which interannual variation in the spatial distribution of spawning anchovy was considered.

7.3 COMPARISON OF THE TWO APPROACHES TO ALTERED ADVECTION

The potential effects of altered advection on anchovy transport and ultimately year-class strength were explored using two approaches. Environmental variation between El-Niño years and others is noticeable in the intensity of south-easterly winds in the ocean surrounding South Africa (J. Taunton-Clark, Sea Fisheries Research Institute, pers. comm.). For this reason, the impact of altering northerly and particularly westerly advection was investigated.

The first approach, whereby fixed components were added to or subtracted from both north and east velocity components, yielded significant differences in both year-class strength and advective losses, and significantly affected the spatial distribution of both young-of-the-year anchovy and losses of batches of eggs (Chapter Five). Reduced advection lead to a mean year-class strength more than double that of the base and enhanced advection scenarios. Young of the year accumulated in all strata under reduced advection, whereas enhanced advection led to advective losses across offshore boundaries, particularly off the west coast of South Africa.

In contrast, the second method, whereby westward advection in all areas was altered by fixed proportions of the mean, led to negligible changes in many instances where westerly components were small, and did not result in significant differences in year-class strength and advective losses (Chapter Six). Despite the non-significant results, trends in the spatial distribution of young-of-the-year anchovy and advective losses were revealed. Model year-class strength increased under an intermediate level of reduced westward advection, but decreased when westward advection was enhanced or further reduced. As mentioned in

Chapter Six, section 6.5, this may be viewed in terms of Cury and Roy's (1989) "optimal environmental window" hypothesis. However, enhanced westward advection served to move anchovy eggs and larvae into the region of the jet current, thereby enhancing the proportion of recruitment off the west coast between 29°S and Cape Columbine.

Owing to large variation in measured currents upon which the model flow field was based, the mean of many separate current measurements in a block may be smaller than the separate observations themselves, since currents in opposite directions negate one another when averaged. In these areas of weak mean currents, altering advection by proportions of the means has less of an effect on advection than does altering advection by set components (Table 7.1). For this reason, it is believed that the first approach may better represent the possible influence of extreme environmental change on advection, and hence on anchovy recruitment. It may be concluded that altered advection may influence anchovy transport and possibly anchovy year-class strength.

Table 7.1 **Comparison of velocity magnitude and direction at points 1 to 4 (Figure 7.1) when vectors were unaltered, when westward vector components were enhanced to 150% that of the unaltered flow scenario (proportional) and when scenario 5 was tested (i.e. westerly components between Cape Columbine (33°S) and Cape Agulhas (20°E) enhanced by 5 cm.s^{-1}, northerly components between Cape Columbine (33°S) and Cape Agulhas (20°E) enhanced by 2 cm.s^{-1}, and elsewhere westerly components enhanced by 2 cm.s^{-1} and northerly components unaltered- "absolute" method).**

POSITION ON FIGURE 7.1	ADVECTION SCENARIO	INTERPOLATED SPEED (cm.s^{-1})	DIRECTION (BEARING IN DEGREES)	COMMENT
1 (weak currents north of Hondeklip Bay)	unaltered	1.1	331	only "absolute" method yielded different resultant
	proportional	1.2	320	
	absolute	2.7	290	
2 (strong north-westerly flow of jet current off Cape Town)	unaltered	21.4	329	both "proportional" and "absolute" methods yielded similar resultants, which differed from unaltered vector
	proportional	24.7	319	
	absolute	25.9	322	
3 (weak currents on CAB)	unaltered	1.3	197	only "absolute" method yielded different resultant
	proportional	1.4	205	
	absolute	2.7	242	
4 (strong offshore currents south-east of Port Elizabeth)	unaltered	12.3	224	resultants varied
	proportional	15.6	236	
	absolute	13.8	230	

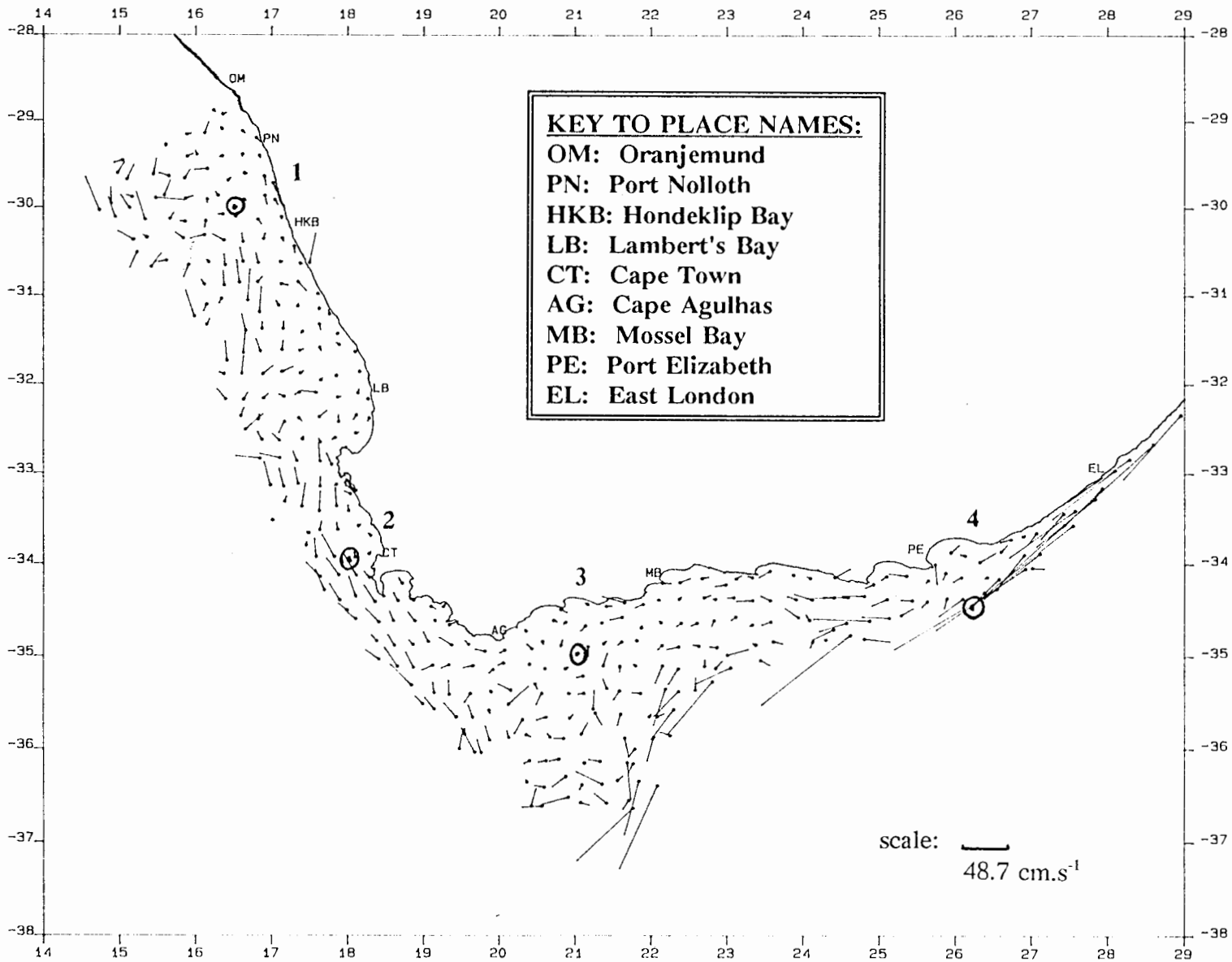

Figure 7.1 Points within the mean 30 and 50 m ADCP velocity field (averaged into quarter degree blocks) at which mean velocity vectors were altered to compare the two methods used to address the effects of altered advection

In total, eight advection scenarios were modelled using spawner distributions from all seven years (Chapters Five and Six). Modelled anchovy year-class strengths and advective losses were correlated with acoustic estimates of year-class strength, in order to find which scenario best modelled observed trends in anchovy recruitment between 1987 and 1993.

Table 7.2 **Correlation coefficients (r) and probability values (p), when model year-class strength under different advection scenarios was correlated with observed year-class strength. Results of correlations of model advective losses with observed year-class strengths are given in parentheses (* indicates significance at the 5% level, ** indicates significance at the 2% level)**

MODELLED ADVECTION SCENARIO	CORRELATION WITH NUMBERS OF RECRUITS (MEASURED ACOUSTICALLY)		CORRELATION WITH BIOMASS OF RECRUITS (MEASURED ACOUSTICALLY)	
	r	p	r	p
reduced westward and northward flow [unaltered ADCP flow field] (scenario 0 of first approach)	0.53 (-0.66)	0.20<p<0.50 (0.10<p<0.20)	0.38 (-0.47)	0.20<p<0.50 (0.20<p<0.50)
normal flow [non El-Niño flow field] (scenario 5 of first approach)	0.36 (-0.77) *	0.20<p<0.50 (0.02<p<0.05)	-0.05 (-0.60)	p>0.50 (0.10<p<0.20)
enhanced westward and northward flow (scenario 6 of first approach)	0.27 (-0.68)	p>0.50 (0.05<p<0.10)	-0.08 (-0.43)	p>0.50 (0.20<p<0.50)
westward flow reduced to 50% of unaltered (second, proportional approach)	-0.27 (0.27)	p>0.50 (p>0.50)	-0.06 (0.12)	p>0.50 (p>0.50)
westward flow reduced to 75% of unaltered (second, proportional approach)	-0.35 (0.23)	0.20<p<0.50 (p>0.50)	-0.10 (0.11)	p>0.50 (p>0.50)
unaltered flow field (original ADCP-based field)	0.53 (-0.66)	0.2<p0.50 (0.10<p<0.20)	0.38 (-0.47)	0.20<p<0.50 (0.20<0.50)
westward flow enhanced to 125% of unaltered (second, proportional approach)	0.46 (-0.67)	0.20<p<0.50 (0.10<p<0.20)	0.31 (-0.47)	0.20<p<0.50 (0.20<p<0.50)
westward flow enhanced to 150% of unaltered (second, proportional approach)	0.87 ** (-0.79) *	0.01<p<0.02 (0.02<0.05)	0.73 (-0.63)	0.05<p<0.10 (0.10<p<0.20)

The first approach showed only weak correlation with observed trends in year-class strength (at most, $0.20<p<0.50$, Table 7.2). In the second approach, whereby westward components were altered proportionally, correlation with measured data improved as westward advection was increased. Westward advection enhanced to 150% over the entire grid yielded model year-class strengths which best correlated to observed year-class strengths (Table 7.2 and Figure 7.2). However, this may simply be due to the small interannual variation shown by this advection scenario (coefficient of variation of 7%, Appendix B, Table B.9, compared to 30% when flow was enhanced by fixed components in Appendix B, Table B.6). Observed year-class strengths correlated negatively with model advective losses under the 150% westward advection scenario.

Correlations between model scenarios and year-class strength in terms of numbers were as significant and often more significant than correlations using biomass estimates (Table 7.2). This is expected since year-class strength was modelled in terms of numbers, and therefore the model does not distinguish between years when young of the year were larger but when there were fewer young of the year, and years when there were many anchovy which were very small.

ADCP data was collected between 1989 and 1993, the period during which the prolonged El-Niño event of 1990/91 to 1992/93 occurred. As discussed in Chapter One, El-Niño events are characterised by weaker south-easterly winds off South Africa, presumably contributing to reduced north-westerly advection in the surface layers of the ocean. In contrast to ADCP data, spawner distributions from which recruitment was modelled spanned the years from 1986 to 1992, and included non-El-Niño years. The 150% westward advection scenario of the

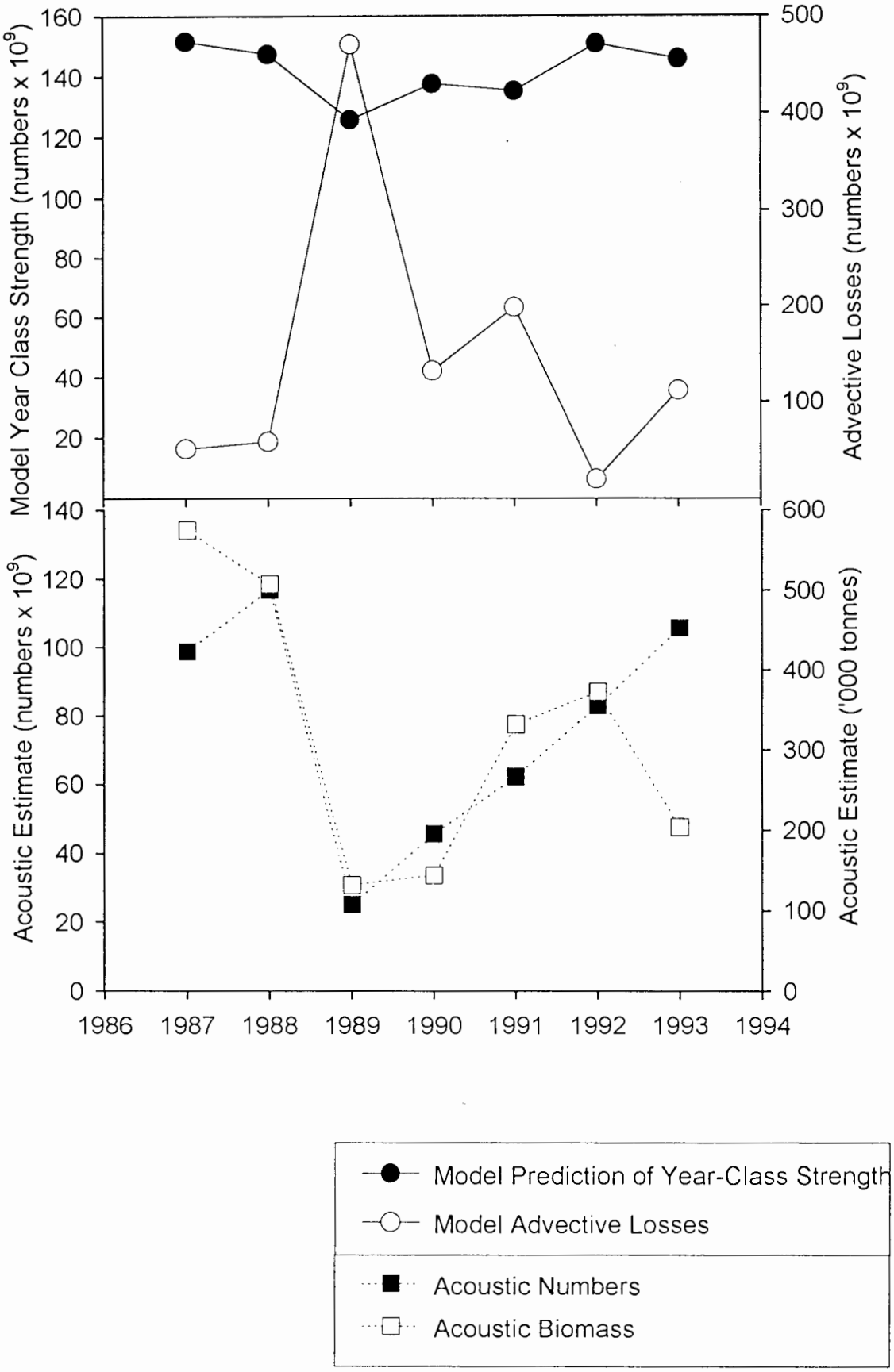

Figure 7.2 **Plot of model year class strength (numbers), year class strength deduced from acoustic surveys (numbers and biomass) and model advective losses in May (note that young of the year were spawned six months earlier, based on the spawner distribution of the previous year)**

second approach accounted for the years in which south-easterly winds were stronger, and possibly for this reason, better represented trends in observed recruitment. Wind-driven currents do not extend to the full depths above the thermocline, and it is likely that the enhanced flow scenario (scenario 6) of the first approach over-compensated for enhanced north-westerly advection of non El-Niño periods.

7.4 THE INFLUENCE OF ADVECTIVE PROCESSES ON TRANSPORT AND ULTIMATELY RECRUITMENT OF ANCHOVY OFF SOUTH AFRICA

Using the model described in this thesis, it is shown that the spatial distribution of adult spawners may influence both the survival, losses by unfavourable advective processes and the distribution of young-of-the-year anchovy. The model shows that the Central Agulhas Bank is an area favourable for survival of anchovy eggs and larvae, since mean currents in this region are weak. On the other hand, regions such as those at the outer edges of the Western and Eastern Agulhas Banks are unfavourable spawning areas, as advection into unproductive waters offshore is likely. Preparations are underway to begin a practical study to explore the findings of this model. Surface drogues to which satellite transmitters are attached will be released and tracked in areas shown by the model to be sensitive to spawning. Through further drogue studies, the possibility will be investigated that anchovy eggs and larvae advected offshore by plumes along the west coast may return to the system via return meanders. The time scales upon which such systems operate are important because anchovy

will starve and therefore not benefit from return transport mechanisms should they remain in unproductive waters for too long.

The model showed that, in the southern Benguela system, the passive transport of anchovy by currents from spawning grounds to nursery areas is a fairly robust process, sensitive only to extreme change. Environmental change may influence advection by altering turbulence levels and/or current vectors, both of which have implications for anchovy transport off South Africa (Chapters Two, Three, Five and Six). Altering the levels of turbulence causes variation in year-class strength. Higher levels of turbulence, changing in amplitude more frequently, cause greater variation than lower, more stable turbulence levels (Chapter Two). Altered advection was shown to have possible impacts on both year-class strength and the distribution of young of the year in particular (Chapters Five and Six). Reduced northward and westward advection lead to strongest year-class strengths and the accumulation of over 50% of young of the year off the west coast between 29oS and Cape Columbine (Chapter Five). The model showed that reducing westward and northward advection leads to larger proportions of young of the year accumulating near the coast or in bays (Chapters Five and Six). In these ways, altered advection may impact on the fishing industry, which has witnessed catches of anchovy between 150 000 and 596 000 tonnes per annum during the seven-year period modelled. It is expected that future studies of the transport mechanisms suggested in section 7.2 and 7.4, and further modelling studies resulting from this work, will improve the ability to predict fluctuations in each forthcoming fishing season, based upon predictions of El-Niño events.

REFERENCES

AGENBAG, J. J. 1992 - A procedure for the computation of sea surface advection velocities from satellite thermal band imagery, with applications to the south east Atlantic ocean. *Ph. D. thesis. University of Cape Town.* 394 p.

ANDERS, A. S. 1965 - Preliminary observations on anchovy spawning off the South African coast. *S. Afr. Shipp. News Fishg Ind. Rev.* **20**(11): 103, 105, 107.

ARMSTRONG, M. [J.], SHELTON, P. [A.], HAMPTON, I., JOLLY, G. [M.] and Y. [C.] MELO 1988 - Egg production estimates of anchovy biomass in the southern Benguela system. *CalCOFI Rep.* **29**: 137-157.

ARMSTRONG, M. J. and R. M. THOMAS 1989 - Clupeoids. In *Oceans of Life off Southern Africa*. Payne, A. I. L. and R. J. M. Crawford (Eds). Cape Town; Vlaeberg: 105-121.

BADENHORST, A. and A. J. BOYD 1980 - Distributional ecology of the larvae and juveniles of the anchovy *Engraulis capensis* Gilchrist in relation to the hydrological environment off South West Africa, 1978/79. *Fish. Bull. S. Afr.* **13**: 83-106.

BAKUN, A. 1990 - Global climate change and intensification of coastal ocean upwelling. *Science, N.Y.* **247**: 198-201.

BAKUN, A. 1994 - Climate change and marine populations: interactions of physical and biological dynamics. Paper presented at the Greenpeace University of Rhode Island "Workshop on the Scope, Significance, and Policy Implications of Global Change and the Marine environment"', 14-17 May.

BANG, N. D. and W. R. H. ANDREWS 1974 - Direct current measurements of a shelf-edge frontal jet in the southern Benguela system. *J. mar. Res.* **32**(3): 405-417.

BARTSCH, J., BRANDER, K., HEATH, M., MUNK, P., RICHARDSON, K. and E. SVENDSEN 1989 - Modelling the advection of herring larvae in the North Sea. *Nature* **340**: 632-636.

BERGH, M. O. and D. S. BUTTERWORTH 1987 - Towards rational harvesting of the South African anchovy considering survey imprecision and recruitment variability. In *The Benguela and Comparable Ecosystems.* Payne, A. I. L., Gulland, J. A. and K. H. Brink (Eds). *S. Afr. J. mar. Sci.* **5**: 937-951.

BERNAL, P. A. 1988 - Consequences of global change for oceans: a review. Paper presented at the IGBP Southern Hemisphere Workshop, Swaziland, 11-16 December.

BERNTSEN, J., SKAGEN, D. W. and E. SVENDSEN 1994 - Modelling the transport of particles in the North Sea with reference to sandeel larvae.
Fish. Oceanogr. 3(2): 81-91.

BJØRKE, H. and R. SÆTRE 1994 - Transport of larvae and juvenile fish into central and northern Norwegian waters. *Fish. Oceanogr.* **3**(2): 106-119.

BLOOMER, S. F. 1994 - Birthdate distributions of anchovy *Engraulis capensis* and sardine *Sardinops ocellata*: implications for recruitment success. Benguela Ecology Programme progress report.

BOYD, A. J. 1980 - A relationship between sea surface temperature variability and anchovy *Engraulis capensis* recruitment off South West Africa, 1970-1978. *Fish. Bull. S. Afr.* **12**: 80-84.

BOYD, A. J. and J. D. HEWITSON 1983 - Distribution of anchovy larvae off the west coast of southern Africa between 32°30' and 26°30'S, 1979-1982. *S. Afr. J. mar. Sci.* **1**: 71-75.

BOYD, A. J., TAUNTON-CLARK, J. and G. P. J. OBERHOLSTER 1992 -Spatial features of the near-surface and midwater circulation patterns off western and southern South Africa and their role in the life histories of various commercially fished species. In *Benguela Trophic Functioning*. Payne, A. I. L., Brink, K. H., Mann, K. H. and R. Hilborn (Eds). *S. Afr. J. mar. Sci.* **12**: 189-206.

BOYD, A. J. and G. P. J. OBERHOLSTER 1994 - Currents off the West and South coasts of South Africa. *S. A. Shipp. News and Fish. Rev.* September/October: 26-28.

BOYD, A. J. and F. A. SHILLINGTON 1994 - Physical forcing and circulation patterns on the Agulhas Bank. *S. Afr. J. Sci.* **90**(3): 114-122.

BOYD, A. J., SHANNON, L. J., SCÜHLEIN, F. H.and J. TAUNTON-CLARK - Food, transport and anchovy recruitment in the Southern Benguela Upwelling System off South Africa. Submitted for publication as part of the procedures of the First International CEOS Meeting entitled "Global versus local changes in upwelling systems", held in California, 6-8 September 1994.

BROWNELL, C. L. 1983 - Laboratory rearing of Cape anchovy *Engraulis capensis* and South African pilchard *Sardinops ocellata* through metamorphosis. *S. Afr. J. mar. Sci.* **1**: 181-188.

BUTLER, J. L., SMITH, P. E. and N. C. H. LO 1993 - The effect of natural variability of life-history parameters on anchovy and sardine population growth. *CalCOFI Rep.* **34**: 104-111.

CRAWFORD, R. J. M. 1980 - Seasonal patterns in South Africa's Western Cape purse-seine fishery. *J. Fish Biol.* **16**(6): 649-664.

CURY, P. and C. ROY 1989 - Optimal environmental window and pelagic fish recruitment in upwelling areas. *Can. J. Fish. aquat. Sci.* **46**: 670-680.

CUSHING, D. H. 1986 - The migration of larval and juvenile fish from spawning ground to nursery ground. *J. Cons. int. Explor. Mer* **43**: 43-49.

CUSHING, D. H. and R. R. DICKSON 1976 - The biological response in the sea to climatic changes. *Adv. mar. Bio.* **14**: 1-122.

DUNCOMBE RAE, C. M., SHANNON, L. V. and F. A. SHILLINGTON 1989 - An Agulhas ring in the South Atlantic ocean. *S. Afr. J. Sci.* 85: 747-748.

DUNCOMBE RAE, C. M., BOYD, A. J. and R. J. M. CRAWFORD 1992 - "Predation" of anchovy by an Agulhas ring: a possible contributory cause for the very poor year-class of 1989. In *Benguela Trophic Functioning*. Payne, A. I. L., Brink, K. H., Mann, K. H. and R. Hilborn (Eds). *S. Afr. J. mar. Sci.* **12**: 167-173.

HAMPTON, I. 1987 - Acoustic study on the abundance and distribution of anchovy spawners and recruits in South African waters. In *The Benguela and Comparable Ecosystems*. Payne, A. I. L., Gulland, J. A. and K. H. Brink (Eds). *S. Afr. J. mar. Sci.* **5**: 901-917.

HAMPTON, I. 1992 - The role of acoustic surveys in the assessment of pelagic fish resources on the South African continental shelf. In *Benguela Trophic Functioning*. Payne, A. I. L., Brink, K. H., Mann, K. H. and R. Hilborn (Eds). *S. Afr. J. mar. Sci.* **12**: 1031-1050.

HEWITT, R. and R. D. METHOT 1982 - Distribution and mortality of northern anchovy larvae in 1978 and 1979. *CalCOFI Rep.* **23**: 226-245.

HSIEH, W. W. and G. J. BOER 1992 - Global climate change and ocean upwelling. *Fish. Oceanogr.* **1**(4): 333-338.

HUNTER, J. R. and S. R. GOLDBERG 1980 - Spawning incidence and batch fecundity in northern anchovy, *Engraulis mordax*. *Fishery Bull., Wash.* **77**(3): 641-652.

HUNTER, J. R. and R. J. H. LEONG 1981 - The spawning energetics of female northern anchovy, *Engraulis mordax*. *Fishery Bull., Wash.* **79**(2): 215-230.

HUNTER, J. R., LO, N. C. H. and R. J. H. LEONG 1985 - Batch fecundity in multiple spawning fishes. In *An Egg Production Method for Estimating Spawning Biomass of Pelagic Fish: Application to the Northern Anchovy, Engraulis mordax*. Lasker, R. (Ed.). *NOAA tech. Rep.* **NMFS 36**: 67-77.

HUNTER, J. R. and B. J. MACEWICZ 1985 - Rates of atresia in the ovary of captive and wild northern anchovy, *Engraulis mordax*. *Fishery Bull., Wash.* **83**(2): 119-136.

HUTCHINGS, J. A., MYERS, R. A. and G. R. LILLY 1993 - Geographic variation in the spawning of Atlantic cod, *Gadus morhua*, in the Northwest Atlantic. *Can. J. Fish. Aquat. Sci.* **50**: 2457-2467.

HUTCHINGS, L. and A. J. BOYD 1992 - Environmental influences on the purse seine fishery in South Africa. *Invest. Presq. (Chile)* **37**: 23-43.

KASAI, A., KISHI, M. J. and T. SUGIMOTO 1992 - Modelling the transport and survival of Japanese sardine larvae in and around the Kuroshio Current. *Fish. Oceanogr.* **1(1)**: 1-10.

KING, D. P. F., ROBERTSON, A. A. and P. A. SHELTON 1978 - Laboratory observations on the early development of the anchovy *Engraulis capensis* from the Cape Peninsula. *Fish. Bull. S. Afr.* **10**: 37-45.

LAMBERTH, R. and G. NELSON 1987 - Field and analytical drogue studies applicable to the St Helena Bay area off South Africa's west coast. In *The Benguela and Comparable Ecosystems*. Payne, A. I. L., Gulland, J. A. and K. H. Brink (Eds). *S. Afr. J. mar. Sci.* **5**: 163-169.

LARGIER, J. L., CHAPMAN, P., PETERSON, W. T. and V. P. SWART 1992 - The western Agulhas Bank: circulation, stratification and ecology. In *Benguela Trophic Functioning*. Payne, A. I. L., Brink, K. H., Mann, K. H. and R. Hilborn (Eds). *S. Afr. J. mar. Sci.* **12**: 319-339.

LASKER, R. 1978 - The relation between oceanographic conditions and larval anchovy food in the California Current: identification of factors contributing to recruitment failure. *Rapp. P-v. Réun. Cons. perm. int. Explor. Mer* **173**: 212-230.

LASKER, R. and P. E. SMITH 1977 - Estimation of the effects of environmental variations on the eggs and larvae of the northern anchovy. *CalCOFI Rep.* **19**: 128-137.

LLUCH-BELDA, D., CRAWFORD, R. J. M., KAWASAKI, T., MacCALL, A. D., PARRISH, R. H., SCHWARTZLOSE, R. A. and P. E. SMITH 1989 - World-wide fluctuations of sardine and anchovy stocks: the regime problem. *S. Afr. J. mar. Sci.* 8: 195-205.

LLUCH-BELDA, D., SCHWARTZLOSE, R. A., SERRA, R., PARRISH, R. [H.], KAWASAKI, T., HEDGECOCK, D. and R. J. M. CRAWFORD 1992 - Sardine and anchovy regime fluctuations of abundance in four regions of the world oceans: a workshop report. *Fish. Oceanogr.* **1**(4): 339-347.

LO, N. C. H. 1985 - A model for temperature-dependent northern anchovy egg development and an automated procedure for the assignment of age to staged eggs. In LASKER, R. (ed.) - An egg production method for estimating spawning biomass of pelagic fish: Application to the northern anchovy, *Engraulis mordax*. *US Department of Commerce, NOAA Technical Report NMFS* **36**: 43-50.

LUTJEHARMS, J. R. E. and R. C. VAN BALLEGOOYEN 1988 - The retroflection of the Agulhas Current. *J. phys. Oceanogr.* **18**(11): 1570-1583.

LUTJEHARMS, J. R. E., CATZEL, R. and H. R. VALENTINE 1989 - Eddies and other boundary phenomena of the Agulhas current. *Continent. Shelf Res.* **9**(7): 597-616.

LUTJEHARMS, J. R. E., SHILLINGTON, F. A. and C. M. DUNCOMBE RAE 1991 - Observations of extreme upwelling filaments in the Southeast Atlantic Ocean. *Science, N.Y.* **253**(5021): 774-776.

MEEHL, G. A., BRANSTATOR, G. W. and W. M. WASHINGTON 1993 - Tropical Pacific interannual variability and CO_2 climate change. *J. Climate* **6**: 42-63.

MELO, Y. C. 1992 - The biology of the anchovy *Engraulis capensis* in the Benguela Current region. *Ph.D. thesis, University of Stellenbosch*. xii + 180 pp.

MELO, Y. C. 1994 - Spawning frequency of the anchovy *Engraulis capensis*. *S. Afr. J. mar. Sci.* **14**: 321-331.

NELSON, G. 1983 - Circulation over the shelf zone of the Cape Peninsula region. *S. Afr. J. Sci.* **79**(4): 147.

NELSON, G. 1989 - Poleward motion in the Benguela area. In *Poleward Flows along Eastern Ocean Boundaries*. Neshyba, S. J., Mooers, C. N. K., Smith, R. L. and R. T. Barber (Eds). New York; Springer: 110-130 (Coastal and Estuarine Studies **34**).

NELSON, G. 1991 - An equatorward jet west of Cape Town. Abstract IAPSO Proceedings XX Assembly Vienna 1991 p189.

NELSON, G. 1992 - Equatorward wind and atmospheric pressure spectra as metrics for primary productivity in the Benguela system. In *Benguela Trophic Functioning*. Payne, A. I. L., Brink, K. H., Mann, K. H. and R. Hilborn (Eds). *S. Afr. J. mar. Sci.* **12**: 19-28.

NELSON, G. and L. HUTCHINGS 1987 - Passive transportation of pelagic system components in the southern Benguela area. In *The Benguela and Comparable Ecosystems.* Payne, A. I. L., Gulland, J. A. and K. H. Brink (Eds). *S. Afr. J. mar. Sci.* **5**: 223-234.

NELSON, G. and A. POLITO 1987 - Information on currents in the Cape Peninsula area, South Africa. In *The Benguela and Comparable Ecosystems*. Payne, A. I. L., Gulland, J. A. and K. H. Brink (Eds). *S. Afr. J. mar. Sci.* **5**: 287-304.

NORCROSS, B. L. and R. F. SHAW 1984 - Oceanic and estuarine transport of fish eggs and larvae: a review. *Trans. Am. Fish. Soc.* **113**(2): 153-165.

O'TOOLE, M. [J.] and I. HAMPTON 1989 -New prospects for surveying and sampling anchovy pre-recruits. *S. Afr. Shipp. News Fishg Ind. Rev.* **44**(5): 32-33.

PARRISH, R. H., NELSON, C. S. and A. BAKUN 1981 - Transport mechanisms and reproductive success of fishes in the California Current. *Biol. Oceanogr.* **1**(2): 175-203.

PARRISH, R. H., BAKUN, A., HUSBY, D. M. and C. S. NELSON 1983 - Comparative climatology of selected environmental processes in relation to eastern boundary current pelagic fish reproduction. In *Proceedings of the Expert Consultation to Examine Changes in Abundance and Species Composition of Neritic Fish Resources, San José, Costa Rica, April 1983.* Sharp, G. D. and J. Csirke (Eds). *F.A.O. Fish. Rep.* **291**(3):731-777.

PARRISH, R. H., MALLICOATE, D. L. and R. A. KLINGBEIL 1986 - Age dependent fecundity, number of spawnings per year, sex ratio, and maturation stages in northern anchovy, *Engraulis mordax. Fishery Bull., Wash.* **84**(3): 503-517.

PIQUELLE, S. J. and HEWITT, R. P. 1983 - The northern anchovy spawning biomass for the 1982-83 Californian fishing season. *CalCOFI Rep.* **24**: 16-28.

POWER, J. H. 1986 - A model of the drift of northern anchovy, Engraulis mordax, larvae in the California Current. *Fish. Bull. natn. mar. Fish. Serv., U.S.* **84**: 585-603.

RAISZ, E. 1948 - *General Cartography*, 2nd ed. New York; McGraw-Hill Book Company: xiii+718pp.

ROBERTS, M. 1993 - The cool ridge on the Eastern Agulhas Bank and its link to coastal upwelling. Abstracts of the 8th Southern African Marine Science Symposium, held in Langebaan, South Africa, 17-22 October.

SHACKLETON, L. Y. 1987 - A comparative study of fossil fish scales from three upwelling regions. In *The Benguela and Comparable Ecosystems.* Payne, A. I. L., Gulland, J. A. and K. H. Brink (Eds). *S. Afr. J. mar. Sci.* 5: 79-84.

SHANNON, L. V. 1985 - The Benguela ecosystem. 1. Evolution of the Benguela, physical features and processes. In *Oceanography and Marine Biology. An Annual Review* 23. Barnes, M. (Ed.). Aberdeen; University Press: 105-182.

SHANNON, L. V. 1989 - The physical environment. In *Oceans of Life off Southern Africa*. Payne, A. I. L. and R. J. M. Crawford (Eds). Cape Town; Vlaeberg: 12-27.

SHANNON, L. V., WALTERS, N. M. and S. A. MOSTERT 1985 - Satellite observations of surface temperature and near-surface chlorophyll in the southern Benguela region. In *South African Ocean Colour and Upwelling Experiment.* Shannon, L. V. (Ed.). Cape Town; Sea Fisheries research Institute: 183-210.

SHANNON, L. V., CRAWFORD, R. J. M., BRUNDRIT, G. B. and L. G. UNDERHILL 1988 - Responses of fish populations in the Benguela ecosystem to environmental change. *J. Cons. perm. int. Explor. Mer* **45**(1): 5-12.

SHANNON, L. V. and G. NELSON (in press) - The Benguela: large scale features and processes and system variability.

SHELTON, P. A. 1979 - The effect of environmental factors on spawning and recruitment of the anchovy *Engraulis capensis* Gilchrist compared with the lightfish *Maurolicus muelleri* (Gmelin). M.Sc. thesis, University of Cape Town: iii + 75 pp. + Appendices 2 & 3.

SHELTON, P. A. and L. HUTCHINGS 1982 - Transport of anchovy, *Engraulis capensis* Gilchrist, eggs and early larvae by a frontal jet current. *J. Cons. perm. int. Explor. Mer* **40**(2): 185-198.

SHELTON, P. A., BOYD, A. J. and M. J. ARMSTRONG 1985 - The influence of large-scale environmental processes on neritic fish populations in the Benguela Current system. *CalCOFI Rep.* **26**: 72-92.

SHILLINGTON, F. A., HUTCHINGS, L., PROBYN, T. A., WALDRON, H. N. and W. T. PETERSON 1992 - Filaments and the Benguela frontal zone: offshore advection or recirculating loops? In *Benguela Trophic Functioning*. Payne, A. I. L., Brink, K. H., Mann, K. H. and R. Hilborn (Eds). *S. Afr. J. mar. Sci.* **12**: 207-218.

SIEGFRIED, W. R., CRAWFORD, R. J. M., SHANNON, L. V., POLLOCK, D. E., PAYNE, A. I. L. and R. G. KROHN 1990 - Scenarios for global-warming induced change in the open-ocean environment and selected fisheries of the west coast of Southern Africa. *S. Afr. J. Sci.* **86**: 281-285.

SINCLAIR, M. and TREMBLAY, M. J. 1984 - Timing of spawning of Atlantic herring (*Clupea harengus harengus*) and the match/mismatch theory. *Can. J. Fish. Aquat. Sci.* **41**: 1054-1065.

SMITH, P. E. 1985 - Year-class strength and survival of 0-group clupeoids. *Can. J. Fish. aquat. Sci.* **42**(Suppl. 1): 69-82.

SWART, V. P. and J. L. LARGIER 1987 - Thermal structure of Agulhas Bank Water. *CalCOFI Rep.* **26**: 72-92. In *The Benguela and Comparable Ecosystems.* Payne, A. I. L., Gulland, J. A. and K. H. Brink (Eds). *S. Afr. J. mar. Sci.* **5**: 79-84.

VALDÉS SZEINFELD, E. [S.] 1991 - Cannibalism and intraguild predation in clupeoids. *Mar. Ecol. Prog. Ser.* **79**: 17-26.

VALDÉS, E. S., SHELTON, P. A., ARMSTRONG, M. J. and J. G. FIELD 1987 - Cannibalism in South African anchovy: egg mortality and egg consumption rates. In *The Benguela and Comparable Ecosystems*. Payne, A. I. L., Gulland, J. A. and K. H. Brink (Eds). *S. Afr. J. mar. Sci.* **5**: 613-622.

VALDÉS SZEINFELD, E. S. and K. L. COCHRANE 1992 - The potential effects of cannibalism and intraguild predation on anchovy recruitment and clupeoid fluctuations. In *Benguela Trophic Functioning*. Payne, A. I. L., Brink, K. H., Mann, K. H. and R. Hilborn (Eds). *S. Afr. J. mar. Sci.* **12**: 695-702.

VALDÉS SZEINFELD, E. S. and Y.C. MELO (unpublished) - Fecundity of the Cape anchovy *Engraulis capensis*.

WALTERS, C. J., HANNAH, C. G. and K. THOMSON 1992 - A microcomputer program for simulating effects of physical transport processes on fish larvae. *Fish. Oceanog.* **1**(1): 11-19.

WALTERS, C. J. 1984 - Managing fisheries under biological uncertainty. In *Exploitation of Marine Communities*. May, R. M. (Ed.). Berlin; Springer: 263-274 (Report of the Dahlem Workshop on Exploitation of Marine Communities, Berlin, April 1984).

ZEBIAK, S.E and M. A. CANE. 1991 -Natural climate variability in a coupled model. pp. 457-469. In *Greenhouse-gas-induced Climate Change: a critical appraisal of Simulations and Observations*. Schlesinger (ed.). Elsevier, New York.

APPENDIX A

MANUAL FOR USE OF THE MODEL

The structure of the model is indicated as a flow diagram in Figure A.1. The model is comprised of three main programs. The first, **ANSHELL.EXE**, facilitates the construction of the necessary run-time information files for the second and third programmes, namely **AUXIL.EXE** and **MONTY.EXE**, and controls their execution.

1. ANSHELL.EXE

a) FUNCTION OF ANSHELL.EXE

This is a shell program for scheduling the other programs of the model. The following can be constructed using this program:

i) **Pilot_an.dat** (fixed name). ANSHELL.EXE initiates the program ANPILOT.EXE which constructs the file specifying batch tracking and graphics display options for MONTY.EXE.

ii) **Rls_tst.dat** (variable name) containing the release site for a batch, seed integer for random number generation, batch size and time at which each batch is to be released in MONTY.EXE. This file is constructed or appended to by the program ANED_RM.EXE or edited or merged with another release file by the program ANED_RE.EXE.

iii) **Coast.dat** (variable name) containing the information required to draw the coastline on the output screen when MONTY.EXE is run. COAST.EXE is the program initiated by ANSHELL.EXE to construct this file.

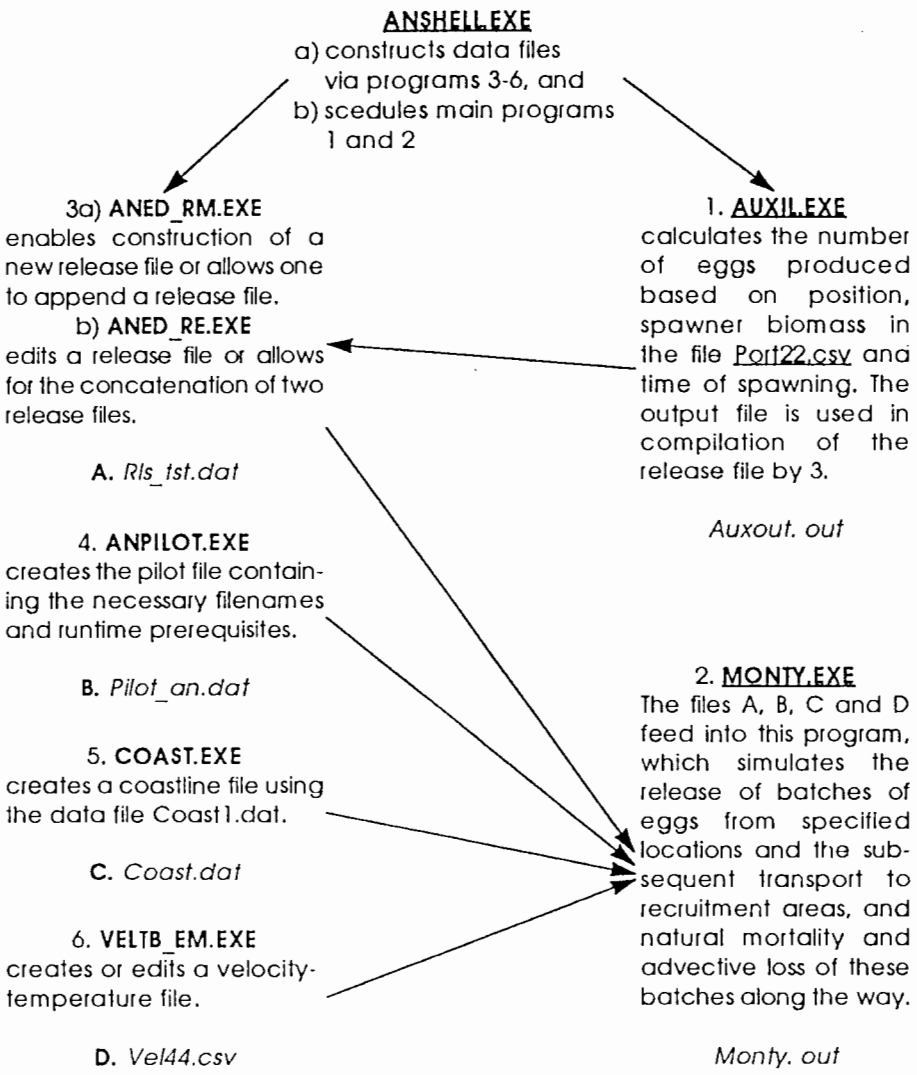

Figure A.1 Flow diagram showing the structure of the model (the three main programs are underlined, all programs are in bold and output files of these programs are in italics)

iv) **Veltbx.dat** (variable name), which for each block in the grid, contains easterly (u) and northerly (v) velocity components, temperature of water above the thermocline, a biomass label corresponding to a record in the biomass file, and a place label indicating whether the block is on land, offshore or beyond a boundary. For these data to be read as arrays by AUXIL.EXE and MONTY.EXE they must be integers; hence the vectors are entered in the data file as values in $cm.s^{-1}X10^2$ and temperature as °CX10 and are later correctly scaled in the programmes.

Veltbx.dat is made or edited by the program VELTB_EM.EXE. A non-zero biomass label refers to a record number in the spawner biomass data file (e.g. **Port22.csv**), a file independently constructed and containing historical spawner biomass sequences for each block. The place labels are used in the boundary checks in MONTY.EXE and AUXIL.EXE.

b) DETAILED INSTRUCTIONS FOR THE USE OF ANSHELL.EXE

To run the programme type "ANSHELL". An information screen will appear, press <enter> for the next information screen, and <enter> again to get to the menu. You may now choose to construct data files by typing the letter in the menu for construction of a pilot data file, release file, coastline file or velocity-temperature file. Similarly, you may view existing files ("v") or choose to run programmes by simply pressing <enter>.

Instructions for the use of data file construction programmes, invoked through ANSHELL.EXE

i) ANPILOT.EXE constructs the pilot file Pilot_an.dat

This program requires the operator to make choices regarding the diffusion amplitude (*da*), turbulence amplitude (*ta*), lapse time (*lapse*), auto graph scaling (*l3*), track display (*l4*), pixel size (*l5*), creation of an output file for MONTY.EXE (*l6*), the number of days to run (*dy*), the first (*r1*) and last (*rn*) records to be read from the release file, the release file name (*rlnm*), the coastline filename (*csnm*), the velocity_temperature file name (*vltnm*), the hours to hatching (*D*), days to prerecruitment (*Dp*) and days to recruitment (*Dr*).

By pressing the character "**A**" which toggles to "yes" or "no", the operator can choose whether diffusion is added as a Monte Carlo component to the ADCP velocity vectors in the grid. Using the character "**B**" the diffusion amplitude can be toggled from 0.0 to 0.9 $cm.s^{-1}$. MONTY.EXE then randomly selects a proportion of this amplitude based on a rectangular distribution on (0,1) and adds it to the ADCP vectors calculated from the linear interpolation. "**C**" toggles to "yes" or "no" to choose whether turbulence is added to the ADCP vectors. "**D**" enables the turbulence amplitude to be entered in $cm.s^{-1}$. Sensible values for turbulence amplitudes lie between 0 and 25 $cm.s^{-1}$. "**E**" enables the operator to enter the turbulence lapse time in hours. MONTY.EXE then randomly selects a proportion of the turbulence amplitude based on a rectangular distribution on (0,1) and adds it to the ADCP vectors calculated from the linear interpolation every "*lapse*" hours.

"**F**" toggles to "yes" for the use of auto graph scaling on the output screen of MONTY.EXE or to "no" for MONTY.EXE to require the operator to enter a graph scaling factor manually. "**G**" toggles to "yes" for the route along which each batch is transported in MONTY.EXE to be tracked on the output screen or to "no" for the release point of each batch to be marked with a "X" and the end point to be marked with a pixel. "**H**" toggles to "yes" if the end pixel is to be enlarged, to "no" if a smaller end pixel is preferred.

"**I**" toggles to "yes" for an output file **Monty.out** to be created after all specified batches have been processed by MONTY.EXE. By pressing "**J**" the number of days for which each batch is to be transported in MONTY.EXE can be entered as an integer. A value of 180 days, for example, will track the batches from spawning to the age at which anchovy should be recruits. **It is important to note that the choice of this value is vital to the end values obtained for year-class strength and mortality by MONTY.EXE.**

The operator can enter the first and last records in the release file that are to be processed by MONTY.EXE by pressing "**L**" and "**M**" respectively. These values must obviously be integers. Pressing "**K**", "**N**" and "**O**" allow the release file name, coastline file name and velocity-temperature file name to be entered.

The number of hours from spawning to hatching is entered by pressing "**P**". This value should be taken from the output file created by AUXIL.EXE and in this version of the model is based on a constant temperature field throughout the grid. The number of days from spawning until larvae become prerecruits (*Dp*) and the number of days until prerecruits recruit to the purse seine fishery (*Dr*) are entered as integers after pressing "Q" and "**R**" respectively.

Sensible values of *Dp* and *Dr* are 101 and 180 days respectively (refer to the discussion in the background section of this document).

ii) ANED_RM.EXE and ANED_RE.EXE constructs the release file Rls_tst.dat

ANED_RM.EXE may be used for constructing or appending to the release file. After choosing "**N**" to create a new release file or "**A**" to append to an existing release file, the operator then chooses from the new purple window that appears; "**N**" to add a new line to the file, "**H**" to obtain more help on using the program or "**E**" to end the session. If "**N**" is chosen the operator is then required to enter the following:

1) Co-ordinates of the release point (x,y) in kilometres along the x and y axes upon which the grid is based. Note that x ranges from 0km (15°E) to 1466km (28°E) and y ranges from 0km (29°S) to 856km (36.75°S) if the files **Vel44.csv** and **Port22.csv** are used.

2) The seed integer (*seed*) for the batch in question. *Seed* specifies a particular sequence of random numbers generated for use in the Monte Carlo part of MONTY.EXE. This allows the same set of conditions to be simulated again if required.

3) The colour of the track, *tclr*, (if chosen) or the start and end pixels (if tracking is switched off). On the right of the user screen a colour test pattern is displayed to aid in this choice.

4) T_0, the time in hours after the start of the flow field to release of the batch in question. This should not be confused with the time from the start of the spawning

season to spawning of the batch, as required in the calculation of the spawning fraction in AUXIL.EXE. T_0 is included in anticipation of later versions of the model which will use time-dependent velocity fields. In MONTY.EXE, random perturbations of the velocity field require that the velocity algorithms (pages A25 and A26) are stepped through until t_0 is reached, in order to preserve comparison of releases at different times at the same point. However, t_0 is also presently set to zero as the flow field is static at this stage.

5) The number of eggs divided by 10^4, as obtained from the output file created when running AUXIL.EXE.

ANED_RE.EXE is an editor written to facilitate the editing of a release file that already exists or the merging of two existing release files. Like **ANED_RM.EXE**, it is user-friendly and self explanatory.

iii) COAST.EXE constructs the coastline file Coast.dat

This program constructs a file required by MONTY.EXE to draw the South African coastline from a data file, **Coast1.dat**. When the program is executed, an information screen appears and the operator is then presented with an input screen containing various choices. By typing the character displayed the operator can enter a value of his/her choice.

The program uses a portion of the data file **Coast1.dat** to draw the coastline; the prescribed number of points (option "**E**") are skipped and the number of subsequent points chosen ("**F**") are used. The boundary of the coastline is closed by returning to the initial point to allow the

map to be filled. A correctly positioned ("**C**" and "**D**") coastline may be drawn to the desired scale ("**A**" and "**B**"), rotated if desired ("**I**") and a research area may be demarcated ("**J**"). Demarcation of the research area serves as a useful reference to the rectangular grid used in the model. The output file ("**G**" and "**H**") is coded to distinguish the coastline from the research box. Through trial and error, the desired coastline can be created.

iv) VELTB_EM.EXE constructs the velocity-temperature file e.g. Vel44.csv

This program is particularly helpful to "beginners" as it guides the user through the task of compiling a velocity-temperature data file to be read by MONTY.EXE and AUXIL.EXE. The velocity-temperature file consists of a series of lines, each representing a single block. The end of a row is recognised by all entries in a block being set to 0. Each line contains 5 variables in the following order: the northerly velocity component (v) in $cm.s^{-1}$ multiplied by 10^2, the easterly velocity component (u) in $cm.s^{-1}$ multiplied by 10^2, the temperature in °C multiplied by 10, the biomass label (refer to page A2) and the place label. A place label of 2 indicates a block on land, a label of 1 refers to an oceanic block with or without ADCP data and a label of 0 defines end-of-row marker blocks and blocks outside the boundaries of the grid but within the program memory. Place labels are used in the boundary checks performed in MONTY.EXE and AUXIL.EXE.

When VELTB_EM.EXE is run, three information screens appear, followed by the input screen. The operator is presented with four choices: "**N**" to make a new file, "**E**" to edit an existing file, "**A**" to append to an existing file and "**Q**" to quit. Selecting "**N**" allows the

operator to choose between entering velocities in the orthogonal form (northerly and easterly velocity components) or the polar form (speed and direction). In the latter case, the orthogonal values are calculated by the program and should this file later be edited or appended, orthogonal values must be entered.

The first line in the velocity-temperature file must contain the block width in kilometres along the x-axis, followed by the block length in kilometres along the y-axis. The file **Vel44.csv** which is based on a 0.25 by 0.25 degree (15 by 15 minutes) grid has block widths of 28.2km and block lengths of 27.6km. These dimensions were derived using the equations presented by Raisz (1948) to calculate the length of one degree of latitude and longitude at a given latitude. For simplicity, the latitude in the middle of the latitude range of the grid, viz 33°S, was used and block size at this latitude was taken to be the constant block size throughout the grid.

After entering data for each block, the operator has three options: "**D**" to enter more data, "**R**" to begin a new row" and "**E**" to end the session. If "**R**" is selected, the program automatically enters an end-of-row marker block of zeroes. Since the file is coded by VELTB_EM.EXE, the novice may have difficulty if he/she elects to use a spreadsheet to compile the file, and it is strongly advised that the beginner rather uses this editor. Note that because of irregularity of the coastline, the interpolation scheme described later in this document requires that a "dummy" land block (having zero velocities, non-zero temperature and a place label of 2) is inserted immediately before the end of a row is signalled. For a file based on the same grid as **Vel44.csv**, for example, the rows 1 to 16 require such blocks (Figure A.2), and these must be entered prior to beginning a new row ("**R**").

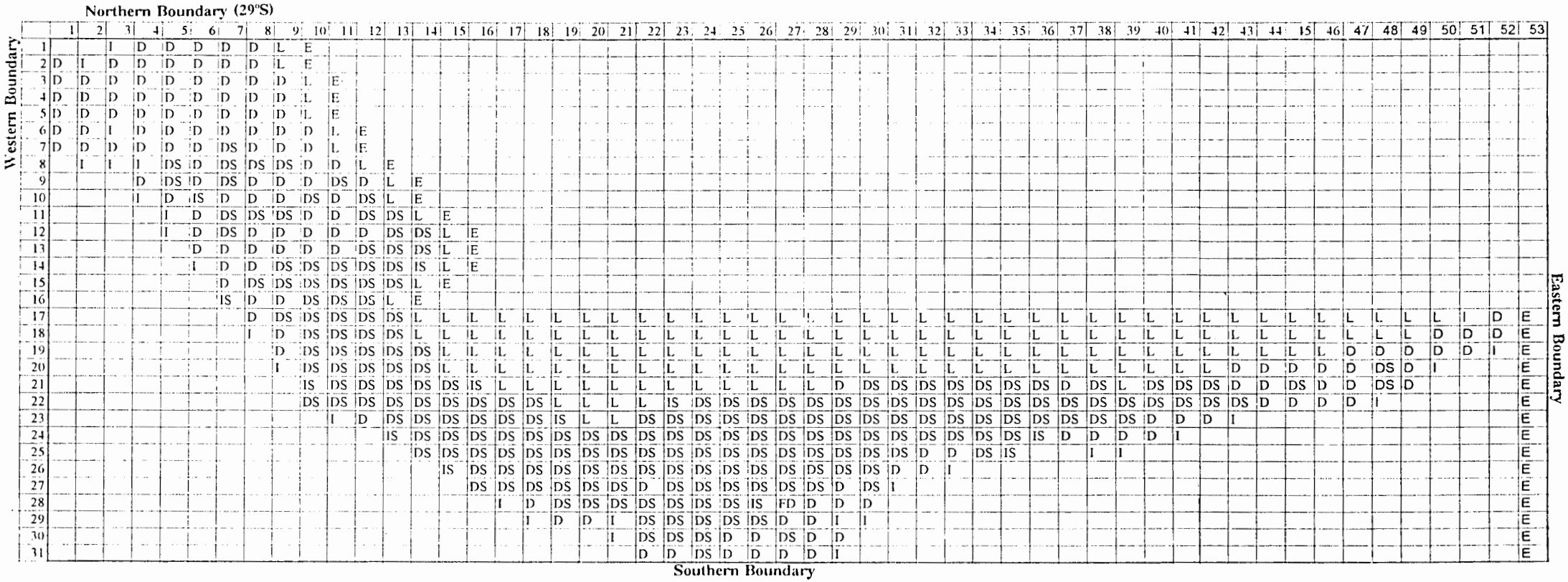

	1	2	3	4	5	6	7	8	9	10	11	12	13	14	15	16	17	18	19	20	21	22	23	24	25	26	27	28	29	30	31	32	33	34	35	36	37	38	39	40	41	42	43	44	45	46	47	48	49	50	51	52	53
1			I	D	D	D	D	D	L	E																																										
2	D	I	D	D	D	D	D	D	L	E																																										
3	D	D	D	D	D	D	D	D	D	L	E																																									
4	D	D	D	D	D	D	D	D	D	L	E																																									
5	D	D	D	D	D	D	D	D	D	L	E																																									
6	D	D	I	D	D	D	D	D	D	D	L	E																																								
7	D	D	D	D	D	D	DS	D	D	D	L	E																																								
8		I	I	I	DS	D	DS	DS	DS	D	D	L	E																																						
9				D	DS	D	DS	D	D	D	DS	D	L	E																																					
10				I	D	IS	D	D	D	DS	D	DS	L	E																																					
11					I	D	DS	DS	DS	D	D	DS	DS	L	E																																				
12					I	D	DS	D	D	D	D	D	DS	DS	L	E																																			
13						D	D	D	D	D	D	DS	DS	DS	L	E																																			
14						I	D	D	DS	DS	DS	DS	DS	IS	L	E																																			
15							D	DS	DS	DS	DS	DS	DS	L	E																																				
16							IS	D	D	DS	DS	DS	L	E																																					
17								D	DS	DS	DS	DS	DS	L	L	L	L	L	L	L	L	L	L	L	L	L	L	L	L	L	L	L	L	L	L	L	L	L	L	L	L	L	L	L	L	L	L	I	D	E
18								I	D	DS	DS	DS	DS	L	L	L	L	L	L	L	L	L	L	L	L	L	L	L	L	L	L	L	L	L	L	L	L	L	L	L	L	L	L	L	L	L	D	D	D	E
19									D	DS	DS	DS	DS	DS	L	L	L	L	L	L	L	L	L	L	L	L	L	L	L	L	L	L	L	L	L	L	L	L	L	L	L	L	L	L	L	D	D	D	D	D	I	E
20									I	DS	DS	DS	DS	DS	L	L	L	L	L	L	L	L	L	L	L	L	L	L	L	L	L	L	L	L	L	L	L	L	L	L	L	L	D	D	D	D	D	DS	D	I			E
21										IS	DS	DS	DS	DS	DS	IS	L	L	L	L	L	L	L	L	L	L	L	L	D	DS	DS	DS	DS	DS	DS	DS	D	DS	L	DS	DS	DS	D	D	DS	D	D	DS	D				E
22										DS	DS	DS	DS	DS	DS	DS	DS	DS	L	L	L	L	IS	DS	DS	DS	DS	DS	DS	DS	DS	DS	DS	DS	DS	DS	DS	DS	DS	DS	DS	DS	DS	D	D	D	D	I						E
23											I	D	DS	DS	DS	DS	DS	IS	L	L	DS	DS	DS	DS	DS	DS	DS	DS	DS	DS	DS	DS	DS	DS	DS	DS	DS	DS	D	D	I													E
24													IS	DS	DS	DS	DS	DS	DS	DS	DS	DS	DS	DS	DS	DS	DS	DS	DS	DS	DS	DS	DS	DS	DS	IS	D	D	D	D	I													E
25														DS	DS	DS	DS	DS	DS	DS	DS	DS	DS	DS	DS	DS	DS	DS	DS	DS	DS	D	D	DS	IS			I	I														E
26															IS	DS	DS	DS	DS	DS	DS	DS	DS	DS	DS	DS	DS	DS	DS	DS	D	D	I																			E
27																DS	DS	DS	DS	DS	DS	D	DS	DS	DS	DS	DS	DS	D	DS	I																				E
28																	I	D	DS	DS	DS	DS	DS	DS	DS	IS	FD	D	D	D																					E
29																		I	D	D	I	DS	DS	DS	DS	DS	D	D	I	I																						E
30																					I	DS	DS	DS	D	D	DS	D	D																							E
31																						D	D	DS	D	D	D	D	I																							E

KEY:

DS:	blocks with *ADCP data available* and where *spawning occurred* in November (month of peak spawning) during at least one of the seven years between 1986 and 1992
IS:	blocks with *interpolated current data* and where *spawning occurred* in November during at least one of the seven years
D:	blocks with *ADCP data available* and where *spawning did not occur* in November during any of the seven years
I:	blocks with *interpolated current data* and where *spawning did not occur* in November during any of the seven years
:	blocks with *no current data* and where *spawning did not occur* in November during any of the seven years
L:	block signalling the land
E:	end of row marker

Figure A.2 Diagram showing the layout of the velocity-temperature file *VEL44.CSV* (numbers indicate rows and columns)

2. AUXIL.EXE

a) FUNCTION OF AUXIL.EXE

The program AUXIL.EXE calculates egg production at the release site stipulated by the operator when creating the release file Rls_tst.dat. The number of eggs produced per night at a particular location is a function of spawner biomass at that site, which depends on the random selection of one of the seven available spawner biomass distributions. In addition egg production depends on batch fecundity, the proportion of females, average female weight and the spawner fraction, which in turn depends on the time within the spawning season. **An output file called Auxout.out**, containing the position and block where spawning occurred, the number of eggs spawned there per hour and the time in hours from spawning until hatching, is created for use in the compilation of the release file **Rls_tst.dat**.

b) DATA SOURCES AND VARIABLES

i) SPAWNER BIOMASS DATA PREPARATION

In order to investigate recruitment resulting from a fixed spawner biomass while accounting for observed spawner biomass distributions, the following steps were taken:

i) Anchovy density, position and interval length (over which acoustic data were integrated) from October, November and December for each year were extracted from Sea Fisheries Research Institute's ACOUSDAT.DAT database using the program

EXTRACT.PAS written by Mark Prowse (Sea Fisheries Research Institute). Data for most of October 1991 were not good and were therefore omitted. Unfortunately there was a problem with the 1984 and 1985 data and for this reason only anchovy spawner distributions of the seven years from 1986 to 1992 were used.

ii) Average anchovy density weighted by interval length (distance over which biomass was estimated during acoustic survey) was calculated for each 0.25 by 0.25 degree block in each year using the program **DENSITY.EXE.**

iii) The average weighted density in each block was then converted to a fraction of the total sum of weighted densities for that year and multiplied by the average spawner biomass for the nine-year period (Table 2.1, Chapter Two), using the program **PORTION.EXE**. These data files were merged into **Port22.csv** and biomass values were multiplied by 10^3 so as to be read into AUXIL.EXE as an array of integers. Despite the fact that only seven years' spatial distributions were modelled, the nine-year mean spawner biomass was used as it was felt this gave a better estimate than the shorter time-series.

AUXIL.EXE therefore chooses one of the seven spawner biomass distributions at random (using TURBO PASCAL'S random number generator) to be used in the egg production calculation. RELEASE5.EXE (described below) simply cycles through all biomass data available for a particular year, calculating daily egg production for each block where spawners were found.

ii) EGG PRODUCTION CALCULATION

In MONTY.EXE egg production (E) in a particular block is calculated per hour according to the following:

$$E = \frac{sb^{hrs} \times \frac{B}{W} \times r \times S \times f}{24.0}$$

.....equation A.1

where B is the spawner biomass in the block in question (**Port22.csv**), W is the mean female weight, r is the female proportion, S is the spawner fraction, f is the batch fecundity, sb is the hourly survival rate of spawners and hrs is the number of hours from start of the spawning season (t_s) to the time of spawning (t_0), i.e. $hrs=t_0-t_s$.

The number of spawning female anchovies in a block is calculated as the product of the spawner biomass in that block (**Port22.csv**) and the female proportion (by mass) divided by the mean weight of a female anchovy.

In order to simulate the release of all eggs spawned in all areas in all seven years, so that the calculated (model) number of anchovy surviving to recruitment can be compared with the observed recruitment over these seven years, AUXIL.EXE was modified into **RELEASE5.EXE**. Release files are compiled by calculating egg production as follows. A year is selected, biomass in all blocks having non-zero biolabels and with biomass data in that year is extracted. For each of these blocks, **daily** egg production is calculated for each day of the spawning season (1 October to 31 March). Batches are released daily rather than hourly

in order to facilitate faster running of the large release files. Release sites are the mid-points of blocks. The program **PREPRAN.EXE** was used to prepare the output file made by RELEASE5.EXE for the running of MONTY.EXE. It allocates random seed integers to each record in the release file, using TURBO PASCAL'S *Random* function.

c) INSTRUCTIONS FOR THE USE OF AUXIL.EXE

1. Enter the names of the velocity-temperature file (**Vel44.csv** for example) and the spawner biomass file (**Port22.csv** for example). If the file does not exist a message pops up on the screen and the operator may try another file instead.
2. A message appears warning the operator to rename the last output file called **Auxout.out** if he/she wishes to retain the old file.
3. Enter the x and y co-ordinates (in kilometres) of the point where spawning is to occur. Note that x ranges from 0km (15°E) to 1466km (28°E) and y ranges from 0km (29°S) to 856km (36.75°S) if the files **Vel44.csv** and **Port22.csv** are used. Figure A.2 is a useful reference if the latter two files are used.
4. The box [i0,j0] in which the chosen point falls (i refers to the row (along the y-axis) and j refers to the column (along the x-axis) is displayed on the screen, as are the proximate row (i1) and column (j1), c1x,c2x,c1y and c2y required for the interpolation process described on pages A25 and A26. In addition, the interpolated easterly velocity (Uu) and northerly velocity (Vv) components, the interpolated temperature, the biomass label and the place label of block [i0,j0] are displayed. Recall that a place label of 1 indicates that the block [i0,j0] is in the ocean, 2 indicates that the block is

on land and 0 that the block lies beyond the boundaries of the grid, lacks ADCP data or is an end-of row marker block.

5. If spawning occurred in the block [i0,j0] in at least one of the seven years from 1986 to 1992, i.e. the biomass label is non-zero, the spawner biomass in this block in kilotonsX10^3 (i.e. thousands of kilotons) is shown for each year and that of a randomly selected year is highlighted. This random selection is made using TURBO PASCAL'S *Random* function. If spawning did not occur in this block in any of the seven years the operator is informed.

In both cases, the operator still has the option of entering a different spawner biomass to that returned using the biomass data in the input file. Note that biomass MUST be entered as kilotonsX10^3, i.e. as an integer. Figure A.2 shows in which blocks spawning occurred in one or more of the seven years. Refer to pages A10 and A11 for the explanation of how spawner biomass was extracted from Sea Fisheries Research Institute records.

6. The next step is to choose the day on which spawning is to occur and in so doing, to obtain the corresponding spawning fraction. This is accomplished by toggling the "+" key to a day subsequent to 1 November and the "-" key to return a day prior to 1 November. The spawning fraction (S) is displayed and corresponds to the chosen day, as computed using the hyperbolic tangent function described in Chapter Two (pages 15-16) of this thesis.

7. At this stage the operator may change any of the biological parameters: female proportion (r), average female weight (W), batch fecundity (f) or hourly spawner survival rate (V).

8. Egg production based on the choice of parameter values, day of spawning and the spawner biomass value in block [i0,j0] is then calculated using the algorithm already described.

9. The time in hours from spawning to hatching of eggs has already been described in Chapter Two by the algorithm

$$D = 43787.93e^{-2.41\ln(x)} + e^{5.02-0.155x}$$

.....equation A.2

where x is the temperature in °C at the position where spawning took place. For model purposes, this algorithm was simplified by the quadratic model

$$D = 0.697x^2 - 23.9x + 417.$$

.....equation A.3

which is a close fit (Figure A.3).

Although the temperature is 17°C everywhere in the grid, the temperature-dependent model is incorporated in anticipation of an altered temperature field, which is to be included in a future application of the model.

10. The screen is now divided into two panels. On the left the egg production (eggs per hour divided by 10^4), time from spawning to hatching (hours), interpolated temperature (°C), interpolated speed ($cm.s^{-1}$) and direction (bearing in degrees) and the release point co-ordinates (in kilometres) are shown. On the right the following are displayed: spawner biomass (kilotons multiplied by 10^3), days from 1 November to the chosen day ("+" indicates subsequent to and "-" indicates prior to 1 November), spawning fraction (per day), average female weight (kilograms), female proportion, batch fecundity (eggs/female/batch) and the hourly survival rate of adult spawners.

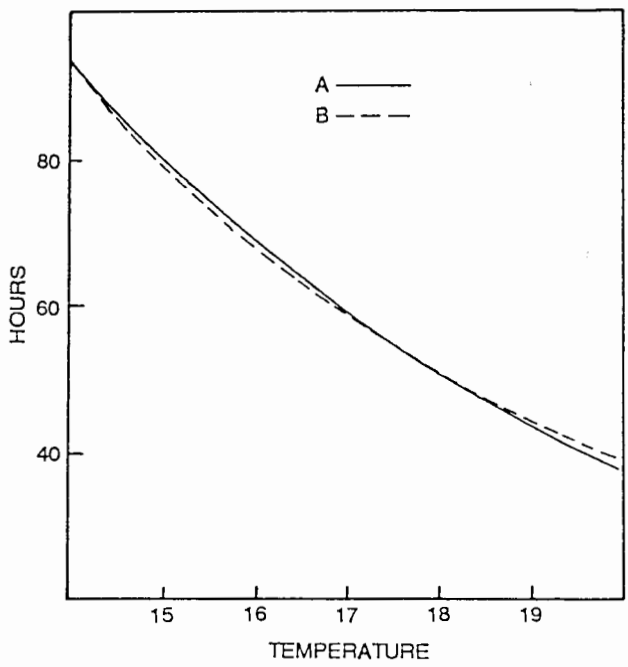

Figure A.3 Graph of hatching time (hours from spawning) as a function of temperature (°C)
(curve A is the fitted model, curve B is the algorithm derived from the literature)

11. Egg production at another point can then be calculated and added to the output file **Auxout.out** or the operator may exit from the program.

d) OUTPUT FROM AUXIL.EXE

The output file **Auxout.out**, created by AUXIL.EXE, contains the following information for each batch selected to be spawned:

a) The row number (i0) and column number (j0) appear on the first line of each record.

b) The second line contains the number of eggs produced per hour, divided by 10^4, the time in hours from spawning to hatching, the temperature in °C at the selected position for spawning, the interpolated speed ($cm.s^{-1}$) followed by direction (bearing in degrees) at the release point and the x (longitudinal) and y (latitudinal) co-ordinates (in kilometres) of the selected spawning site.

c) Written on the third line of each record are: the spawner biomass (in kilotons) multiplied by 10^3, days from 1 November to the day selected for spawning, the fraction of females spawning per day, the average weight (kg) of female spawners, the female proportion by mass, the batch fecundity (eggs produced per batch per female) and finally, the hourly survival rate of spawners on the day selected for spawning.

3. MONTY.EXE

a) FUNCTION OF MONTY.EXE

MONTY.EXE is the principal program of the model. **Pilot_an.dat**, **Rls_tst.dat**, **Coast.dat** and **Veltb.dat** all feed information into MONTY.EXE, which then proceeds to simulate the release of batches of eggs of Cape anchovy at specified locations within the spawning area off the South African coast. Each batch of eggs released is then moved as a point on an hourly time scale according to the interpolated velocity at each new position. The number of individuals dying per hour depends on the mortality rate allocated to individuals of that age class. Should the batch cross one of the "loss" boundaries, all the individuals surviving at that time are counted as advective losses. The total number of individuals surviving to recruitment, the total number of individuals dying due to causes excluding unfavourable advection and the total number of individuals lost due to unfavourable advection are summed for all the batches in the release file in question.

The output file **Monty.out** gives the number of anchovy surviving to recruitment (180 days), the position reached after the specified number of days, total mortality and the proportion of total mortality resulting from advective loss for each release file run.

b) DATA SOURCES AND VARIABLES:

Each batch is moved as a unit which remains intact until recruitment. It was originally planned that batches spawned in a single night would be released over the whole 24 hour period, the total number of eggs spawned per day equivalent to those produced during a real night's spawning. By releasing many small batches at hourly intervals in the same block, diffusion would have been at least partially simulated. However, owing to this process being very time-consuming, **RELEASE5.EXE** was written to calculate daily egg production so that one larger batch is released per night at a particular site.

Each batch is moved with a velocity obtained from linearly interpolating the ADCP velocity vectors in eight neighbouring blocks and if desired, adding to this diffusion, turbulence or both.

i) ACOUSTIC DOPPLER CURRENT PROFILE (ADCP) DATA

The program written by Caroline Zauner (Sea Fisheries Research Institute) was used to average ADCP northerly and easterly vectors for the 0.25 by 0.25 degree (15 by 15 minutes of latitude and longitude) blocks at 30m and 50m depths. Data from the cruises listed in Table A.1 were averaged. Only cruises between September and March were used, as advised by Dr A.J. Boyd (Sea Fisheries Research Institute), since these cruises cover the areas where anchovy are found at the times relevant to anchovy transport from spawning grounds to recruitment areas.

Interpolated vectors were used in those 41 blocks lacking ADCP data but which were bordered by at least 3 blocks having ADCP data. Weighted interpolated northerly vector components (Vv) were calculated by using the following formula:

$$Vv = \frac{\sum (n \times \frac{v}{d})}{\sum (\frac{n}{d})}$$

.....equation A.4

where v is the average ADCP vector component, n is the number of observations used in calculating this average component and d is the fraction of a degree between the mid-point of the block in question and the mean position of all observations used in the bordering block. Weighted interpolated easterly vector components were similarly calculated. Figure A.2 shows which blocks have ADCP data, which have interpolated ADCP data and which have no current data at all.

Table A.1 **Cruises from which ADCP data were extracted to compile the velocity file Vel44.csv.**

VOYAGE	DATE	TYPE OF CRUISE
V078	November 1989	Pelagic biomass
V079	January 1990	Hake recruitment
V086	September 1990	Hake recruitment
V087	November 1990	Pelagic recruitment
V088	January 1991	Hake recruitment
V090	March 1991	Pelagic prerecruitment
V095	September 1991	Hake recruitment
V096	October 1991	Horse Mackerel
V097	November 1991	Pelagic biomass
V100	February 1992	Hake recruitment
V101	March 1992	Pelagic prerecruitment
V106	September 1992	Hake recruitment
V107	October 1992	Horse mackerel
V108	November 1992	Pelagic biomass
V109	January 1993	Hake recruitment

ii) SURVIVAL RATES

Mortality rates taken from the literature discussed in Chapter Two were converted to hourly survival rates. Table 3.1 (Chapter Three) summarises the survival rates used in the model for the Cape anchovy in the egg, larval, prerecruit and recruit stages.

c) INSTRUCTION FOR THE USE OF MONTY.EXE

Once the input files **Pilot_an.dat**, **Rls_tst.dat**, **Coast.dat**, **Veltbx.dat** (i.e. **Vel44.csv**) and **Port22.csv** have been compiled, MONTY.EXE can be run from ANPILOT.EXE without any further input required by the operator.

d) THE RUNNING OF MONTY.EXE; BEHIND THE SCENES

1. MONTY.EXE begins by reading in the file **Pilot_an.dat** which contains the chosen diffusion and turbulence amplitudes, graphics requirements, the number of days for which the program is to run, the release file name, the coastline file name, the velocity-temperature file name and the timescales of the various stages in the life cycle of the anchovy. MONTY.EXE then cycles through its loop for each record specified in the release file. Note that all time scales are converted to be hourly.
2. Next is the loading of the specified velocity-temperature data file **Veltbx.dat**.
3. The graphics is initialised and the coastline is drawn in the "icon" on the output screen according to the specifications contained in **Coast.dat**.
4. The position of spawning, time of spawning (t_0 set to zero at present) and number of eggs to be released are extracted from the release file.
5. The loop "*loop*" is initiated to cycle through the number of hours (*it*X24) for which a batch is to be tracked.
6. The *Box* procedure begins. This procedure finds the box (block) in which the batch is located at a particular time and calculates the distances required for the linear interpolations of the velocity vectors. The procedure reads in the x, y co-ordinates (in kilometres) of the position of the batch at this time, and the block width (*dltx*) and length (*dlty*) defined in the velocity-temperature file. It steps through the rows by incrementing half the block length and through the columns by incrementing half the block width until the row (i0) and column (j0) in which the point lies are found. The procedure then calculates the distances xl, xr, yu and yd from the point P(x,y) (Figure A.4) to the midpoints of the blocks on the left, right, above and below

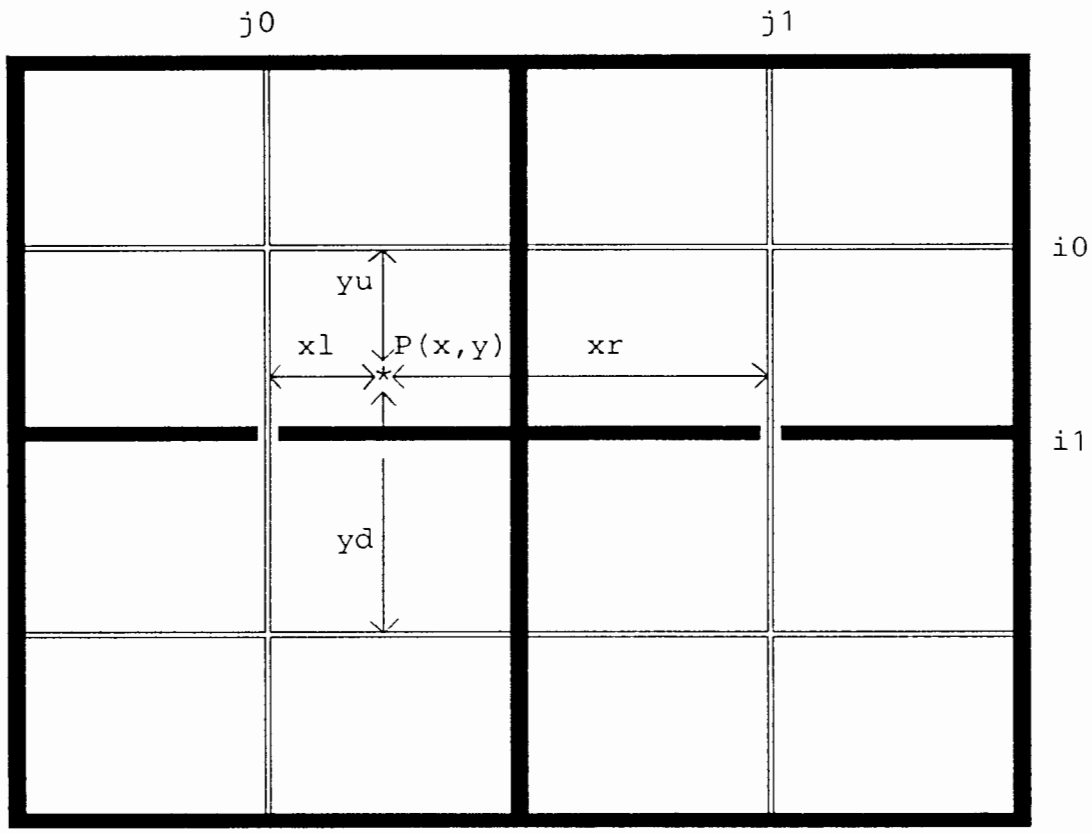

Figure A.4 Distances required for velocity interpolation later in *MONTY.EXE* (each block is subdivided into four equal parts which are recognised in the program by the values of the monitor *l*)

respectively. The procedure uses a monitor (*l*) to differentiate between the case when x lies in the left half of the box and when x is in the right half of the box, and between y in the top half and the bottom half of the box, so that the correct distances are used. The proximate column and row are then found, also depending on the monitor.

7. If the block position lies outside the program bounds (120 by 120 blocks) due to an initial absurd choice of release position or a velocity field filling the memory space, MONTY.EXE is halted and an explanatory message appears on the screen.

8. If the proximate row returned by the box procedure lies outside the range of rows in the grid (i.e. less than 1 or greater than 31 for the grid upon which **Vel44.csv** is based) then the proximate row is set to the row in which the block itself lies, viz i0. Similarly, if the proximate column lies outside the column range (less than 1 or greater than 53 in **Vel44.csv**) j0 is taken to be the proximate column.

9. At this stage two of the boundary checks are carried out. If the block (i0,j0) is on land, i.e. *place*=2, then the boundary check is set to 4. If the block is beyond the zone having ADCP or interpolated ADCP data, i.e. if *place*=1 (oceanic block) and the u and v velocity components are zero, then the boundary check is set to 5.

10. The interpolation procedure described below requires four blocks (viz [i0,j0], [i1,j0], [i0,j1] and [i1,j1]). Since the west coastal land belt (i=1 to i=16 in **Vel44.csv**) is irregular some of the blocks used in the interpolation procedure may be on land or even in non-existent blocks. The latter case is avoided by the insertion of a band of "dummy" land blocks (Figure A.2) immediately before the end-of-row marker blocks, which have all parameters in the velocity-temperature file set to zero.

If one or more of the three blocks [i1,j0], [i1,j1] and [i0,j1] are end-of-row marker blocks it/they are substituted with the temperature in box [i0,j0]. Velocities still assume the same values, i.e. zero at the end of a row. In this way the velocity field is effectively tapered at the coastal boundary but the temperature field is not.

11. If the boundary check is not 4 or 5, (i.e. if it is 0 at this stage), the four-block three-stage proportionally-weighted linear interpolation scheme is applied to obtain the easterly (Uu) and northerly (Vv) velocity components and the temperature at the position of the batch. The information required to perform this interpolation is returned by the *box* procedure.

There are four cases for the position of the point in block [i0,j0], namely

i) the proximate column (j1) is to the right of j0 and the proximate row (i1) is below i0, i.e. xl is less than or equal to xr and yu is less than or equal to yd,

ii) the proximate column is to the left of j0 and the proximate row is below i0, i.e. xl is greater than xr and yu is less than yd,

iii) the proximate column is to the left of j0 and the proximate row is above i0, i.e. xl is greater than xr and yu is greater than yd,

iv) the proximate column is to the right of j0 and the proximate row is above i0, i.e. xl is less than or equal to xr and yu is greater than yd.

These four cases are handled by the following algebra, where u[i,j] is the easterly velocity vector in block [i,j] and v[i,j] is the northerly velocity vector in block [i,j]:

if xl<=xr then q=1 else q=0

$$c1x=(1-q)xl+xr\times q;c2x=xl\times q+(q-1)xr$$

.....equation A.5

if yu<=yd then q=1 else q=0

$$c1y=(1-q)yu+yd\times q;c2y=yu\times q+(q-1)yd$$

.....equation A.6

$$Uu1=\frac{u[i0,j0]\times c1x+u[i0,j1]\times c2x}{xl+xr}$$

.....equation A.7

$$Uu2=\frac{u[i1,j0]\times c1x+u[i1,j1]\times c2x}{xl+xr}$$

.....equation A.8

$$Uu=\frac{c1y\times Uu1+c2y\times Uu2}{yu+yd}$$

.....equation A.9

$$Vv1=\frac{v[i0,j0]\times c1x+v[i0,j1]\times c2x}{xl+xr}$$

.....equation A.10

$$Vv2=\frac{v[i1,j0]\times c1x+v[i1,j1]\times c2x}{xl+xr}$$

.....equation A.11

$$Vv=\frac{c1y\times Vv1+c2y\times Vv2}{yu+yd}$$

.....equation A.12

Finally, velocity components are scaled by dividing by 10^2 to represent currents in $cm.s^{-1}$.

12. It is optional at this point that the extra easterly velocity component of 3 $cm.s^{-1}$ is added to the Uu component if the anchovy are in the prerecruit stage and in the recruitment area, i.e. between 30 and 33°S, 16°E and the coast. The program called **SWIM.EXE** is identical to MONTY.EXE but has this option permanently switched on here. However, for purposes of this thesis, active swimming was not included, so that passive transport alone could be modelled and its importance assessed.

13. Two pairs of random numbers are generated in the *rnd* procedure, which maps random numbers generated by TURBO PASCAL'S *Random* function (distributed on [0,1]) onto [-1,1]. If the latch *l1* is set to 1 in the pilot file **Pilot_an.dat**, i.e. if the operator chose to add a Monte Carlo component simulating diffusion, each of the first pair of random numbers is multiplied by the diffusion amplitude, the first product is added to the easterly (Uu) velocity component, the second to the northerly (Vv) velocity component. If the operator chose to add a Monte-Carlo component to simulate turbulence, i.e. if the latch *l2* is set to one, and if the hour ("*loop*") is equal to the lapse time (*lapse*) prescribed in **Pilot_an.dat**, then each of the second pair of random numbers is multiplied by the turbulence amplitude, the first product is added to the easterly component and the second to the northerly component. Hereafter, the turbulence component is added hourly. If the hour is a multiple of the lapse time, the second pair of random numbers generated for this hour is then multiplied by the turbulence amplitude to give a new turbulence component, which in turn is added hourly until the next *lapse* hours have passed. In this way the hourly-added turbulence component only changes every *lapse* hours, whereas a "new" randomly selected diffusion component is added hourly.

14. MONTY.EXE then checks for the crossing of the other four boundaries. The boundary check is set to 1 if the batch crosses the western boundary, 2 if it crosses the northern boundary, 3 if is transported through the southern boundary and 6 if the batch reaches the eastern boundary. For details of what these boundaries are in **Vel44.csv** please refer to the section "Output from MONTY.EXE" beginning on page A29.

15. The counter "*stage*" keeps track of the number of hours from the spawning of the batch. The *biol* procedure is initiated to choose the correct survival rate depending on the hour ("*stage*") within the life cycle of the batch and to then calculate anchovy survival to the end of the hour in question. Recall that Table 3.1 (Chapter Three) gives the hourly survival rates of anchovy in the egg, larval, prerecruit and recruit stages that are used in this procedure and that the durations of each of these stages are set in the pilot file **Pilot_an.dat.**

    The loop "*loop*" is repeated for each hour until the batch has been tracked for the specified number of hours or until the boundary check is 1, 2, 3, 5 or 6. If no boundary is reached or if the batch has reached land (i.e. the boundary check is 4) the loop is repeated. The reasoning behind continuing despite the land boundary being crossed is that anchovy are unlikely to be washed ashore. They are far more likely to survive in small shoals in nearshore regions or bays in such areas. This being the case, hourly natural mortality must still be summed until the required number of days have passed.

16. If the boundary check is still 0 after the batch has been tracked for the required number of days, the end point reached is marked with a pixel.

17. The five output "icons" are set up on the screen and updated once each batch released has been tracked for the specified time. They represent a) percentage of the "job" completed so far, b) relative mortality due to natural processes and counterproductive advective processes,

c) total number of recruits, d) number of eggs initially released multiplied by 10^{-4}, (this number should therefore be multiplied by 10^{4} to get actual number of eggs), and e) the subsequent percentage of these eggs that survive to recruitment.

The number of anchovy dying due to natural processes excluding adverse advection is calculated each hour as a cumulative total. If the boundary check is 4 (land), or if the specified number of days has passed and the boundary check is 0, the total number of recruits is computed as a cumulative sum for all the batches. If the boundary check is 1 (western boundary), 2 (northern boundary), 3 (southern boundary), 5 (region lacking ADCP data) or 6 (eastern boundary), the number of anchovy surviving at the time at which one of these boundaries was crossed is added to the cumulative sum of potential recruits lost as a result of unfavourable advection.

18. The loop "*cycl*" is repeated for the next record in the release file, i.e. for the next batch destined to be released, until all specified batches have been released and tracked.

e) OUTPUT FROM MONTY.EXE

The output file **Monty.out** created by MONTY.EXE contains the following information for each batch released and tracked:

a) the record number, corresponding to the batch in the release file,

b) the x and y co-ordinates (in kilometres) of the final position reached by the batch after the selected number of days,

c) the box row number (i0) and column number (j0) of the final position reached,

d) a value corresponding to the boundary check, (recall that a boundary check of

1 indicates the batch crossed the western offshore boundary

(i.e. 15°E for the grid upon which **Vel44.csv** is based),

2 indicates that the batch went through the northern boundary (i.e. 29°S),

3 indicates that the batch was transported across the southern boundary (36°45'S),

4 indicates that the batch reached land, i.e. remained in nearshore areas and bays,

5 indicates that the batch was transported into the region of the grid where no ADCP or interpolated ADCP data are available and

6 indicates that the batch reached the maximum eastern grid boundary, i.e. 28°E),

e) the number of anchovy in the batch that were still surviving after the chosen number of days had passed or at the time when one of the "loss" boundaries (viz boundary 1, 2, 3, 5 or 6) was reached and

f) the hour (*loop*) when tracking of the batch ceased i.e. when tracking time was over or when boundary 1,2,3,5 or 6 was crossed.

Appended to the end of the output file **Monty.out** are the following:

g) the total number of anchovy in all batches in the release file that survived to recruitment,

h) the total number of anchovy in all batches that died due to causes excluding unfavourable advection,

i) the total number of anchovy in all batches that were advected across the boundaries 1, 2, 3, 5 or 6 and therefore assumed lost to the system,

j) the total number of anchovy in all batches that died or were lost due to natural mortality including adverse advective processes and

k) the overall percentage of anchovy in all batches that survived to recruitment.

Output files created by MONTY.EXE are then run through the program **BOUNDAL.EXE**, which processes MONTY.OUT files so that the distributions of recruits and advective losses can be considered. This program calculates the proportion of advective losses that occur in each of the five strata depicted in Figure 2.4 of Chapter Two. In addition, it calculates the proportion of recruits that accumulate offshore (i.e. crossing no boundaries) and in coastal regions (i.e. crossing the land boundary). The distribution of recruits (offshore and near the coast, together) is computed as proportions accumulating in the four strata within the boundaries of the grid, viz. between 29°S and Cape Columbine (stratum 2), between Cape Columbine and Cape Agulhas (stratum 3), between Cape Agulhas and Mossel Bay (stratum 4) and between Mossel Bay and 28°E (stratum 5).

Since the flow field is at this stage not yet time-dependent, BOUNDAL.EXE also calculates the mean hour (after spawning) at which those batches of anchovy lost to the system by unfavourable advection crossed loss boundaries. Whether advection across boundaries occurs soon after spawning or later in the 180 day period to recruitment, no anchovy survive in a batch which is lost. For this reason, the mean hour of loss is of no real significance for

anchovy survival. However, it is useful in the sensitivity tests since it does provide an indication of the likelihood of advection across boundaries at different levels of diffusion and turbulence.

IMPORTANT NOTES: MONTY.EXE assumes the natural mortality rates exclude mortality due to unfavourable advection. Strictly speaking, this is not correct because egg, prerecruit and recruit mortality rates used in this model are estimates of observed mortality in the field, which theoretically include all causes ranging from disease to advection into regions unfavourable for survival. Mortality due to adverse advective processes is simulated separately by the model and added to "natural mortality" to give total mortality, hence advective mortality is effectively being added twice. Only larval mortality, which was estimated from laboratory experiments, excludes mortality due to advection.

An attempt was made to solve this problem by separating MONTY.EXE into two parts; one part which tracked the paths of batches and summed the advective losses and one part that merely cycled through the required number of days, allowing the number of potential recruits (initially equal to number of eggs produced) to decrease according to the mortality rates obtained from the literature (field estimates except for the larval stage). On closer examination, however, this method is not a solution because by separating the advective processes, it is impossible to tell whether and when a batch is advected offshore, and therefore how long one should continue decreasing anchovy numbers to simulate mortality.

With the exception of larval mortality, laboratory work has not been undertaken to estimate mortality rates during the other stages of the life cycle of *E. capensis*. For this reason and

because separating the model into two parts was not feasible, the model was "tuned" by adjusting the mortality rate of the least-known stage, viz. the prerecruit stage.

APPENDIX B

TABLES CONTAINING EXTRA INFORMATION RELEVANT TO CHAPTERS THREE, FOUR, FIVE AND SIX

Table B.1 **Percentages and numbers of young of the year occurring in the five strata and, in parentheses, percentage of year-class accumulating offshore but within grid boundaries (ofs) and inshore in bays (ins), obtained by simulation when altered advection scenarios were modelled**

* indicates a percentage between 0 and 1%

ADVECTION SCENARIO	NORTH OF CAPE COLUMBINE: - STRATUM 2	BETWEEN CAPE COLUMBINE AND CAPE AGULHAS: - STRATUM 3	BETWEEN CAPE AGULHAS AND MOSSEL BAY: - STRATUM 4	EAST OF MOSSEL BAY: - STRATUM 5
0	49.5 $2.182X10^{11}$ (0.5 ins 49.1 ofs)	25.6 $1.127X10^{11}$ (all ins)	21.3 $9.371X10^{10}$ (1.2 ins 20.1 ofs)	3.6 $1.599X10^{10}$ (1.8 ins 1.8 ofs)
0t	44.6 $1.962X10^{11}$ (0.6 ins 44.0 ofs)	30.5 $1.340X10^{11}$ (30.5 ins 0.0* ofs)	21.3 $9.353X10^{10}$ (1.2 ins 20.1 ofs)	3.7 $1.608X10^{10}$ (1.6 ins 2.0 ofs)
0T	39.9 $1.748X10^{11}$ (0.8 ins 39.1 ofs)	34.2 $1.500X10^{11}$ (34.2 ins 0.0* ofs)	22.2 $9.733X10^{10}$ (1.2 ins 21.0 ofs)	3.7 $1.619X10^{10}$ (1.4 ins 2.3 ofs)
1	20.1 $2.655X10^{10}$ (all ofs)	8.6 $1.133X10^{10}$ (all ins)	63.6 $8.400X10^{10}$ (9.2 ins 54.4 ofs)	7.7 $1.016X10^{10}$ (all ins)
1t	19.3 $2.370X10^{10}$ (all ofs)	9.4 $1.150X10^{10}$ (9.3 ins 0.0* ofs)	62.7 $7.699X10^{10}$ (11.7 ins 51.1 ofs)	8.6 $1.050X10^{10}$ (all ins)
2	24.1 $4.241X10^{10}$ (all ofs)	13.5 $2.374X10^{10}$ (all ins)	53.3 $9.371X10^{10}$ (2.9 ins 50.4 ofs)	9.1 $1.599X10^{10}$ (4.6 ins 4.5 ofs)
2t	17.9 $3.166X10^{10}$ (all ofs)	20.0 $3.541X10^{10}$ (20.0 ins 0.0* ofs)	52.9 $9.353X10^{10}$ (3.0 ins 50.0 ofs)	9.1 $1.608X10^{10}$ (4.0 ins 5.1 ofs)

3	22.3 $4.241X10^{10}$ (all ofs)	20.2 $3.839X10^{10}$ (19.8 ins 0.3 ofs)	49.2 $9.371X10^{10}$ (2.7 ins 46.5 ofs)	8.4 $1.599X10^{10}$ (4.2 ins 4.2 ofs)
3t	15.8 $3.001X10^{10}$ (all ofs)	26.4 $5.006X10^{10}$ (26.1 ins 0.3 ofs)	49.3 $9.352X10^{10}$ (2.8 ins 46.6 ofs)	8.5 $1.608X10^{10}$ (3.7 ins 4.7 ofs)
4	22.3 $4.241X10^{10}$ (all ofs)	20.0 $3.805X10^{10}$ (all ins)	49.3 $9.371X10^{10}$ (2.7 ins 46.6 ofs)	8.4 $1.599X10^{10}$ (4.2 ins 4.2 ofs)
4t	15.8 $3.001X10^{10}$ (all ofs)	26.3 $4.981X10^{10}$ (26.3 ins 0.0* ofs)	49.4 $9.353X10^{10}$ (2.8 ins 46.6 ofs)	8.5 $1.608X10^{10}$ (3.7 ins 4.7 ofs)
5	52.5 $1.050X10^{11}$ (all ofs)	19.2 $3.839X10^{10}$ (18.9 ins 0.3 ofs)	19.7 $3.927X10^{10}$ (2.3 ins 17.3 ofs)	8.6 $1.717X10^{10}$ (7.8 ins 0.8 ofs)
5t	51.8 $1.035X10^{11}$ (all ofs)	21.8 $4.353X10^{10}$ (19.2 ins 2.6 ofs)	17.8 $3.561X10^{10}$ (2.3 ins 15.5 ofs)	8.6 $1.717X10^{10}$ (7.8 ins 0.8 ofs)
6	34.1 $8.219X10^{10}$ (all ofs)	25.4 $6.120X10^{10}$ (10.6 ins 14.7 ofs)	33.5 $8.077X10^{10}$ (4.9 ins 28.5 ofs)	7.1 $1.717X10^{10}$ (6.4 ins 0.7 ofs)
6t	32.6 $7.698X10^{10}$ (all ofs)	27.3 $6.447X10^{10}$ (13.5 ins 13.8 ofs)	33.5 $7.910X10^{10}$ (4.9 ins 28.6 ofs)	6.6 $1.551X10^{10}$ (5.9 ins 0.7 ofs)
7	36.2 $8.219X10^{10}$ (all ofs)	20.7 $4.689X10^{10}$ (5.0 ins 15.7 ofs)	35.6 $8.077X10^{10}$ (5.2 ins 30.3 ofs)	7.6 $1.717X10^{10}$ (6.8 ins 0.7 ofs)
7t	34.7 $7.698X10^{10}$ (all ofs)	22.6 $5.007X10^{10}$ (7.9 ins 14.7 ofs)	35.7 $7.910X10^{10}$ (5.3 ins 30.4 ofs)	7.0 $1.551X10^{10}$ (6.2 ins 0.8 ofs)

Table B.2 **Percentages and numbers of advective losses occurring in the five strata, obtained by simulation when altered advection scenarios were modelled**

* indicates a percentage between 0 and 1%

ADVECTION SCENARIO	NORTH OF 29°S: - STRATUM 1	NORTH OF CAPE COLUMBINE: - STRATUM 2	BETWEEN CAPE COLUMBINE TO CAPE AGULHAS: - STRATUM 3	BETWEEN CAPE AGULHAS AND MOSSEL BAY: - STRATUM 4	EAST OF MOSSEL BAY: - STRATUM 5
0	0.0	0.0	0.0	100.0 $1.795X10^{14}$	0.0
0t	0.0	0.0	0.0	100.0 $1.809X10^{14}$	0.0
0T	0.0	0.0	0.0	100 $1.838X10^{14}$	0.0
1	0.0	19.6 $2.642X10^{13}$	80.4 $1.081X10^{14}$	0.0	0.0
1t	0.0	21.7 $2.540X10^{13}$	78.3 $9.150X10^{13}$	0.0* $1.152X10^{10}$	0.0
2	0.0	9.1 $2.426X10^{13}$	23.9 $6.417X10^{13}$	67.0 $1.795X10^{14}$	0.0
2t	0.0	8.6 $2.329X10^{13}$	24.3 $6.544X10^{13}$	67.1 $1.809X10^{14}$	0.0
3	0.0* $1.122X10^{11}$	14.6 $3.549X10^{13}$	11.5 $2.785X10^{13}$	73.9 $1.795X10^{14}$	0.0
3t	2.5 $6.127X10^{12}$	7.6 $1.882X10^{13}$	16.5 $4.054X10^{13}$	73.4 $1.809X10^{14}$	0.0
4	0.0	44.9 $2.272X10^{14}$	19.7 $9.976X10^{13}$	35.4 $1.795X10^{14}$	0.0
4t	0.0	45.1 $2.292X10^{14}$	19.4 $9.845X10^{13}$	35.6 $1.809X10^{13}$	0.0
5	0.0	15.5 $3.549X10^{13}$	12.2 $2.785X10^{13}$	72.3 $1.655X10^{14}$	0.0
5t	2.6 $6.014X10^{12}$	8.2 $1.882X10^{13}$	17.6 $4.054X10^{13}$	71.6 $1.652X10^{14}$	0.0
6	0.0	69.1 $2.230X10^{14}$	30.9 $9.976X10^{13}$	0.0	0.0
6t	0.0	69.6 $2.250X10^{14}$	30.4 $9.845X10^{13}$	0.0	0.0
7	0.0	38.6 $2.411X10^{14}$	61.4 $3.835X10^{14}$	0.0	0.0
7t	0.0	38.7 $2.423X01^{14}$	61.3 $3.837X10^{14}$	0.0	0.0

Table B.3 **Numbers of young of the year and advective losses obtained by simulation when advection scenario 5 was modelled using spawning distributions in the years listed**

YEAR'S SPAWNING DISTRIBUTION	NUMBER OF ANCHOVY SURVIVING TO 180 DAYS (NUMBERS X 10^9) % SURVIVING IN PARENTHESES	PERCENTAGE ACCUMULATING OFFSHORE BUT WITHIN GRID BOUNDARIES (AS OPPOSED TO COASTAL AREAS)	NUMBER OF ANCHOVY LOST THROUGH ADVECTION ACROSS BOUNDARIES (NUMBERS X 10^{12})	PERCENTAGE OF BATCHES LOST BY ADVECTION; AVERAGE TIME OF LOSS (HOURS AFTER SPAWNING) IN PARENTHESES
1986	122.44 (0.0025)	64.9	85.24	49.5 (1424)
1987	179.08 (0.0037)	79.3	160.78	45.6 (1397)
1988	139.10 (0.0029)	67.5	540.33	50.6 (1426)
1989	135.09 (0.0028)	60.4	225.12	38.1 (1432)
1990	214.36 (0.0044)	69.3	115.17	44.1 (1765)
1991	199.84 (0.0041)	71.0	228.80	34.7 (1535)
1992	218.64 (0.0045)	78.8	104.41	34.5 (1682)

Table B.4 **Percentages and numbers of young of the year occurring in the five strata and, in parentheses, percentage of year-class accumulating offshore but within grid boundaries (ofs) and inshore in bays (ins), obtained by simulation when advection scenario 5 was modelled using spawning distributions in the years listed**

YEAR'S SPAWNING DISTRIBUTION	NORTH OF CAPE COLUMBINE: - STRATUM 2	BETWEEN CAPE COLUMBINE AND CAPE AGULHAS: - STRATUM 3	BETWEEN CAPE AGULHAS AND MOSSEL BAY: - STRATUM 4	EAST OF MOSSEL BAY: - STRATUM 5
1986	33.2 $4.060X10^{10}$ (all ofs)	42.1 $5.155X10^{10}$ (33.6 ins 8.5 ofs)	22.2 $2.714X10^{10}$ (0.1 ins 22.1 ofs)	2.6 $3.151X10^{9}$ (1.5 ins 1.1 ofs)
1987	44.0 $7.885X10^{10}$ (all ofs)	43.3 $7.762X10^{10}$ (17.5 ins 25.8 ofs)	8.0 $1.43X10^{10}$ (0.9 ins 7.1 ofs)	4.6 $8.289X10^{9}$ (2.3 ins 2.3 ofs)
1988	63.2 $8.794X10^{10}$ (2.6 ins 60.6 ofs)	27.1 $3.763X10^{10}$ (25.7 ins 1.4 ofs)	0.3 $3.840X10^{8}$ (all ofs)	9.5 $1.315X10^{10}$ (4.2 ins 5.3 ofs)
1989	47.9 $6.468X10^{10}$ (all ofs)	24.3 $3.289X10^{10}$ (23.8 ins 0.5 ofs)	11.6 $1.565X10^{10}$ (0.1 ins 11.5 ofs)	16.2 $2.188X10^{10}$ (15.7 ins 0.5 ofs)
1990	39.0 $8.359X10^{10}$ (all ofs)	24.0 $5.136X10^{10}$ (all ins)	32.9 $7.051X10^{10}$ (2.6 ins 30.3 ofs)	4.1 $8.883X10^{9}$ (all ins)
1991	52.5 $1.050X10^{11}$ (all ofs)	19.2 $3.839X10^{10}$ (18.9 ins 0.3 ofs)	19.7 $3.927X10^{10}$ (2.3 ins 17.3 ofs)	8.6 $1.717X10^{10}$ (7.8 ins 0.8 ofs)
1992	37.9 $8.282X10^{10}$ (all ofs)	18.0 $3.941X10^{10}$ (16.5 ins 1.6 ofs)	25.4 $5.548X10^{10}$ (0.4 ins 25.0 ofs)	18.7 $4.092X10^{10}$ (4.4 ins 14.4 ofs)

Table B.5 **Percentages and numbers of advective losses occurring in the five strata, obtained by simulation when advection scenario 5 was modelled using spawning distributions in the years listed**

YEAR'S SPAWN-ING DISTRI-BUTION	NORTH OF 29°S: - STRATUM 1	NORTH OF CAPE COLUMBINE: - STRATUM 2	BETWEEN CAPE COLUMBINE AND CAPE AGULHAS: - STRATUM 3	BETWEEN CAPE AGULHAS AND MOSSEL BAY: - STRATUM 4	EAST OF MOSSEL BAY: - STRATUM 5
1986	0.0	32.4 $2.764X10^{13}$	20.2 $1.720X10^{13}$	19.5 $1.660X10^{12}$	27.9 $2.380X10^{13}$
1987	1.7 $2.702X10^{12}$	34.5 $5.550X10^{13}$	52.8 $8.482X10^{13}$	11.0 $1.776X10^{13}$	0.0
1988	0.1 $7.020X10^{11}$	4.2 $2.269X10^{13}$	93.1 $5.031X10^{14}$	2.0 $1.062X10^{13}$	0.6 $3.174X10^{12}$
1989	0.0	8.2 $1.852X10^{13}$	88.4 $1.990X10^{14}$	0.0	3.4 $7.633X10^{12}$
1990	0.0	9.3 $1.072X10^{13}$	90.7 $1.044X10^{14}$	0.0	0.0
1991	0.0	15.5 $3.549X10^{13}$	12.2 $2.785X10^{13}$	72.3 $1.655X10^{14}$	0.0
1992	0.0	19.1 $1.991X10^{13}$	46.4 $4.843X10^{13}$	34.5 $3.607X10^{13}$	0.0

Table B.6 **Mean numbers of young of the year and advective losses obtained by simulation when advection was altered (means of runs using 7 years of spawning distributions). Standard deviations are in parentheses and in bold are the coefficients of variation (CVX100%).**

	REDUCED FLOW FIELD (SCENARIO 0)	NEW BASELINE FLOW FIELD (SCENARIO 5)	ENHANCED FLOW FIELD (SCENARIO 6)
MEAN YEAR-CLASS STRENGTH (NUMBERS $X10^9$)	461.63 (22.68) **4.91**	172.65 (40.19) **23.28**	171.84 (51.87) **30.19**
MEAN % RECRUITS ACCUMULATING OFFSHORE	66.99 (6.06) **9.05**	70.17 (6.95) **9.90**	73.3 (12.86) **17.54**
MEAN ADVECTIVE LOSS (NUMBERS $X10^{12}$)	115.70 (136.75) **118.19**	208.55 (156.96) **75.26**	501.50 (192.79) **38.44**
MEAN % BATCHES LOST THROUGH ADVECTION	4.7 (3.5) **74.5**	42.2 (6.7) **15.9**	42.8 (7.6) **17.8**
AVERAGE TIME OF ADVECTIVE LOSS (HOURS AFTER SPAWNING)	245 (143) **58**	1523 (146) **10**	708 (43) **6**

Table B.7 **Mean numbers of young of the year accumulating in each of the four strata when advection was altered (means of 7 years of spawning distributions). Standard deviations are in parentheses, coefficients of variation (CVX100%) are in bold.**

	REDUCED FLOW FIELD (SCENARIO 0)	NEW BASELINE FLOW FIELD (SCENARIO 5)	ENHANCED FLOW FIELD (SCENARIO 6)
BETWEEN 29°S AND CAPE COLUMBINE (STRATUM 2)	$2.361X10^{11}$ ($0.433X10^{11}$) **18.340** most offshore	$7.764X10^{10}$ ($2.024X10^{10}$) **26.069** all offshore	$6.072X10^{10}$ ($1.477X10^{10}$) **24.325** all offshore
BETWEEN CAPE COLUMBINE AND CAPE AGULHAS (STRATUM 3)	$1.386X10^{11}$ ($0.256X10^{11}$) **18.470** all inshore	$4.698X10^{10}$ ($1.525X10^{10}$) **32.461** most inshore	$6.920X10^{10}$ ($2.339X10^{10}$) **33.801** in- and offshore
BETWEEN CAPE AGULHAS AND MOSSEL BAY (STRATUM 4)	$7.102X10^{10}$ ($3.790X10^{10}$) **53.365** most offshore	$3.182X10^{10}$ ($2.480X10^{10}$) **77.938** most offshore	$3.153X10^{10}$ ($2.772X10^{10}$) **87.916** most offshore
EAST OF MOSSEL BAY (STRATUM 5)	$1.629X10^{10}$ ($1.248X10^{10}$) **76.611** in- and offshore	$1.621X10^{10}$ ($1.252X10^{10}$) **77.236** in- and offshore	$1.040X10^{10}$ ($0.692X10^{10}$) **66.538** most inshore

Table B.8 **Mean numbers of advective losses accumulating in each of the five loss strata (means of 7 year's of spawning distributions). Standard deviations are in parentheses, coefficients of variation (%) are in bold**

	REDUCED FLOW FIELD (SCENARIO 0)	NEW BASELINE FLOW FIELD (SCENARIO 5)	ENHANCED FLOW FIELD (SCENARIO 6)
BEYOND 29°S (STRATUM 1)	$4.757X10^{10}$ ($1.259X10^{11}$) **264.663** only from 1988 spawning	$4.863X10^{11}$ ($10.115X10^{11}$) **207.999** only from 1987 and 1988 spawning	no advective losses
BETWEEN 29°S AND CAPE COLUMBINE (STRATUM 2)	no advective losses	$2.721X10^{13}$ ($1.466X10^{13}$) **53.877** advective losses in all years	$2.875X10^{14}$ ($0.727X10^{14}$) **25.287** advective losses in all years
BETWEEN CAPE COLUMBINE AND CAPE AGULHAS (STRATUM 3)	$7.173X10^{13}$ ($14.036X10^{13}$) **195.678** none from 1990, 1991, 1992 spawning	$1.407X10^{14}$ ($1.711X10^{14}$) **121.606** advective losses in all years	$2.085X10^{14}$ ($1.886X10^{14}$) **90.456**; advective losses in all years
BETWEEN CAPE AGULHAS AND MOSSEL BAY (STRATUM 4)	$3.867X10^{13}$ ($6.359X10^{13}$) **164.443** 100% from 1991 and 1992 spawning	$3.309X10^{13}$ (5.980E13) **180.719** none from 1989 and 1990 spawning	$1.056X10^{12}$ (2.795E12) **264.678** only from 1986 spawning
EAST OF MOSSEL BAY (STRATUM 5)	$5.256X10^{12}$ ($9.578X10^{12}$) **182.230** none from 1990, 1991 and 1992 spawning	$4.944X10^{12}$ ($8.791X10^{12}$) **177.811** only from 1986, 1988 and 1989 spawning	$4.399X10^{12}$ ($8.893X10^{12}$) **202.160** only from 1986, 1988 and 1989 spawning

Table B.9 **Mean, standard deviation and coefficient of variation (CVX100%) for year-class strength (number of recruits) and advective losses of anchovy obtained by simulation under different scenarios of westward advection.**

WESTWARD ADVECTION (PROPORTION OF MEASURED)	MEAN YEAR-CLASS STRENGTH (10^9)	STANDARD DEVIATION OF YEAR-CLASS STRENGTH (10^9) %CV IN PARENTHESES	MEAN NUMBER LOST BY OFFSHORE ADVECTION (10^{12})	STANDARD DEVIATION OF MEAN NUMBER LOST BY OFFSHORE ADVECTION (10^{12}) %CV IN PARENTHESES
0.5	142.11	10.26 (7.22)	103.75	93.16 (89.79)
0.75	149.33	6.63 (4.44)	60.71	75.36 (124.13)
1.00	147.61	7.26 (4.92)	116.60	137.14 (117.62)
1.25	146.96	7.00 (4.76)	122.47	145.86 (119.10)
1.5	142.09	9.55 (6.72)	149.00	153.73 (103.17)

Table B.10 **Mean numbers ($X10^{10}$) of young of the year accumulating in the four strata, obtained by simulation under different scenarios of altered westward advection. Coefficients of variation (CVX100%) are in parentheses.**

WESTWARD ADVECTION (PROPOR-TION OF MEASURED)	NORTH OF CAPE COLUMBINE: - STRATUM 2	BETWEEN CAPE COLUMBINE AND CAPE AGULHAS: - STRATUM 3	BETWEEN CAPE AGULHAS AND MOSSEL BAY: - STRATUM 4	EAST OF MOSSEL BAY: - STRATUM 5
0.50	2.949 (77.552)	8.850 (8.204)	1.938 (46.213)	0.474 (82.300)
0.75	3.799 (55.462)	8.181 (11.552)	2.433 (55.528)	0.519 (76.393)
1.00	6.871 (20.128)	5.101 (17.467)	2.268 (53.351)	0.522 (76.538)
1.25	9.088 (11.290)	3.187 (9.319)	1.900 (64.526)	0.520 (77.521)
1.50	9.256 (16.141)	2.481 (24.248)	1.974 (72.239)	0.496 (82.052)

Table B.11 **Percentage of young of the year remaining within the area under observation and retained in coastal regions, obtained by simulation under different scenarios of westward advection. Standard deviations are in parentheses.**

WESTWARD ADVECTION (PROPORTION OF MEASURED)	% RECRUITS REMAINING WITHIN BOUNDARIES BUT NOT IN COASTAL REGIONS	% RECRUITS RETAINED IN COASTAL REGIONS
0.50	32.8 (9.8)	67.2 (9.8)
0.75	42.1 (5.9)	57.9 (5.9)
1.00	62.5 (6.3)	37.5 (6.3)
1.25	75.6 (1.5)	24.4 (1.5)
1.50	79.7 (3.5)	20.3 (3.5)

Table B.12 **Mean numbers of anchovy lost by advection and accumulating in the four strata, obtained by simulation under different scenarios of altered westward advection. Coefficients of variation (CVX100%) are in parentheses.**

WESTWARD ADVECTION (PROPOR-TION OF MEASURED)	NORTH OF 29°S: - STRATUM 1	BETWEEN 29°S AND CAPE COLUMBINE: - STRATUM 2	BETWEEN CAPE COLUMBINE AND CAPE AGULHAS: - STRATUM 3	BETWEEN CAPE AGULHAS AND MOSSEL BAY: - STRATUM 4	EAST OF MOSSEL BAY: - STRATUM 5
0.50	$1.120X10^{10}$ (257.054)	0.000 (0.000)	0.000 (0.000)	$6.929X10^{13}$ (81.267)	$3.445X10^{13}$ (181.916)
0.75	$3.237X10^{10}$ (264.597)	0.000 (0.000)	$3.431X10^{12}$ (264.617)	$5.234X10^{13}$ (151.146)	$4.899X10^{12}$ (172.892)
1.00	$4.756X10^{10}$ (264.550)	0.000 (0.000)	$7.219X10^{13}$ (195.152)	$3.912X10^{13}$ (163.804)	$5.249X10^{12}$ (182.206)
1.25	$3.499X10^{11}$ (230.294)	$1.974X10^{11}$ (176.292)	$8.197X10^{13}$ (185.409)	$3.463X10^{13}$ (165.001)	$5.307X10^{12}$ (186.282)
1.50	$5.329X10^{11}$ (224.432)	$3.139X10^{12}$ (132.112)	$1.406X10^{14}$ (111.380)	0.000 (0.000)	$4.777X10^{12}$ (181.516)

APPENDIX C

FURTHER SENSITIVITY ANALYSIS RELEVANT TO CHAPTER TWO

Table C.1 **Year-class strength obtained when turbulence amplitude and lapse period are varied, expressed as a percentage of year-class strength obtained when turbulence is excluded from the model.**

	TURBULENCE AMPLITUDE ($CM.S^{-1}$)		
LAPSE PERIOD (HOURS)	5	15	30
6	100.000	99.515	98.058
24	100.000	99.515	99.515
48	100.000	100.485	100.485
72	100.000	100.000	100.000
144	100.000	100.000	100.000

Table C.2 **Total advective losses obtained when turbulence amplitude and lapse period are varied, expressed as a percentage of total advective losses obtained when turbulence is excluded from the model.**

	TURBULENCE AMPLITUDE ($CM.S^{-1}$)		
LAPSE PERIOD (HOURS)	5	15	30
6	99.848	99.045	111.476
24	100.005	104.292	103.325
48	100.005	98.979	98.855
72	100.474	100.586	100.770
144	100.417	100.481	100.632

Table C.3 **Total advective losses obtained when diffusion amplitude is varied, expressed as a percentage of total advective losses obtained when diffusion is excluded from the model.**

DIFFUSION AMPLITUDE	PERCENTAGE DEVIATION
0.1	100.162
0.3	100.094
0.5	99.894
0.7	99.796
0.9	99.664

APPENDIX D

ADCP CURRENT DATA AMENDMENT

After all simulations were completed, and the thesis had been submitted, it was established that some of the current data used were biased. This resulted from a mistake in the settings of the Acoustic Doppler Current Profiler. Instead of the constant heading offset being set to -2° or -3° for the ADCP on *Research Ship Africana*, it was incorrectly set to +2° in November 1990, and this was only corrected in November 1994 when new software was installed.

Since ADCP data used in this thesis were based on cruises between 1989 and 1992, three quarters of the data have been collected with this small bias in operation. It was therefore decided that tests be undertaken to establish to what extent this positive offset affected the results presented. Since most current data were collected relative to the bottom and not to the navigation device, this was accomplished by correcting all current vectors by -3° (three quarters of -4° out).

Results of simulations using the uncorrected current field were compared to results of the same scenario when currents were corrected by -3°. Paired t-tests were used to test for significant differences between year-class strengths with and without the heading correction added to currents, when each of the seven years spawner distributions were modelled. Similarly, losses to advection were compared. Two-factor Anova tests with replication were used to test for significant differences between numbers of young of the year accumulating in four strata defined in this thesis, with and without the heading correction, and when each of the seven years spawner distributions were modelled. In this way the distribution of young

of the year which resulted from modelling the uncorrected heading offset was compared to the distribution when the corrected offset was modelled. Advective losses from five defined loss strata were similarly tested.

Results:

Paired t-tests showed significantly different year-class strengths and advective losses between scenarios when ADCP data were uncorrected and corrected (Table D.1). Year-class strengths were slightly lower and advective losses were higher when ADCP heading was corrected (Table D.1).

Table D.1 **Summary of results of two paired t-tests, performed on i) year-class strength and ii) total advective losses**

	i) YEAR-CLASS STRENGTH	ii) TOTAL ADVECTIVE LOSSES
UNCORRECTED MEAN	$4.61628X10^{11}$	$1.15704X10^{14}$
UNCORRECTED VARIANCE	$5.14467X10^{20}$	$1.87018X10^{28}$
CORRECTED MEAN	$4.56296X10^{11}$	$1.29453x10^{14}$
CORRECTED VARIANCE	$5.06824X10^{20}$	$1.89527X10^{28}$
CALCULATED t-TEST STATISTIC	2.545203	-2.969426
CRITICAL t-TEST STATISTIC	2.446914	2.446914
P-VALUE	0.04377	0.024976
CONCLUSION	significant difference at 5% level	significant difference at 5% level

Tables D.2 and D.3 show that neither numbers of young of the year nor advective losses in the various strata show significant differences at the 5% level between the uncorrected and corrected simulations.

Table D.2 **Results of two-way Anova with replication performed on young of the year in the four strata in which anchovy accumulate** (results relevant to this discussion are in bold)

SOURCE OF VARIATION	SS	df	MS	F	P-value	$F_{critical}$ (5%)
STRATA	4305.210	3	1435.070	182.733	$2.97X10^{-26}$	2.798
CORRECTED VS UNCORRECTED	**0.286**	**1**	**0.286**	**0.036**	**0.849**	**4.043**
INTERACTION	63.538	3	21.179	2.697	0.056	2.798
WITHIN SUBGROUPS (ERROR)	376.962	48	7.853			
TOTAL	4745.996	55				

Table D.3 **Results of two-way Anova with replication performed on numbers lost to advection from the five strata around the coast** (results relevant to this discussion are in bold)

SOURCE OF VARIATION	SS	df	MS	F	P-value	$F_{critical}$ (5%)
STRATA	613.769	4	153.442	3.088	0.022	2.525
CORRECTED VS UNCORRECTED	**1.326**	**1**	**1.326**	**0.027**	**0.871**	**4.001**
INTERACTION	2.505	4	0.626	0.013	0.999	2.525
WITHIN SUBGROUPS (ERROR)	2981.832	60	49.697			
TOTAL	3599.432	69				

Conclusion:

The corrected heading offset yielded significantly lower year-class strengths, and significantly higher advective losses at the 5% level of significance, although the mean values differed by only 1% for year-class strength, and 11% for advective losses. However, it was the relative differences between scenarios which were considered in this thesis. Distributions of young of the year and advective losses were insignificantly affected and yielded important results. It is concluded that the incorrectly set heading offset in Acoustic Doppler Current Profile data, from November 1990 onwards, did not alter the conclusions drawn from this work. In fact, the dependence of recruitment on the alignment of the flow field vectors suggests that this could be viewed as a further method of investigating the impact of flow field variability on anchovy.